Not the outside but the inside matters: Functional analysis of Capricious and Tartan during *Drosophila* tracheal morphogenesis

Dissertation

Am Fachbereich Naturwissenschaften

der Universität Kassel

Cindy Krause

2003

Dissertation

zur Erlangung des akademischen Grades

doctor rerum naturalium

(Dr. rer. nat.)

im Fach Biologie

eingereicht an der

Fachbereich Naturwissenschaften

der Kassel Universität

Tag der mündlichen Prüfung: 12.01.2004

Erstgutachterin: Prof. Dr. Mireille A. Schäfer

Zweitgutachter: PD. Dr. Reinhard Schuh

Abbreviations

A	abdominal segment
Ac	acetate
AEL	after egg laying
AP	alkaline phosphatase
A-P	anterior-posterior
BCIP	5-bromo-chloro-3-indolyl phosphate
bp	base pair
CB	cerebral branch
cDNA	complementary DNA
CNS	central nervous system
DB	dorsal branch
DMSO	dimethyl sulfoxide
DNA	desoxyribonucleic acid
dNTP	desoxyribonucleoside triphosphate
DT	dorsal trunk
DTa	dorsal trunk anterior
DTp	dorsal trunk posterior
dUTP	desoxyuridine triphosphate
D-V	dorso-ventral
ECM	extracellular matrix
Ed	extracellular domain
EDTA	ethylenediaminetetra acetate
EGF	epidermal growth factor
EST	expressed sequence tag
EtBr	ethidium bromide
ExPASy	expert protein analysis system
FGF	fibroblast growth factor
GB	ganglionic branch
HIF	hypoxia inducible factor
HRP	horseradish peroxidase
Id	intracellular domain
IPTG	isopropylthio-β-D-galactoside
kb	kilobase pairs
LB	Luria-Bertani
LRR	Leucine Rich Repeat
LT	lateral trunk
LTa	lateral trunk anterior
LTp	lateral trunk posterior
MN	motorneuron
mRNA	messenger RNA
NBT	nitro blue tetrazolium chloride
OD	optical density
PB	pharyngeal branch
PBS	phosphate-buffer saline
PCR	polymerase chain reaction
PDZ	PSD-95, Discs-large, ZO-1

PS	position-specific
PSP	posterior spiracle
RNA	ribonucleic acid
RNAse	ribonuclease
rpm	rotation per minute
SDS	sodium dodecyl sulfate
sec	seconds
SRF	serum response factor
St.	stage
T	thoracic segment
TC	transverse connective
TGF	transforming growth factor
TP	tracheal placode
Tris	tris(hydroxyethyl)aminoethane
tRNA	transfer RNA
UAS	upstream activating sequence
U	unit (for enzyme activity)
VB	visceral branch
VNC	ventral nerve cord

Table of contents

1 Introduction

1.1 Branching morphogenesis

The fundamental aspects of developmental biology include morphogenesis, the process that organizes cells into specific tissues and organs. In the past years, much effort was given especially to understand branching morphogenesis, the organization of ramified tubes. The tubular structures, which transport essential gases, liquids, or cells from one site to another, are essential components of common organs shared among various divergent organisms. These highly organized tubular networks include lung, kidney, vasculature and mammary gland in mammals as well as trachea and salivary gland in *Drosophila melanogaster* (Bard, 1990; Gumbiner, 1992). Although these tubes vary in their forms and sizes, the basic molecular mechanisms underlying their development are analogous. Branching morphogenesis initiates almost invariably with differentiation of epidermal cells into tube specific anlagen, often in the form of placodes. Then, the placodes invaginate into the underlying tissues to form primary branches, which subsequently grow out in diverse directions. Finally, specific proximal and distal branches that permeate or contact the target tissues are formed (reviewed in Affolter et al., 2003). A detailed comprehension of branching morphogenesis is important for medicine as well as biology, since many human diseases such as polycystic kidney diseases and atherosclerotic heart disease are results of defective development of tubular structures (reviewed in Lubarsky and Krasnow, 2003).

Recent discoveries reveal that many signaling molecules such as Fibroblast Growth Factor (FGF), Hedgehog (Hh), Wingless (Wnt) and Transforming Growth Factor-β (TGF-β) play similar roles in lung morphogenesis in mammals as well as in tracheogenesis in *Drosophila* (Chuang and McMahon, 2003; Metzger and Krasnow, 1999). Although these works provided considerable progress in gaining insights into complex mechanisms underlying the formation of three dimensional tubular networks, many fundamental questions remain to be answered. What dictates the epithelial cells to differentiate specifically to form particular tubes? What initiates such dramatic changes in cell shape? What guides the differentiated cells to their corresponding targets through different tissues? These questions cannot be addressed sufficiently by investigating mammalian organs because their structures are extremely complex and therefore, systematic analysis of

the genetic and cellular programs guiding their development is not possible. In contrast, *Drosophila* tracheal development provides an excellent model system to explore such crucial issues since many molecular markers and powerful tools for genetic manipulations are available. Furthermore, recent advances in real time lapse microscopy allow *in vivo* imaging of developing tracheal system and thus analysis of branching morphogenesis at a cellular resolution (Ribeiro et al., 2002). Therefore, by studying the molecular and genetic pathways involved in the development of tracheal system, tubulogenesis in other organisms can be elucidated.

1.2 Morphogenesis of embryonic *Drosophila* tracheal system

The *Drosophila* trachea follows a complex but highly stereotyped pattern, in which ten highly similar segmental units on either side of embryo undergo a similar sequence of developmental events. The ten tracheal metameres span from the second thoracic (T2) segment to the eighth abdominal (A8) segment (**Figure 1.1**). However, this localization becomes less clear later in development as tracheal branches migrate towards their target tissues and eventually fuse with each other to form a continuous three-dimensional network. The dorsal trunk (DT) is the major airway, linking each tracheal metameres and the anterior spiracle in T1 to the posterior spiracle in A8 in larva (**Figure 1.1**). A continuous lateral trunk (LT) is formed during late embryogenesis as the lateral trunk anterior (LTa) in each metameres fuse with the lateral trunk posterior (LTp). Although the LT spans approximately the same length as the DT, it is thinner and curvier (**Figure 1.2.G-H**). Both DT and LT migrate anterior-posteriorly, in parallel from each other. The transverse connective (TC), one of the dorsal-ventral branches, grows perpendicular to DT and LT and interconnects both branches (**Figure 1.1**).

From this central framework, other specific branches extend in various directions. From the DT, dorsal branches (DB) grow towards the heart and dorsal epidermis and become connected to the dorsal branches on the opposite side of the embryo through dorsal anastomosis. From the TC, visceral branches (VB) extend inward towards the gut. Ganglionic branches (GB) targeting the central nervous system (CNS) grow ventrally from the lateral trunk. From the most anterior hemisegment, the cerebral branch (CB) and pharyngeal branch (PB) grow anterodorsally. This typical structure arises during embryogenesis and persists during larval life, but it is extensively modified at

metamorphosis to form the pupal and adult tracheal system (Whitten, 1972; Manning and Krasnow, 1993).

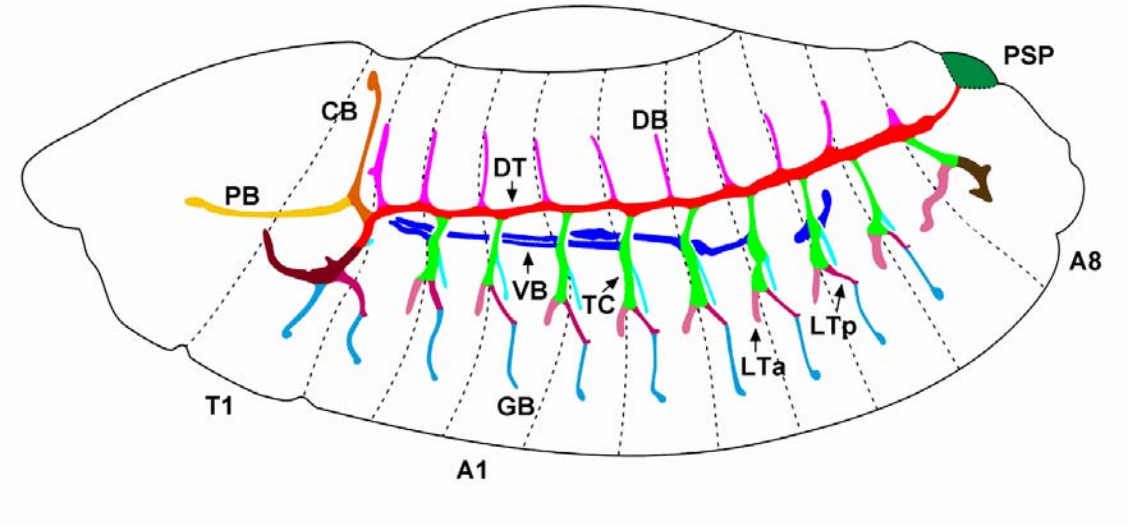

Figure 1.1. Schematic description of major branches in *Drosophila* tracheal system.
A lateral view of stage 14 embryo is shown here. CB, cerebral branch (orange); PB, pharyngeal branch (yellow); DT, dorsal trunk (red); DB, dorsal branch (pink); VB, visceral branch (blue); TC, transverse connective (green); GB, ganglionic branch (sky blue); LTa, lateral trunk anterior (light pink); LTp, lateral trunk posterior (maroon); PSP, posterior spiracle (dark green); T, thoracic segment; A, abdominal segment.

The formation of this highly complex tracheal system begins around 6 hours AEL (after egg laying) and lasts until 17 hours AEL (all embryonic stages and times are according to Campos-Ortega and Hartenstein, 1985). Each developmental stage of tracheogenesis is marked by distinct morphological events and genetic mechanisms that specify and control those events. Generally, the development of tracheal tubes in *Drosophila* can be subdivided into the following sequential stages: (1) formation of tracheal placodes (**Section 1.2.1**); (2) formation of primary branches (**Section 1.2.2**); (3) specification of individual branches (**Section 1.2.3**); (4) formation of secondary branches (**Section 1.2.4**) as well as determination of fusion cells (**Section 1.2.5**); and finally (5) formation of terminal branches (**Section 1.2.6**), which respond to various oxygen needs in target tissues (**Section 1.2.7**).

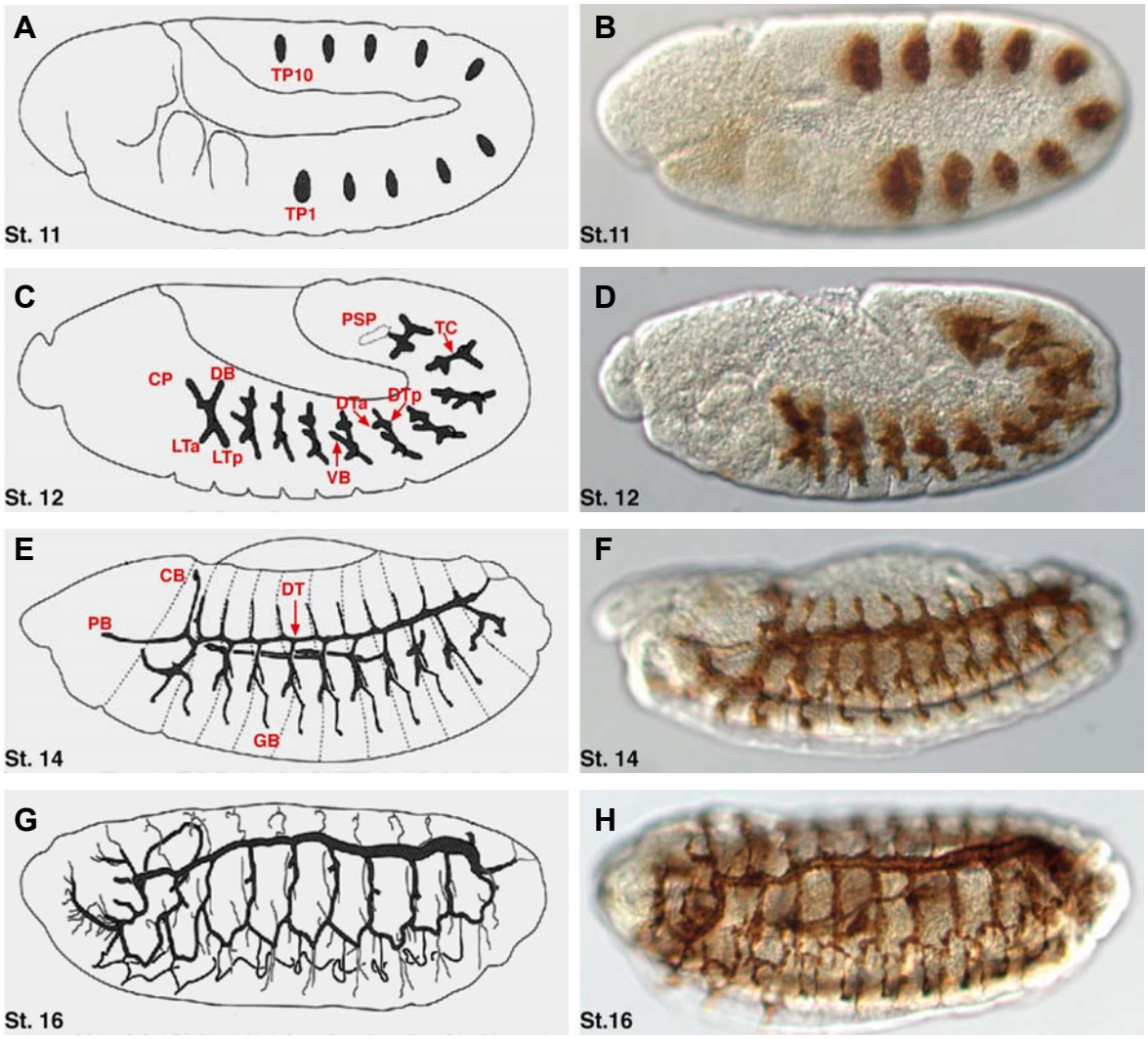

Figure 1.2. Developmental stages during embryonic tracheogenesis in *Drosophila melanogaster*.
Lateral views of the embryonic tracheal system at different stages are shown. The left panel (**A**, **C**, **E**, **G**) shows schematic illustrations of the tracheal network (modified after Manning and Krasnow, 1993). Right panel (**B**, **D**, **E**, **H**) shows tracheal system in *1-eve-1* enhancer trap line embryos at corresponding stages. The tracheal system can visualized through antibody staining with anti β-Galactosidase in *1-eve-1* enhancer trap line embryos because they contain a *lacZ* insertion within the enhancer region of *trachealess*, which is expressed in all tracheal cells throughout the tracheal development (Perrimon, 1991).
(**A**-**B**) During stage 11, ten tracheal placodes (TP1-10) on either side of the embryo can be detected.
(**C**-**D**) During stage 12, the tracheal cells start to migrate into diverse directions and form finger-like structures called primary branches consisting of cerebropharyngeal branch (CP), dorsal branch (DB), lateral trunk anterior (LTa), lateral trunk posterior (LTp), visceral branch (VB), dorsal trunk anterior (DTa), dorsal trunk posterior (DTp), and transverse connective (TC). PSP, posterior spiracle.
(**E**-**F**) By stage 14, the dorsal trunk anteriors and dorsal trunk posteriors of adjacent metameres have fused to form a continuous dorsal trunk (DT). Cerebral branch (CB), pharyngeal branch (PB), and ganglionic branch (GB) have also grown.
(**G**-**H**) Finally, during stage 16, fine terminal branches start to sprout from the interconnected tracheal branches and permeate target tissues.

Initially, between 5 and 7 hours AEL, groups of ectodermal cells in segments T2 though A8 invaginate almost completely into the underlying mesoderm to form irregularly shaped

ovoid sacs called tracheal placodes (Turner and Mahowald, 1977; Fullilove and Jacobson, 1978). In either side of the embryo, the placodes lie on the lateral surface between the amnioserosa and the midline (**Figure 1.2.A-B**). After the tracheal pits, consisting of approximately 80 ectodermal cells each, are generated, no further mitoses take place in the tracheal system until the onset of metamorphosis (Poulson, 1950; Madhavan and Schneiderman, 1977; Campos-Ortega and Hartenstein, 1985). Thus, these tracheal cells in limited number must undergo dramatic change in cell shape and size and migrate extensive distances towards their targets to accommodate the increasing body size throughout the embryogenesis.

Between 7 and 9 hours AEL, the tracheal cells start to grow out in defined directions and form a finger-like structure called the primary branch, which consists of 4 branches that grow along the anterior-posterior (A-P) axis and 3 branches along the dorso-ventral (D-V) axis (**Figure 1.2.C-D**). By 10 hours AEL, the DTa and the DTp of neighboring metameres have fused to form a continuous dorsal trunk (**Figure 1.2.E-F**).

Subsequently, all primary branches, except the dorsal trunk, give rise to finer, unicellular secondary branches. For instance, between 11 and 13 hours AEL, one secondary branch sprouts from the dorsal branch towards the dorsal midline to fuse with its counterpart from the opposite hemisegment and to interconnect the right and left side of the tracheal network.

Finally, most secondary branches generate hundreds of fine terminal branches that permeate the whole embryo (**Figure 1.2.G-H**). Terminal branches are seamless thin intracellular capillaries that enable gas diffusion in distinct cells and tissues by closely associating with the plasma membranes (Manning and Krasnow, 1993). Exquisite ramifications of single cells, which might extend more than 50μm throughout the embryogenesis, generate these intracellular tubes during terminal branching. At the onset of terminal branching, the terminal-cell nucleus remains almost stationary and the cytoplasmic extensions are adjacent to the cell nucleus (Guillemin et al., 1996; Samakovlis et al., 1996a). As terminal branching proceeds, the cytoplasmic extensions stretch away from the nucleus and the intracellular lumens are formed repeatedly, eventually permeating the whole target area.

These distinct steps during tracheal morphogenesis are associated with a particular set of genes and their products that have been identified through systematic screens for tracheal markers and mutants. In the following sections, the function of those genes as well as the

molecular pathways that regulate and mold each developmental step during tracheogenesis will be described.

1.2.1 Differentiation of ectodermal cells into tracheal cells

At the onset of tracheal morphogenesis, 20 groups of cells within lateral ectodermal cells become selected as tracheal cells to form the tracheal placode (**Figure 1.2.A-B**). For this differentiation of ectodermal cells into tracheal cells, the restricted expression of two transcriptional factors encoded by *trachealess* (*trh*) and *drifter/ventral veinless* (*dfr/vvl*) are essential (reviewed in Affolter and Shilo, 2000). Expression of *trh* can be detected specifically in tracheal precursor cells as early as about 4 hours AEL, before the tracheal placodes are formed, and therefore serve as the earliest specific marker known for the tracheal cells (Issac and Andrew, 1996; Wilk et al., 1996). Trh is a bHLH-PAS domain protein that forms a heterodimeric complex with Tango, another bHLH-PAS domain protein that is expressed more broadly (Ohshiro and Saigo, 1997; Sonnenfeld et al., 1997; Zelzer et al., 1997). On the other hand, *dfr/vvl* encodes a POU domain transcription factor that is expressed also in the tracheal precursor cells either simultaneously at or immediately after the onset of *trh* expression (Anderson et al., 1995; de Celis et al., 1995; Anderson et al., 1996; Llimargas and Casanova, 1997).

The initial function of Trh and Dfr/Vvl is to activate invagination of tracheal placodes. For example, tracheal placodes fail to invaginate completely in lack of *trh* function mutants and partially in *dfr/vvl* mutants as a target gene *rhomboid* (*rho*), a component of EGF signaling, fails to become activated (Llimargas and Casanova, 1999; Boube et al., 2000). Another essential role of Trh and Dfr/Vvl is to induce expression of various tracheal-specific genes such as *breathless* (*btl*) and *thick veins* (*tkv*) that are necessary for subsequent morphological steps (Wilk et al., 1996; Ohshiro and Saigo, 1997; Boube et al., 2000). Most likely, Trh/Tango heterodimer and Vvl cooperate in specifying the tracheal cellular fate, probably by directly interacting with each other (Zelzer and Shilo, 2000). Recently, another transcription factor encoded by *jing*, which may also be involved in determining the tracheal cell fate, was identified (Sedaghat et al., 2002)

Specific expression of *trh* and *vvl* in tracheal precursor cells seem to be crucial for inducing particular marker genes in the tracheal cells only. What initiate and/or restrict the *trh* and *vvl* expressions to particular anterior-posterior (A-P) and dorso-ventral (D-V) position within each segment? Recent studies indicate that *domeless*, which encodes an

interleukin receptor homolog, and *stat92E* encoding a transcription factor in the JAK/STAT pathway are both required to induce *trh* expression (Brown et al., 2001; Chen et al., 2002). In addition, *decapentaplegic* (*dpp*) and *wingless* (*wg*) are involved in confining *trh* and *dfr*/*vvl* expression to their corresponding A-P and D-V positions (de Celis et al., 1995; Isaac and Andrew, 1996; Wilk et al., 1996).

1.2.2 Induction of primary branches through FGF signaling pathway

During stage 12, the tracheal cells stretch in defined directions and form a finger-like primary branch (**Figure 1.2. B-C**). From the dorsal end of the transverse connective (TC), the anterior branch of the dorsal trunk (DTa), the very short posterior branch of the dorsal trunk (DTp), and the dorsal branch (DB), which appears as if it were continuation of the transverse connective, grow out. In addition, the visceral branch (VB) extends anteriorly inward towards the gut. Ventral from the transverse connective, the lateral trunk anterior (LTa) and the lateral trunk posterior (LTp) are formed.

What induces these tracheal cells to migrate in such a stereotypical pattern? Identification of *Drosophila* homologs of mammalian FGF and FGF receptors in the last decades provided an initial understanding of the complex process of primary branching. *branchless* (*bnl*) encodes the *Drosophila* FGF ligand (Sutherland et al., 1996) whereas *breathless* (*btl*) encodes the FGF receptor, a receptor tyrosine kinase (Glazer and Shilo, 1991; Klämbt et al., 1992). Prior to initiation of primary branching, the heterodimeric transcription factors Trh/Tango, together with another transcription factor Vvl, activate the expression of the FGF receptor gene *btl* in all tracheal cells. At the same time, several clusters of epidermal and mesodermal cells near the tracheal placodes start to express *bnl*, the FGF ligand. Interestingly, these small clusters of *bnl* cells are located at positions where the primary branches will grow out. When the outgrowing primary branches reach the source of FGF ligand, the expression of *bnl* in these cells disappear and the tracheal cells cease to migrate. Soon, in a more distal location, another cell cluster starts to express *bnl* and the primary branches begin to extend towards the new Bnl source. These findings demonstrate that the pattern of primary branching depends on the pattern of Bnl expression and thus, Bnl is a chemoattractant that guides primary branch outgrowth.

Recent studies have identified several additional components that are important for the function of FGF signaling in primary branch outgrowth. For example, mutations in *sugarless* (*sgl*) or *sulfateless* (*sfl*), which encode enzymes that catalyze biosynthesis of

heparan sulfate proteoglycans (HSPGs), inhibit extension of primary branches (Lin et al., 1999). Inactivation of another HSPG biosynthesis gene, *heparan sulfate 6-Osulfotransferase* (*dHS6ST*), also blocks primary branch outgrowth (Kamimura et al., 2001). These results suggest that a specific structure of HSPG may be critical for FGF signaling during primary branch formation. As HSPGs are known to function as co-receptors that build active FGF-FGF receptor complexes in FGF signaling pathways during other developmental processes (Pellegrini, 2001), it is likely that HSPGs play similar roles in FGF signaling during primary branch outgrowth.

How the signal is mediated from the activated FGF receptor Btl to the downstream targets that eventually induce tracheal cells to migrate is not clearly understood. Recent discoveries show that activation of FGF signaling induces formation of dynamic filopodia-like cellular extensions at the tip of primary branches leading to tracheal cell migration (Shim et al., 2001; Ribeiro et al., 2002; Wolf et al., 2002). This formation of filopodial protrusions might be mediated partially by activation of mitogen-activated protein kinase (MAPK) signaling components. For instance, active phosphorylated MAPK is detected in the leading cells of primary branches but is reduced in *bnl* or *btl* mutant embryos (Vincent et al., 1998). One essential downstream component known is *stumps* (*sms*), which is also called *downstream of fgf* (*dof*) or *heartbroken* (*hbr*) encoding a novel cytosolic protein containing potential docking sites for various intracellular signaling proteins (Michelson et al., 1998; Vincent et al., 1998; Imam et al., 1999). *sms* is expressed not only in the developing tracheal cells but also in the mesodermal cells. In mutant embryos lacking *sms* function, tracheal cells fail to generate filopodial extensions and thus the primary branch cannot develop. This observation and the structure of Sms protein suggest that Sms may operate as an adapter that couples exclusively FGF receptors to downstream components (Dossenbach et al., 2001).

As the leading cells of primary branches send out filopodial extensions, the remaining cell bodies start to move towards the source of Bnl and the apical cell surface grows; these processes appear to require the putative transcription factors Ribbon (Rib) and Grainyhead (Grh). In embryos lacking *rib*, the tracheal cells are able to form filopodial protrusions but cell bodies fail to move and the lumen cannot grow (Bradley and Andrew 2001; Shim et al., 2001). Similarly, when *grh* is absent, the tracheal cells migrate normally but produce excess apical membrane; as a result, elongated, convoluted tubes are formed at the end of embryogenesis (Hemphala et al., 2003).

1.2.3 Specification of individual branches through diverse signaling pathways

As primary branching continues, individual branches acquire different number of cells, grow along or through different substrates and form tubes of distinctive sizes, shapes and patterns. For example, some individual branches such as DB, GB and VB develop into narrow branches that involve substantial modulations in cell contacts and shapes and repositioning of cells into a single row, similar to intercalation of cells in epithelial sheets. In contrast, DTa and DTp branches have the largest diameter, three to ten times the size of other primary branches, and neither develop elongated cells, undergo intercalation, nor sprout new branches. Clonal analysis indicates that different domains of cells within the tracheal placode are assigned with various branch fates as soon as the tracheal placodes invaginate (Samakovlis et al., 1996a). Numerous works in the last decade show that distinctive branch fate is regulated by genes expressed in regional- and branch-specific patterns.

Ectodermal stripes, dorsal and ventral to the tracheal placode, express Dpp (member of TGFβ family), which determines branch fate in dorsal and ventral tracheal domains (Vincent et al., 1997). Dpp, which is secreted from a dorsal stripe of cells near the tracheal placode, activates its receptors Thickveins and Punt in tracheal cells, leading to phosphorylation of the transcription factor Mad (Affolter et al., 1994b; Ruberte et al., 1995; Vincent et al., 1997). Activated Mad induces expression of *knirps* (*kni*) and *knirps-related* (*knrl*), which encode partially redundant zinc-finger transcription factors, in the dorsal-most tracheal cells (Vincent et al., 1997; Chen et al., 1998). When Dpp signaling is absent, *kni* fails to be induced and formation or maintenance of DBs is disrupted; moreover, the presumptive DB cells become integrated into the DT (Vincent et al., 1997; Chen et al., 1998; Ribeiro et al., 2002). On the other hand, when the Dpp signaling pathway or its effectors *kni* and *knrl* are ectopically expressed, the DT cells are recruited into the DB (Llimargas and Casanova, 1997; Vincent et al., 1997; Chen et al., 1998).

While the transcription factors *kni* and *knrl* establish dorsal branch identity, another transcription factor Spalt (Sal) determines DT identity. In lack of *sal* mutants, DT cells assume a DB fate and consequently, the DT fails to form (Kühnlein and Schuh, 1996). Initially, *sal* is expressed in the dorsal half of the tracheal placode, containing precursor cells of DT and DB; however, its expression soon becomes restricted to DT only. This

down-regulation of *sal* in DB cells is controlled by Kni/Knrl, which most likely bind directly to an enhancer element of *sal* (Chen et al., 1998).

Localized expression of Bnl induces tracheal cell migration whereas localized expression of transcription factors, mediating various signal pathways, destine the tracheal cells to different developmental fates and establish fundamental boundaries between each branches. However, not much is known about the downstream target genes of these branch identity transcription factors. Which genes play direct roles in changing the cell shape, controlling the tube size and length, or guiding the tracheal cells through various substrates? These important downstream target genes and their respective functions remain yet to be identified and analyzed.

1.2.4 Induction and inhibition of secondary branching by FGF signaling

Similar to primary branching, secondary branching also follows a stereotypical pattern that is regulated by *bnl* and *btl* activity. However, different sets of genes involved in novel molecular mechanisms are activated. As primary branches migrate towards their targets, cells at the tip of each branch express a pantip marker gene *pointed* (*pnt*), which encodes a transcription factor (Scholz et al., 1993). Activation of FGF signaling leads to induction of *pnt* through phosphorylation and consequently, degradation of AOP/Yan, an ETS domain transcriptional repressor (Samakovlis et al., 1996a; Hacohen et al., 1998; Ohshiro et al., 2002). When *bnl* is ectopically expressed, *pnt* and other secondary and terminal branch genes throughout the tracheal system become induced, and as a result, ectopic secondary and terminal branches are produced (Lee et al., 1996; Sutherland et al., 1996). These observations indicate that almost all tracheal cells can potentially activate genes necessary to form secondary and terminal branches, which are normally restricted by localized expression of Bnl.

Interestingly, FGF signaling activates *sprouty* (*spry*) that inhibits secondary branching as well. *spry* is induced in the tracheal cells upon activation of FGF pathway and functions cell non-autonomously to stop neighboring cells from inducing secondary branch genes. When *spry* function is absent, the secondary branch genes are not inhibited anymore and form ectopic secondary and terminal branches. Spry is evolutionarily conserved and contains a novel cysteine-rich motif that antagonizes FGF and other RTK signaling pathways (Hacohen et al., 1998; Casci et al., 1999; Kramer et al., 1999; Reich et al., 1999).

1.2.5 Determination of fusion cells

Another process that is as essential as cell migration for tubular construction is branch fusion. There are approximately 50 fusion points in the tracheal network. Among the tip cells that gain secondary branch fate, two cells, one at the tip of each connecting branch, acquire a fusion cell fate and undergo a complex process of target recognition as well as intracellular tube formation (Samakovlis et al., 1996a; Tanaka-Matakatsu et al., 1996). First, the fusion cells on either side of interconnecting branches extend filopodial protrusions that come in contact with each other. This contact between two fusion partners triggers deposition of DE-cadherin and subsequently formation of a ring of DE-cadherin at the contact site. DE-cadherin, an epidermal transmembrane adhesion protein localized at adherens junctions, interacts with Armadillo (β-catenin) and Dα-catenin, which in turn binds actin filaments linking the plasma membrane to the cytoskeleton. In addition, Short Stop (Shot), a cytoskeleton-associated plakin that interacts with both actin and microtubules, is similarly distributed as DE-cadherin throughout the fusion process and is required for accumulation of DE-cadherin at the fusion cell interface (Lee and Kolodziej, 2002). Eventually, a new apical membrane appears and a new lumen is formed in each fusion cells following the rearrangement of DE-cadherin and F-actin. As the two growing lumens approach the fusion cell interface, the fusion cells contract and pull the flanking tracheal cells closer to the fusion site. Finally, the adherens ring expands to the same size as the connecting primary branches and lumens of the two fusion cells, which are attached face-to-face, fuse to form doughnut-shaped tubes.

Yet another zinc finger transcription factor Escargot (Esg) controls the fusion of tracheal branches (Samakovlis et al., 1996b; Tanaka-Matakatsu et al., 1996). *esg* is the earliest fusion specific gene known so far as its expression begins in fusion cells about 2 hours prior to the initiation of fusion process. When *esg* function is disrupted, most fusion events are inhibited and other fusion genes such as *shotgun*, *members only*, and *headcase* are not expressed (Uv et al., 2000; Steneberg et al., 1998). However, expression of *shotgun* (*shg*) in DT fusion cells and the fusion process of the dorsal trunk is only slightly affected when *esg* function is absent, suggesting that a separate mechanism might be responsible for fusion of DT cells.

Only one cell at each outgrowing primary braches is selected as a fusion cell, requiring an elaborate interplay between several signaling pathways. For example, localized expression

of Bnl and Wg in surrounding tissues seems to provide combinatorial cues that induce *esg* expression in individual cells at the tips of primary branches (Ikeya and Hayashi, 1999; Chihara and Hayashi, 2000; Llimargas, 2000). In addition, the Dpp signaling pathway triggers Delta expression in the prospective fusion cell, which in turn activates Notch but represses Esg in neighboring cells (Llimargas and Casanova, 1999; Ikeya and Hayashi, 1999; Steneberg et al., 1999; Chihara and Hayashi, 2000). This regulatory mechanism called lateral inhibition ensures that only a single cell containing the highest initial level of Esg and Delta becomes the fusion cell at the end of each primary branch.

1.2.6 Specification of terminal cells through *Drosophila* SRF

At least one gene, which is specifically expressed in the terminal cells and is required for terminal branch growth, has been identified; *blistered* (*bs*), also known as *pruned*, encodes the *Drosophila* homolog of mammalian Serum Response Factor (SRF), (Affolter et al., 1994a; Guillemin et al., 1996; Montagne et al., 1996). In embryos lacking *bs*, terminal cells undergo the initial sprouting from secondary branches, but fail to develop the intracellular tube distal to the nucleus. Together with an ETS domain protein Elk-1, a MADS domain transcription factor, SRF comprises part of transcription complex whose activity is regulated by RTK signaling and the Ras/MAPK cascade (Treisman, 1994). Consistent with this observation, FGF signaling, which plays a role in primary and secondary branching, also regulates terminal branching and induces *bs* expression in terminal cells (Reichman-Fried and Shilo, 1995; Jarecki et al., 1999; Sutherland et al., 1996). However, the downstream target genes of *bs* are not yet known.

1.2.7 Response of terminal branches to oxygen level

Unlike the primary or secondary branching, which follows a predetermined stereotypical pattern, terminal branching is highly variable readily adapting to fulfill different oxygen needs in target tissues. However, certain guidelines seem to exist as the branch points are regularly spaced and terminal branches do not cross over one another. Like in mammalian angiogenesis, low oxygen or hypoxia stimulates sprouting of terminal branches whereas high oxygen or hyperoxia suppresses them (Wigglesworth, 1954; Locke, 1958; Jarecki et al., 1999). Under hypoxia, cells secrete Bnl to attract new terminal branches even from one segment away. As secondary branches begin to bud and expressions of early terminal

branch genes start, *bnl* expression disappears; however, it turns on again several hours later when larval development begins. Which genes restart the FGF signaling during larval life and elicit complex cellular events in response to low or high oxygen level remain yet unknown. One of the possible regulators is *sima*, a *Drosophila* homolog of mammalian HIFα (Hypoxia Inducible Factor alpha subunit), which is a heterodimeric transcription factor (Nagao et al., 1996; Adryan et al., 2000; Bruick and McKnight, 2001; Lavista-Llanos et al., 2002). In the mammalian system, HIF plays central role in hypoxic response including activation of glycolytic pathway genes and angiogenic factors to restore oxygen balance or help cells to survive under low oxygen (Semenza, 2001).

1.3 Interaction between tracheal cells and surrounding substrates

During lung morphogenesis, interaction between the epithelium and its surrounding mesenchyme is the major driving force for the outgrowth of epithelial cells (Hogan et al., 1997). Recent discoveries reveal that surrounding substrates also play significant roles in guiding individual tracheal branches in their migratory paths. On one hand, localized expression of Bnl in the surrounding substrates guides tracheal branches to migrate in designated path by inducing FGF signaling in the tracheal cells. On the other hand, substrates provide particular surface properties that are distinctively identified by individual branches or physical constraints such as grooves, which shape or guide outgrowth of branches (Franch-Marro and Casanova, 2000). Recent works elucidate how visceral and ganglionic branches are distinctively guided in their specific paths through adhesion to contiguous substrate cells (**Section 1.3.1**). In particular, recent findings reveal that the interaction between dorsal trunk cells and the juxtaposing mesodermal cells called bridge-cells is essential for proper guidance of outgrowing dorsal trunk cells (**Section 1.3.2**).

1.3.1 Cell surface molecules that guide visceral and ganglionic branches

Presumably, the interaction between substrates and the tracheal cells involve cell surface molecules that mediate direct cell-to-cell contact. For example, a recent study reveals that position-specific (PS) integrins play essential roles for extension of visceral branches along the visceral mesoderm during formation of gut constriction (Boube et al., 2001). PS integrins are a class of heterodimeric molecules that consist of two transmembrane

proteins, α and β subunits. These molecules are activated by extracellular matrix (ECM) ligands to promote contacts and adhesion of cells with the matrix (Brown et al., 2000). In *Drosophila*, *multiple edematous wings* (*mew*) encodes αPS1 integrin, expressed specifically on the surface of visceral branch cells, whereas *inflated* (*if*) encodes αPS2 integrin, expressed on the surface of visceral mesoderm. Defects in either of the PS integrins lead to impaired migration of the visceral branches. However, the initial movement of visceral branch as well as formation of the terminal branch is not affected, indicating that the visceral branches can still respond to the Bnl signal.

During terminal branching, each ganglionic branch (GB) enters hemisegments of the embryonic ventral nerve cord (VNC), attracted by a cluster of *bnl*-expressing cells directly outside of CNS (Englund et al., 2002). Inside the CNS, the GB initially migrates towards the midline, but turns dorsally through the neuropil just before it crosses the midline. For this abrupt change in migration direction of the GB inside the CNS, a phylogenetically conserved axonal guidance molecule Slit (Rothberg et al., 1988) and its receptors Roundabout (Robo) (Brose et al., 1999; Kidd et al., 1998) and Roundabout 2 (Robo2) (Rajagopalan et al., 2000; Simpson et al., 2000) are required. At the CNS midline, Slit (Sli) functions as a repellent for ganglionic branches expressing Robo. In contrast, Robo2 mediates the tracheal response to Sli functioning as an attractant. Thus, ganglionic branches expressing different combinations of Robo and Robo2 receptors on the cell surface are guided by its substrate CNS that express the cell surface molecule Sli to either attract or repel the tracheal branches.

1.3.2 Bridge-cells as specific guidance for outgrowing dorsal trunk cells

Apparently, local expression of Bnl can provide the outgrowing tracheal branches with general guidance. However, previous experiments showed that other mechanisms providing specific local guidance for individual branches must exist. For example, constitutive activation of FGF signaling in lack of *bnl* function mutants restored the outgrowth of the dorsal trunk whereas it failed to generate the other primary branches (Sutherland et al., 1996). Thus, it seemed that a mechanism independent of FGF signaling provides local guidance specifically for the dorsal trunk cells. Indeed, a recent study reveals single mesodermal cells that guide exclusively the outgrowing dorsal trunk cells (Wolf and Schuh, 2000). The transcription factor Hunchback (Tautz, 1988; Hülskamp et

al., 1990) is initially expressed in the single mesodermal cells positioned posteriorly from each tracheal metamere (**Figure 1.3.A**). This cell divides once and consequently, two daughter cells are formed (**Figure 1.3.B**). While the more ventrally located daughter cell remains round in its shape and stationary in its position, the more dorsal daughter cell stretches posteriorly towards the adjacent DTa cell and interconnects the juxtaposing DTp and DTa cells in the next metamere as if it were a bridge (**Figure 1.3.C**). Thus, this dorsal daughter cell was named bridge-cell.

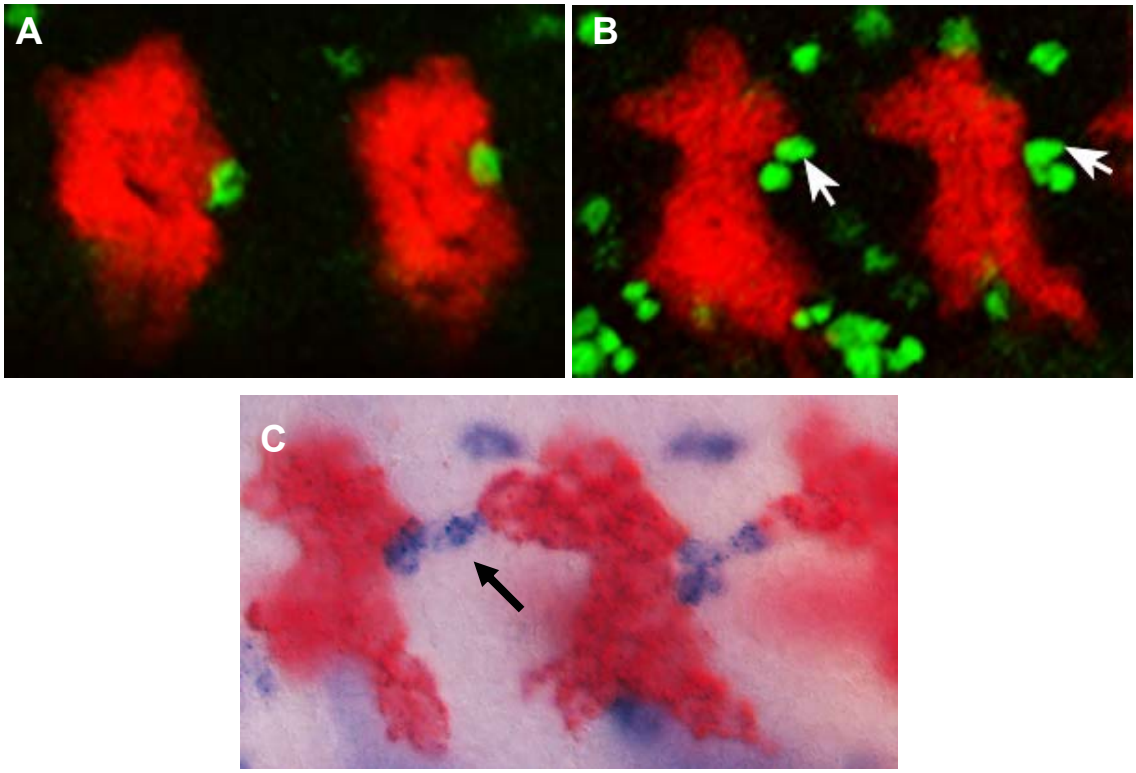

Figure 1.3. Single mesodermal cells called bridge-cells provide guidance for adjacent dorsal trunk cells.
Double antibody staining with anti-Hb (green) and anti-β-Gal (red) of *1-eve-1* embryos at stage 10 (**A**) and 11 (**B**) are shown. Hb expressing single mesodermal cells, located on the posterior lateral side of tracheal placodes, divides once and gives rise to two daughter cells: the ventral anchor cell and the dorsal bridge-cell (arrows in **B**).
(**C**) *In situ* hybridization with *hb* antisense RNA probes (blue) and antibody staining with anti-β-Gal (red) in *1-eve-1* embryos at early stage 12 are shown. Bridge-cell (arrow) stretches posteriorly and forms tight interconnection between adjacent dorsal trunk cells (Wolf and Schuh, 2000).

Hb is essential for the identity of the bridge-cell as well as for its viability. For example, cells expressing *hb* ectopically seem to acquire bridge-cell identity and attract dorsal trunk cells. As a result, dorsal trunk cells become misguided and grow in unusual directions. Conversely, in the absence of *hb*, the bridge-cells undergo apoptosis and the dorsal trunk becomes interrupted at several positions, although *bnl* expression is normal. Moreover,

lack of *bnl* function does not affect formation of bridge-cells. Therefore, general guidance provided by Bnl and local guidance by bridge-cells are independent mechanisms.

Prior to fusion, cells at the tip of the dorsal trunk send out filopodia-like protrusions and contact the bridge-cells directly. These protrusions from either of the juxtaposing dorsal trunk tip cells grow along the surface of bridge-cells until they connect with each other. Subsequently, the remaining dorsal trunk cells move along and finally undergo fusion process to generate a continuous multicellular tube. In vertebrate fibroblasts, a Rho-like GTPase Cdc42 induces filopodial extensions (Nobes and Hall, 1995; Caron and Hall, 1998). Similarly, in the *Drosophila* tracheal system, formation of filopodial cell protrusions is regulated by Cdc42 activity, which in turn is controlled by FGF signaling pathway.

For the formation of a continuous dorsal trunk, the main airway and the only multicellular tube in tracheal system, three mechanisms are important: (1) induction of primary branch migration through localized expression of Bnl: (2) extension of filopodial protrusions regulated by by FGF signaling: (3) expression of Hb in the bridge-cells, which provides specific local guidance for outgrowing dorsal trunk cells. Since Hb is a transcription factor, it is unlikely that Hb is directly involved in making a contact with the tracheal cell. Then, what kinds of molecules mediate such cell-to-cell interaction between the bridge-cell and the tracheal cell? Does such an interaction involve receptor proteins that allow communication between the tracheal cells and the bridge-cells? Or is the guidance function of the bridge-cell mediated rather by cell adhesion molecules localized on the surface? Does *hb* regulate expression of genes encoding such cell surface molecules? Identification of novel genes, which are expressed specifically in the bridge-cells, would help to obtain some answers to these questions. In addition, functional analysis of such genes would elucidate which molecular mechanisms underlie the guidance function of bridge-cell for the outgrowing dorsal trunk cells.

2 Results

2.1 *capricious* mediates the guidance function of bridge-cells.

Previous results demonstrated that the bridge-cells are specifically required for guiding the outgrowing dorsal trunk cells towards each other as they stretch posteriorly towards the adjacent DTa cells (Wolf and Schuh, 2000). These tracheal cells establish direct contact with the bridge-cells and extend along their surface (Wolf et al., 2002). Which mechanisms induce such dramatic change in the shape of bridge-cells? What kinds of molecules mediate this direct and specific contact between the bridge-cells and the tracheal cells? The only gene identified to be expressed in the bridge-cells is *hunchback* (*hb*), which encodes a transcription factor. Obviously, as a transcription regulator, Hb can hardly induce cell form change or directly bind cell surface molecules localized on the dorsal trunk cells. Rather, Hb probably activates downstream target genes that mediate such functions. Thus, in collaboration with C. Samakovlis, 2460 lethal P-element *Drosophila* strains from the Szeged Stock Center (Deak et al., 1997) were screened for reporter gene expressions in the bridge-cells.

One of the P-element lines showed expression in metamerically repeated cells that appeared to be at the presumptive bridge-cell positions. Sequencing of genomic DNA flanking the P element revealed a gene called *capricious* (*caps*). *caps* has been mapped cytologically to 70A2-3 on the third chromosome and consists of 5 exons spanning approximately 40 kb (Shishido et al., 1998; Milan et al., 2001). Exon 5 contains the open reading frame encoding a transmembrane protein with 14 Leucine-rich-repeat (LRR) motifs in the extracellular domain (Shishido et al., 1998). These LRR motifs are often found in cell adhesion molecules that are expressed on the cell surface and may mediate cell-to-cell interactions (Kobe and Deisenhofer, 1994). Previous works showed that Caps, which is localized on the cell surface as well, affects the target specificity of muscle 12 motorneurons during innervation of motorneurons in larva (Shishido et al., 1998). It also contributes to affinity boundary formation of between the dorsal and ventral compartments during wing development (Milan et al., 2001). These observations suggested that Caps might be a cell adhesion molecule interacting specifically with other cell surface molecules to mediate its functions. Possibly, *caps* is one of the downstream target genes of Hb and

may act as a cell adhesion molecule mediating the function of bridge-cells in guiding the outgrowing dorsal trunk cells.

2.1.1 *capricious* is specifically expressed in the bridge-cells.

Previously, analysis of the enhancer trap line (E2-3-27) containing *lacZ* reporter gene within *caps* genomic sequence revealed that *caps* is expressed in four dorsal (1, 2, 9, and 10) and six ventral (12, 14 to 17, and 28) muscles as well as in motorneurons aCC, RP2, RP5, and the most medial U, which all innervate muscles that express *caps* (Shishido et al., 1998). However, expression pattern of *caps* during early embryogenesis was not shown. Thus, the early expression of *caps* was investigated through *in situ* hybridization with *caps* antisense RNA probes in OreR wild-type embryos.

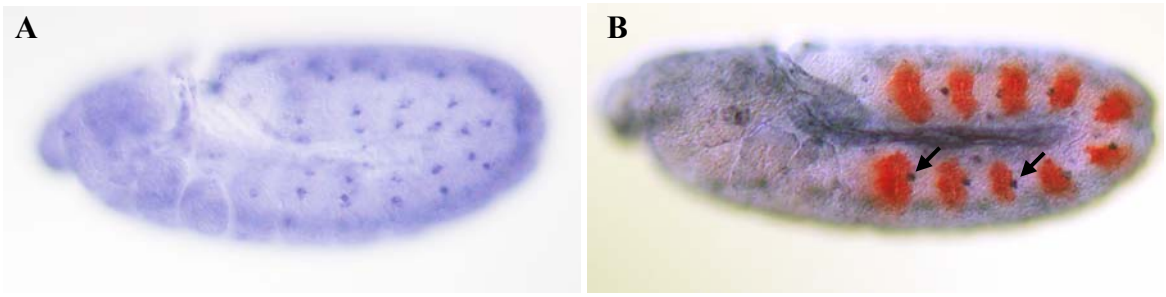

Figure 2.1. *caps* is expressed in metamerically repeated cells at presumptive bridge-cell positions.
A. Wild-type (OreR) embryos were hybridized *in situ* with *caps* antisense RNA probes. A stage 10 embryo shows specific expression of *caps* in metamerically repeated cells on the lateral side of embryo.
B. *1-eve-1* enhancer trap line embryos were stained with anti-β-Gal antibody (red) to visualize the tracheal cells. Simultaneously, the embryos were hybridized *in situ* with *caps* antisense RNA probes (blue). A stage 10 embryo reveals that *caps* expressing cells (arrows) are directly adjacent to the posterior lateral side of each tracheal metamere.

During stage 10, *caps* expression appears in metamerically repeated single cells (**Figure 2.1.A**). This expression pattern looks quite similar to *hb* expression in mesodermal cells during the primary branching of tracheal system. In addition, visualization of *caps* expressing cells and the tracheal cells reveal *caps* expression specifically in the single cells that are positioned on the posterior lateral side of each tracheal metamere (**Figure 2.1.B**). Notably, the bridge-cells are also located in such pattern and possibly, those single cells expressing *caps* might be the bridge-cells.

During stage 11, a single mesodermal cell divides once to give rise to a dorsal bridge-cell and a ventral anchor-cell. *hb* is expressed in both cells and thus serves as a marker for the anchor-cell as well as the bridge-cell (**Figure 2.2**). Earlier work demonstrated that *lacZ*

expression in *caps-lacZ* enhancer trap line containing nuclear *lacZ* is identical to the expression pattern of endogenous *caps* (Shishido et al., 1998). In order to verify that the metamerically repeated cells expressing *caps* are indeed the bridge-cells, *caps-lacZ* embryos were fluorescently stained with anti-Hb antibody to label the bridge-cells and anti-β-Gal antibody to visualize *caps* expression.

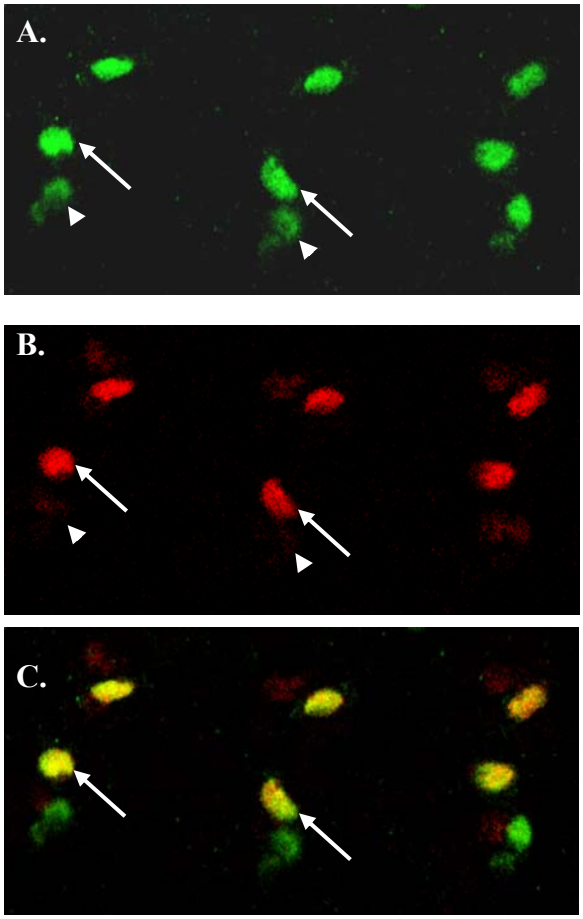

Figure 2.2. Caps co-localizes with Hb specifically in the bridge-cells but not in the anchor-cells.
caps-lacZ enhancer trap line embryos were stained with anti-β-Gal (red) and anti-Hb (green) antibodies.
A. A stage12 embryo shows Hb expression in the bridge-cells (arrows) and the more ventral anchor-cells (arrowheads).
B. The same embryo shows Caps expression in the bridge-cells (arrows) but not in the anchor-cells (arrowheads).
C. The overlay of green and red channels reveals co-localization of Caps and Hb exclusively in the bridge-cells (arrows) and the cells lying more dorsally.

Co-localization of *lacZ* and *hb* can be clearly seen in the bridge-cells and the cells located more dorsally (**Figure 2.2.C**). This result confirms that *caps* expressing cells, which associate with the tracheal metameres, are indeed the bridge-cells. However, there is a striking discrepancy between *hb* and *caps* expressions. Surprisingly, whereas *hb* is induced both in the bridge-cells and the sibling anchor-cells, *caps* is expressed exclusively in the bridge-cells (compare **Figure 2.2.A** and **B**).

2.1.2 Hb requires a co-factor for *caps* activation.

As *caps* and *hb* are both expressed in the bridge-cells, *caps* might be a direct downstream target of Hb and its expression may depend on the activity of Hb. In such a case, ectopic expression of *hb* would result in ectopic induction of *caps* expression as well. To analyze if *hb* regulates *caps* expression, *hb* was misexpressed in the tracheal cells using *btl-GAL4* driver, which induces expression in all tracheal cells throughout the tracheal development (Shiga et al., 1996). Since the tracheal cells normally do not contain *caps* expression, any induction of *caps* in the tracheal cells would be solely due to ectopic *hb* function. *In situ* hybridization with *caps* RNA probes in embryos carrying *btl-GAL4* and *UAS-hb* reveal that ectopic *hb* in the tracheal cells cannot induce *caps* expression (**Figure 2.3.A**). Although endogenous expression of *caps* in the bridge-cells and the dorsal cells are present, no ectopic *caps* expression can be observed in the tracheal cells. This result reveals evidently that *hb* alone cannot induce *caps*.

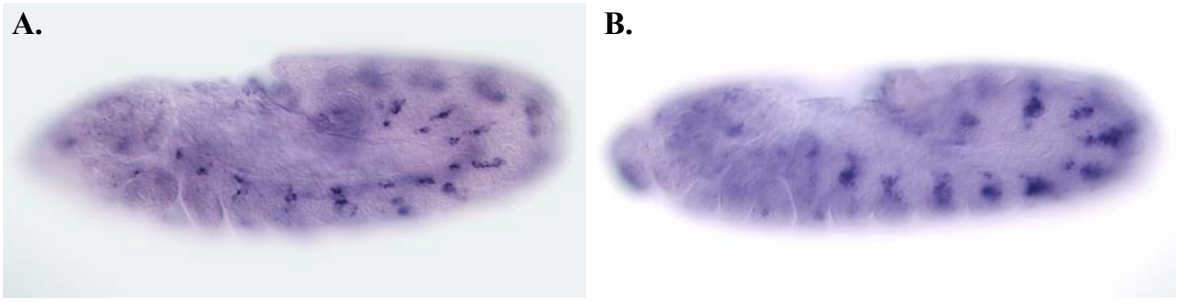

Figure 2.3. Ectopic *hb* in the mesodermal cells can induce ectopic expression of *caps*.
Stage 11 embryos containing *UAS-hb*, which is ectopically expressed either in all tracheal cells through *btl-GAL4* (**A**) or in the mesodermal cells through *twi-GAL4* (**B**), are shown. In both embryos, *caps* expression is labeled through *in situ* hybridization with *caps* antisense RNA probes.
A. Even though endogenous *caps* can be detected in the bridge-cells and the cells lying more dorsally, no ectopic *caps* is observed in the tracheal cells.
B. Ectopic expression of *caps* can be seen in the broad patch of mesodermal cells.

Notably, *caps* is expressed only in the bridge-cells whereas *hb* is found both in the bridge-cells and the anchor-cells (**Figure 2.2**). Thus, it is unlikely that the distinctive expression of *caps* in the bridge-cells depends solely on *hb* activity. Probably, *hb* requires another co-factor for specific expression of *caps* in the bridge-cells. Since the bridge-cells are of mesodermal origin, this unidentified co-factor might be found explicitly in the mesodermal cells. Therefore, it was investigated whether ectopic *hb* in the mesodermal cells can induce ectopic *caps*. A mesodermal driver line *twi-GAL4* was used in order to generate misexpression of *hb* in the mesodermal cells (Greig and Akam, 1993). When *hb* is induced

in the mesodermal cells, then ectopic *caps* expression can be detected in the mesodermal cells (**Figure 2.3.B**). Whereas *hb* fails to activate *caps* in the tracheal cells, it can elicit ectopic expression of *caps* in a subset of mesodermal cells. These findings suggest that *hb* alone is not sufficient to activate transcription of *caps* and requires a mesodermal specific co-activator.

2.1.3 Lack of *caps* function results in disrupted dorsal trunk formation.

In *hb* mutant embryos lacking the bridge-cells, the outgrowth of dorsal trunk cells towards their adjacent targets is impaired and as a result, a discontinuous dorsal trunk is formed (Wolf and Schuh, 2000). Since *caps* is very specifically expressed in the bridge-cells similar to *hb*, the next obvious question is if *caps* mutant embryos reveal an analogous tracheal defect to that found in *hb* mutant embryos. *caps* loss-of-function mutant allele ($caps^{65.2}$), which lacks the first exon and does not express Caps protein (Shishido et al., 1998), was first balanced with *ftz-lacZ* to enable unambiguous identification of homozygous mutant embryos. Similarly as in *hb* mutant embryos, the outgrowth of dorsal trunk cells is disrupted at several positions and consequently, a discontinuous dorsal trunk is formed in $caps^{65.2}$ mutant embryos (**Figure 2.4**). Moreover, as seen in *hb* mutants, the development of lateral trunk and other tracheal branches is not significantly affected.

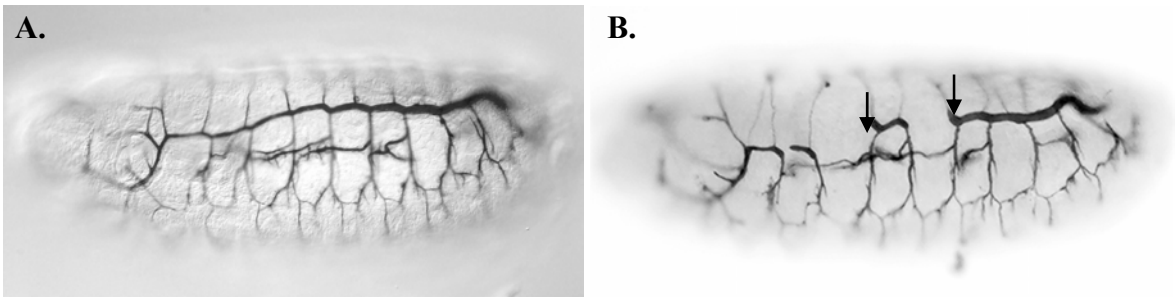

Figure 2.4. Dorsal trunk is interrupted at several positions in $caps^{65.2}$ mutant embryos.
Wild-type (**A**) or *caps* loss-of-function mutant allele, $caps^{65.2}$, embryos (**B**) were stained with the 2A12 antibody to visualize tracheal lumen.
A. A wild-type embryo at stage 14 shows continuous dorsal trunk.
B. In contrast, a whole-mount $caps^{65.2}$embryo at stage 14 reveals gaps in the dorsal trunk at several positions (arrows). Other tracheal branches appear to be as in wild-type embryos.

When the tracheal defects in $caps^{65.2}$ mutant embryos were analyzed, a significant variation in the severity of the phenotypes between embryos at early stages and at late stages was noticed. Early stages are defined as stages before the lateral trunk fusion takes place, i.e. stage 10 to stage 13. On the other hand, late stages represent developmental stages at and

after the fusion of lateral trunk, i.e. stage 14 and later. In order to measure quantitatively the variations between the tracheal phenotypes of *caps*$^{65.2}$ mutant embryos at early and late stages, interruptions in the dorsal trunks and the lateral trunks were counted and represented as percentage of total possible fusion points.

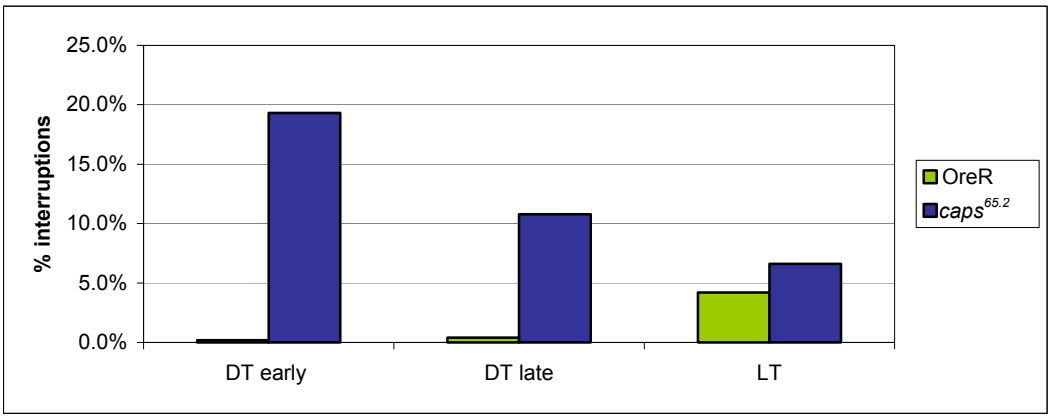

Figure 2.5. Chart showing percentage of interruptions in tracheal branches of *caps*$^{65.2}$ mutant embryos.
Interruptions of fusion points were counted for the dorsal trunks in early and late stage embryos and for the lateral trunks. There are 18 fusion points each for a dorsal trunk and a lateral trunk in an embryo. Early stage is defined as stages between10 and 13. Late stage is defined as stage 14 and later.
DT early = dorsal trunk in early stage embryos; DT late = dorsal trunk in late stage embryos; LT = lateral trunk.
For OreR (wild-type) embryos, the values are as following: DT early = 0.2% (N=1260), DT late = 0.4% (N=1224), LT=4.2% (N=936)
For homozygous *caps*$^{65.2}$ mutant embryos, the values are as following: DT early = 19.3% (N=1278), DT late =10.8 % (N=1782), LT = 6.6% (N=684)
N = total number of fusion points counted.

While *caps*$^{65.2}$ mutant embryos at early stages show 19.3% interruptions in the dorsal trunks, embryos at late stages show 10.8%, which is only half as many as the interruptions observed in embryos at early stages (**Figure 2.5**). In comparison, wild-type (OreR) embryos show 0.2% and 0.4% interruptions in the dorsal trunk at early and late stages, respectively. Although interruptions in the dorsal trunk, which is the only multicellular tracheal branch, are extremely rare in wild-type (OreR) embryos, interruptions in the lateral trunk seem to be more frequent. Possibly, the unicellular lateral trunk is not required to be perfectly continuous for the tracheal system to function properly. As interruptions in the lateral trunk of *caps*$^{65.2}$ mutant embryos (6.6%) is comparable to interruptions in the lateral trunk of wild-type (OreR) embryos (4.2%), the development of the lateral trunk does not appear to be affected significantly in *caps*$^{65.2}$ mutant embryos.

2.1.4 The bridge-cells cannot stretch properly when *caps* is lacking.

Lack of *hb* function results in lack of bridge-cells, which guide the outgrowing dorsal trunk cells, and consequently, a discontinuous dorsal trunk is formed (Wolf and Schuh, 2000). Similarly, when *caps* is absent, formation of continuous dorsal trunk is also inhibited. Is this tracheal defect like that seen with *hb* mutants a subsequent consequence of lacking bridge-cells? In order to determine if the bridge-cells are viable when *caps* function is absent, $caps^{65.2}$ mutant embryos were stained with anti-Hb antibody. Hb expression can be clearly observed in the bridge-cells as well as the anchor-cells, demonstrating that the bridge-cells are still viable in the absence of *caps* expression (**Figure 2.6**). Thus, the formation of discontinuous dorsal trunk in $caps^{65.2}$ mutant embryos is not due to the lost bridge-cells.

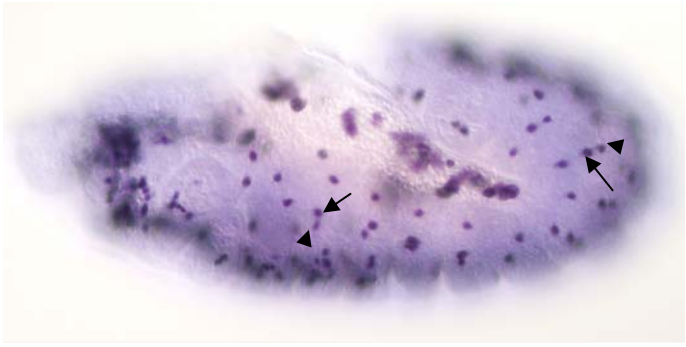

Figure 2.6. Viability of the bridge-cells is not affected when *caps* function is absent.
$caps^{65.2}$ mutant embryos were stained with anti-Hb antibody to label the bridge-cells. A stage 12 embryo reveals *hb* expression in the bridge-cells (arrows) as well as the anchor-cells (arrowheads), similarly as in the wild-type embryos.

Immediately prior to interconnection of juxtaposing dorsal trunk cells, the bridge-cells stretch posteriorly towards adjacent tracheal metameres (Wolf and Schuh, 2000). To investigate whether the bridge-cells are able to stretch properly in the absence of *caps* function, the bridge-cells and the tracheal cells were labeled fluorescently in $caps^{65.2}$ mutant embryos. Although some bridge-cells extend posteriorly to contact the adjacent dorsal trunk cells, other bridge-cells fail to do so and remain in their initial round form (**Figure 2.7**). This observation suggests that one of *caps* functions is to regulate the cell shape change in the bridge-cells so that they can stretch and interconnect the dorsal trunk cells.

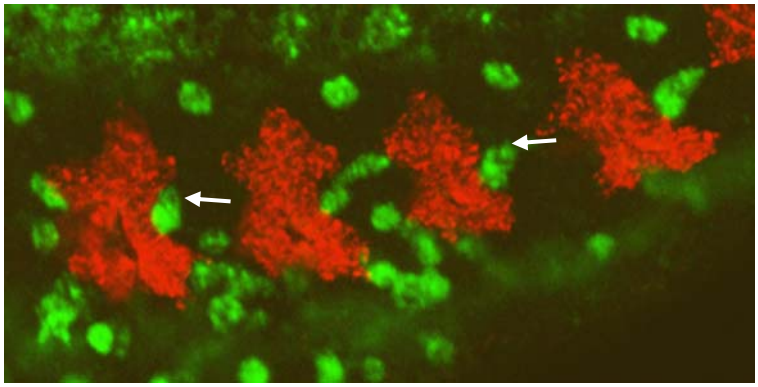

Figure 2.7. The bridge-cells cannot extend properly towards the dorsal trunk cells when *caps* is lacking.
caps$^{65.2}$ mutant embryos were hybridized *in situ* with *hb* antisense RNA probes (green) to label the bridge-cells and with *btl* antisense RNA probes (red) to label the tracheal cells. Tracheal metameres 1-4 in a stage 12 embryo are shown. Some bridge-cells (arrows) fail to stretch towards the adjacent dorsal trunk cells and remain round in their form

2.1.5 Misexpression of *caps* inhibits proper outgrowth of tracheal branches.

While loss of *caps* function resulted in unusual innervation of nerve terminal into a neighboring *caps*-negative muscle, ectopic overexpression of *caps* in all embryonic muscles caused formation of more ectopic synapses (Shishido et al., 1998). Therefore, both lack and gain of *caps* function are involved in specific motorneurons forming synaptic endings in non-target muscles. The previous section described that a lack of *caps* function resulted in discontinuous dorsal trunks. How would then ectopic *caps* function affect the tracheal formation? By misexpressing *caps* in the mesodermal cells, which normally do not express *caps*, the effect of ectopic *caps* on the formation of tracheal branches was investigated

To drive *caps* expression ectopically in the mesoderm, the *twi-GAL4* construct, which drives expression in the mesodermal primordium starting at stage 7 as the embryo gastrulates until at least stage 12 when the germ band retracts, was used (Baylies et al., 1995). Since the bridge-cells are of mesodermal origin, *twi-GAL4* may drive ectopic expression in the bridge-cells as well. In order to analyze in detail whether *twi* drives the expression in the bridge-cells, co-localization of *lacZ* and *hb* in the bridge-cells was determined in the embryos carrying *UAS-lacZ* driven by *twi-GAL4*.

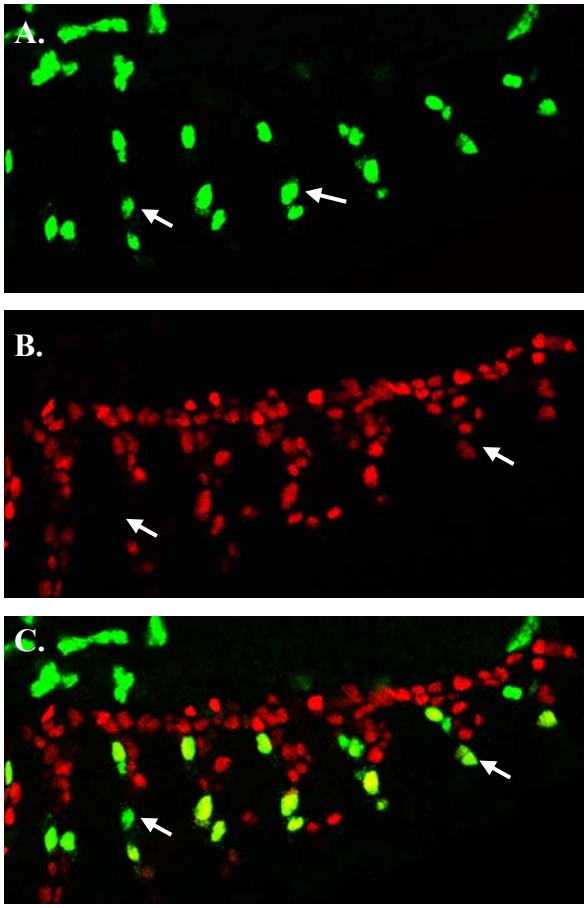

Figure 2.8. *twi* drives expression in the bridge-cells transiently and partially.
Embryos bearing *twi-GAL4* and *UAS-lacZ* were fluorescently labeled with anti-β-Gal (red) and anti-Hb (green) antibodies.
A. A stage 12 embryo reveals normal *hb* expression in the bridge-cells (arrows). The first 7 tracheal metameres are shown.
B. The same embryo reveals that either very weak or no expression of *lacZ* can be observed in the bridge-cells (arrows).
C. An overlay of green and red channel demonstrates that *hb* and *lacZ* do not consistently co-localize in the bridge-cells (arrows).

Even though *twi* drives expression broadly in the mesodermal cells, it does not seem to induce ectopic expression in the bridge-cells consistently. Whereas endogenous *hb* is expressed in the bridge-cells (**Figure 2.8.A**), *lacZ* expression driven by *twi-GAL4* cannot be detected in most bridge-cells (**Figure 2.8.B**). Lack of clear co-localization of *lacZ* and *hb* indicates that *twi-GAL4* does not consistently induce *lacZ* expression in the bridge-cells (**Figure 2.8.C**). Nevertheless, *twi-GAL4* activates expression generally in other mesodermal cells and therefore, is used as the mesodermal driver throughout this thesis.

When *caps* is ectopically expressed in the mesodermal cells through *twi-GAL4*, the outgrowth of dorsal trunk cells is impaired and as a result, the dorsal trunk becomes discontinuous (**Figure 2.9.A**). Usually, dorsal trunk cells extend anterior-posteriorly in a relatively straight line towards their adjacent targets so that a continuous linear tube can be formed. Interestingly, in embryos misexpressing *caps*, some of dorsal trunk cells seem to become disoriented and grow in wrong directions, for example, towards dorsal (**Figure 2.9.A**). This observation indicates that one of Caps function might be to provide the

outgrowing dorsal trunk cells with guidance signal so that they can extend anteriorly towards their adjacent fusion partners.

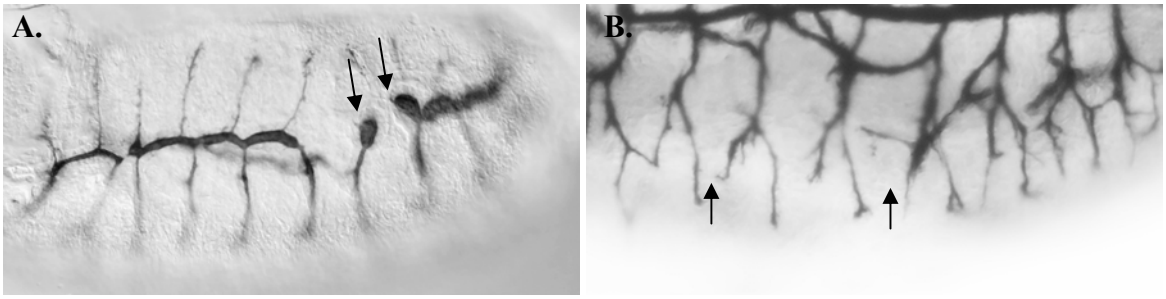

Figure 2.9. Tracheal branches are disrupted in the embryos misexpressing *caps* in mesodermal cells.
Embryos carrying *UAS-caps* and *twi-GAL4* were stained with the 2A12 antibody to visualize the tracheal lumen.
A. Whole-mount embryo at stage 13 shows dorsal trunk that is interrupted at several fusion points. In addition, some of the dorsal trunk cells extend in ectopic directions (arrows) instead of towards the adjacent targets.
B. Whole-mount embryo at stage 15 reveals that not only the dorsal trunk but also the lateral trunk is discontinuous (arrows point to the interruptions in the lateral trunk).

In contrast to lack of *caps* function, ectopic *caps* expression in mesoderm affects the outgrowth of another anterior-posterior branch, the lateral trunk. As found with the dorsal trunk cells, some lateral trunk cells also seem to be incapable of finding their targets properly in order to fuse with each other and form a continuous lateral trunk.

As the phenotype caused by ectopic expression of *caps* was variable in its severity, the interruptions in dorsal trunks and lateral trunks were counted to compare the phenotypes more quantitatively. To verify that the defective tracheal system observed in embryos misexpressing *caps* is not a general effect of *twi-GAL4* driver line, tracheal development in embryos carrying *UAS-lacZ* and *twi-GAL4* were also analyzed. Since *lacZ* is not endogenous to *Drosophila*, overexpression of *lacZ* should not affect any developmental morphogenesis in *Drosophila*. However, overexpression of *lacZ* by *twi-GAL4* causes 3.7% and 0.8% interruptions in dorsal trunk at early stages (stage 11-13) and late stages (stage 14-16), respectively (**Figure 2.10**). The effect on lateral trunk development is even stronger as 5.8% of fusion points are disrupted. This observation shows that under an artificial genetic condition, such as misexpression of bacterial *lacZ*, the development of tracheal system is affected to small extent during embryogenesis, even when the gene has no explicit function during the tracheal morphogenesis. Nevertheless, the percentage of interruptions in dorsal trunks and lateral trunks observed in embryos misexpressing *caps* is significantly higher than in embryos misexpressing *lacZ*. Therefore, ectopic expression of

caps in the mesodermal cells seems to significantly influence the outgrowth of anterior-posterior tracheal branches.

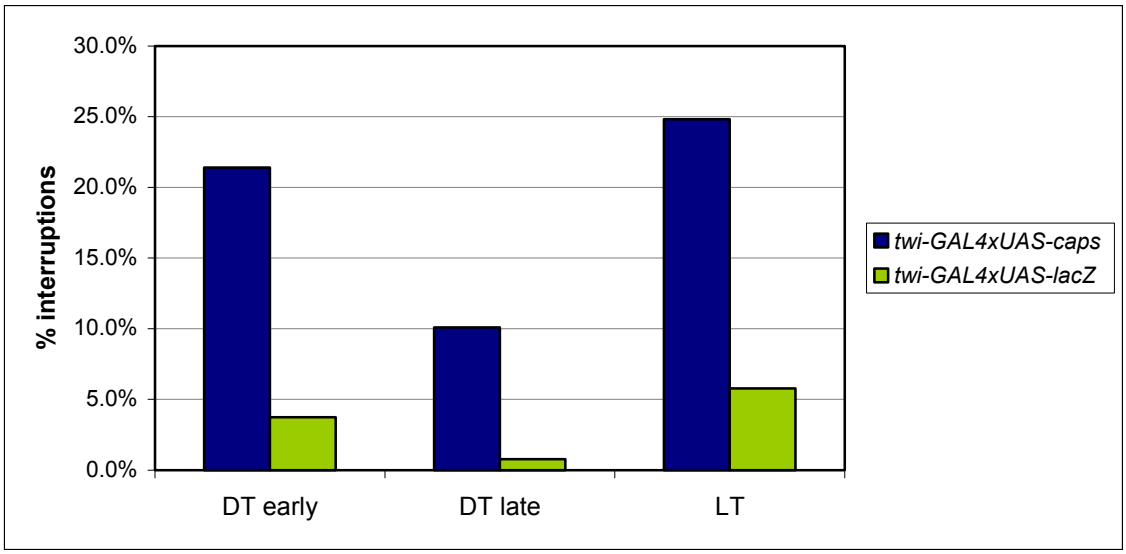

Figure 2.10. Chart showing percentage of interruptions in dorsal and lateral trunks of embryos overexpressing *caps* in the mesodermal cells.
Interruptions of fusion points were counted for the dorsal trunks in embryos at early and late stages and for the lateral trunks.
DT early = dorsal trunk in early stage embryos; DT late = dorsal trunk in late stage embryos; LT = lateral trunk.
For embryos bearing *twi-GAL4* and *UAS-caps*, the values are as following: DT early = 21.4% (N=990), DT late = 10.1% (N=1170), LT=24.5% (N=954)
For embryos bearing *twi-GAL4* and *UAS-lacZ*, the values are as following: DT early = 3.7% (N=990), DT late = 0.8 % (N=900), LT = 5.8% (N=900)
N = total number of fusion points counted.

2.1.6 Ectopic *caps* induces tracheal cells to extend in abnormal directions.

When *caps* is misexpressed in the mesodermal cells, some dorsal trunk cells grow dorsally or ventrally instead of anteriorly towards the juxtaposing tracheal metameres (**Figure 2.9.A**). The extending dorsal trunk cells follow the guidance signal provided by ectopic *caps* in the nearby mesodermal cell rather than by endogenous *caps* in the bridge-cells. In order to investigate whether ectopic expression of *caps* is the reason why some tracheal cells extend in anomalous directions, the outgrowth of tracheal cells in embryos carrying *twi-GAL4* and *UAS-caps* was analyzed through fluorescent labeling of *caps* and the tracheal cells.

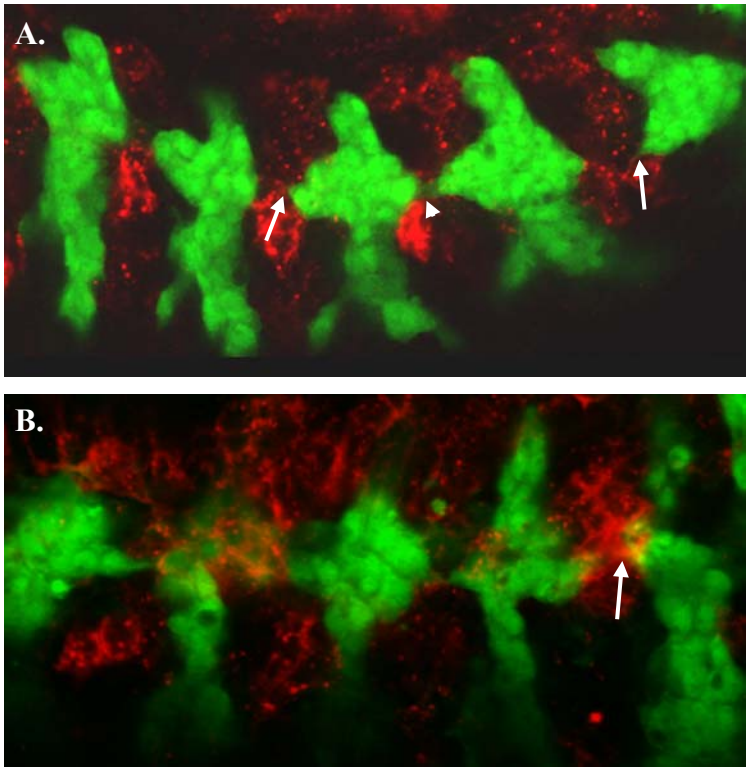

Figure 2.11. Ectopic *caps* in the mesodermal cells affects the outgrowth of tracheal cells.
Double fluorescent antibody staining with anti-Caps (red) and anti-β-Gal (green) antibodies were performed in embryos bearing *twi-GAL4*, *UAS-caps* and *1-eve-1* enhancer trap allele.
A. A stage 12 embryo reveals that some dorsal trunk cells (arrows) extend towards the mesodermal cells expressing ectopic *caps* and make contact with those cells whereas some grow along the bridge-cells (arrowhead).
B. During stage 13, when endogenous *caps* is no longer expressed in the bridge-cells but ectopic *caps* expression in other mesodermal cells persists, some dorsal trunk cells (arrow) grow towards these *caps* expressing cells and thus cannot fuse with the adjacent target metameres.

Although some dorsal trunk cells grow normally along the bridge-cells towards the neighboring tracheal metameres, some dorsal trunk cells contact instead other mesodermal cells ectopically expressing *caps* (**Figure 2.11.A**). While the dorsal trunk cells stretching along the bridge-cells interconnect with each other, other dorsal trunk cells contacting ectopic Caps appear to be either delayed or inhibited to join each other. Consequently, a disconnected dorsal trunk is formed. During stage 13, the bridge-cells disappear and the dorsal trunk cells fuse with each other to form a linear and continuous dorsal trunk. However, upon continual induction of ectopic *caps* in the mesodermal cells, some tracheal cells maintain contact with the mesodermal cells rather than with the tracheal cells (**Figure 2.11.B**). Again, these anomalous attractions of tracheal cells towards Caps result in discontinuous dorsal and lateral trunks with interruptions at several positions. Thus, it seems that the tracheal cells become disoriented and cannot find their fusion targets efficiently when cells other than the bridge-cells express *caps*. These observations indicate

that ectopic Caps misguides the outgrowing dorsal trunk cells in abnormal directions so that the dorsal trunk cells fail to locate their corresponding fusion partners properly.

2.1.7 Caps requires intracellular and extracellular domains for ectopic function.

Previous studies of Caps function in boundary formation during wing disc morphogenesis revealed that Caps requires only its extracellular domain for its function (Milan et al., 2002). Would Caps operate analogously during tracheal morphogenesis? Is the extracellular domain sufficient to mediate the function of Caps in the bridge-cells? To determine which of the two domains is essential for Caps function, two deletion constructs containing either the extracellular domain or the intracellular domain were misexpressed in the mesodermal cells and their effects on the tracheal development were analyzed.

UAS-caps^{Ed} contains the amino terminal 470 amino acids of Caps without the intracellular domain under *UAS* promoter. Conversely, *UAS-caps*^{Id} contains the amino terminal 71 amino acids, which include the signal peptide, fused to amino acid sequence 450-532 that encodes the transmembrane domain and the C-terminal intracellular domain. As a result, *UAS- caps*^{Id} lacks the region extending from the second LRR domain to the amino acid just before the transmembrane domain (Taniguchi et al., 2000). Both constructs were designed so that they would be correctly localized to the membrane, where Caps is normally expressed. These deletion constructs of Caps were overexpressed in the mesodermal cells using *twi-GAL4*. In order to compare the resulting tracheal phenotypes quantitatively, the interruptions in the dorsal trunks of early and late stage embryos and in the lateral trunks were counted.

Surprisingly, when either the extracellular or the intracellular domain is lacking, Caps can no longer influence the development of tracheal system. For example, while the misexpression of complete Caps in the mesodermal cells resulted in 21.4% interruptions in the dorsal trunk of early stage embryos, only 3.7% or 3.3% interruptions were observed in the embryos misexpressing either the extracellular domain (Ed) or the intracellular domain (Id) of Caps, respectively (**Figure 2.12**). As these low values are comparable to the reference values observed in the embryos misexpressing *UAS-lacZ*, the tracheal system appears to be normal in the embryos misexpressing either *UAS-caps*^{Ed} or *UAS-caps*^{Id}. This significant contrast in the tracheal phenotypes between the embryos overexpressing whole

Caps and only certain domains of Caps indicates that both extracellular and intracellular domains are required for Caps function during tracheal morphogenesis.

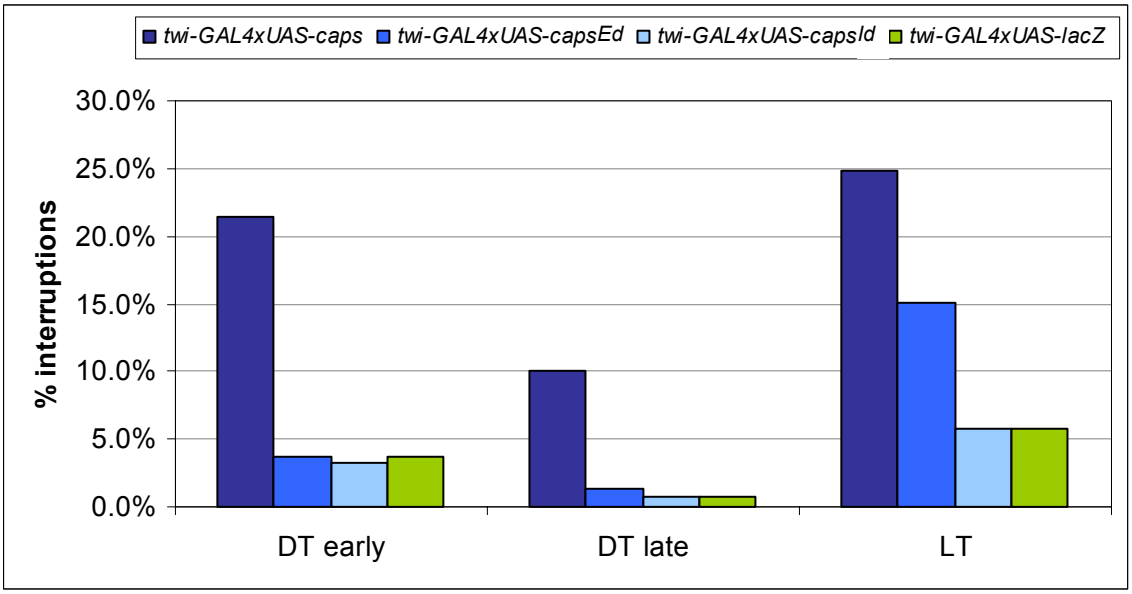

Figure 2.12. **Chart showing percentage of interruptions in dorsal and lateral trunks of embryos misexpressing *caps* deletion constructs**.
Interruptions of fusion points were counted for the dorsal trunks in embryos at early and late stages and for the lateral trunks.
DT early = dorsal trunk in early stage embryos; DT late = dorsal trunk in late stage embryos; LT = lateral trunk.
For embryos bearing *twi-GAL4* and *UAS-caps*, the values are as following: DT early = 21.4% (N=990), DT late = 10.1% (N=1170), LT=24.5% (N=954)
For embryos bearing *twi-GAL4* and *UAS-caps^{Ed}*, the values are as following: DT early = 3.7% (N=900), DT late = 1.4% (N=954), LT=15.1% (N=918)
For embryos bearing *twi-GAL4* and *UAS-caps^{Id}*, the values are as following: DT early = 3.3% (N=954), DT late = 0.7 % (N=954), LT = 5.8% (N=936)
For embryos bearing *twi-GAL4* and *UAS-lacZ*, the values are as following: DT early = 3.7% (N=990), DT late = 0.8 % (N=900), LT = 5.8% (N=900)
N = total number of fusion points counted.

2.2 Mesodermal *tartan* affects outgrowth of dorsal and lateral trunk.

Caps is most closely related to another cell adhesion molecule Tartan (Trn) in *Drosophila* (Shishido et al., 1998). Using the lalign program (Myers and Miller, 1989), Caps and Trn amino acid sequences were aligned against each other (**Figure 2.13**). Overall, Caps and Trn share 43.1% identity throughout the whole sequences. Surprisingly, most amino acid residues comprising the extracellular domains and the transmembrane domains in Caps and Trn are either similar or identical. The alignment reveals that while the extracellular and transmembrane domains of Caps and Trn are almost identical, the intracellular domains are

distinct. Caps intracellular domain is significantly smaller than Trn intracellular domain and shares few identical amino acid residues.

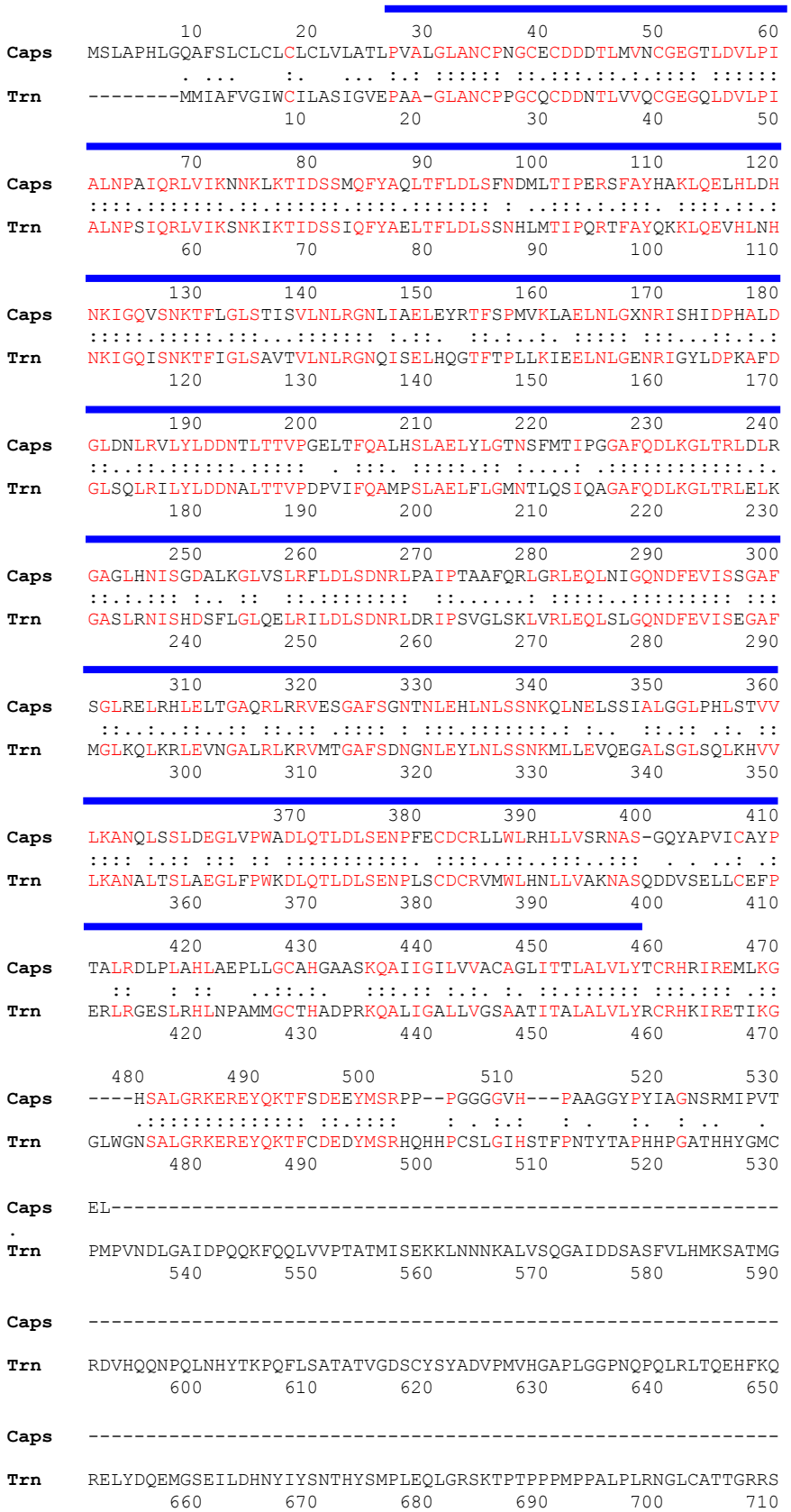

```
Caps    ----------------------

Trn     FQQKSASQKQQQNNNTLRQFTH
                720       730
```

Figure 2.13. Trn containing 14 LRRs in the extracellular domain is most similar to Caps.
Caps protein sequence was aligned against Trn protein sequence using the lalign program. The numbers indicate the positions of amino acid residues. Identical residues are highlighted in red letters and are marked by (**:**). In addition, similar residues are marked by (**.**). Overall, Caps and Trn share 43.1% identity throughout the whole sequences. Most amino acid residues comprising the extracellular and transmembrane domains of Caps and Trn are either similar or identical. In contrast, the intracellular domains reveal low similarity. Blue bars above the sequences denote the extracellular and transmembrane domains.

2.2.1 Lack of *trn* disrupts outgrowth of dorsal and lateral trunk.

It was shown that proteins, which are highly similar in their primary sequences, often carry out redundant functions in certain mechanisms (Chen et al., 1998; Boutros et al., 2000; Reim et al., 2003). The striking similarity in the extracellular and the transmembrane domains between Caps and Trn raised the question whether they could substitute for each other in their respective functions. Although it was not investigated if Caps function in pathfinding of motorneurons could be replaced by Trn function, it was demonstrated that Caps and Trn share redundant function in the formation of the affinity boundary between dorsal and ventral compartments during wing imaginal disc development (Milan et al., 2001). Although clones of cells mutant for either only *caps* or *trn* had no effects for the wing disc development, clones of cells double mutant for *caps* and *trn* revealed defective formation of the affinity boundary. Do Caps and Trn play redundant roles during the tracheal morphogenesis as well? Analysis of the tracheal system in the embryos lacking *trn* would reveal whether *trn* plays any role during tracheal morphogenesis.

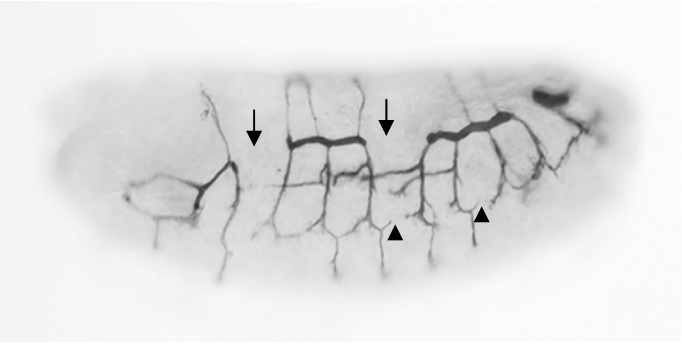

Figure 2.14. $trn^{28.4}$ mutant embryos show discontinuous dorsal and lateral trunks.
The lack of *trn* allele, $trn^{28.4}$ mutant embryos were stained with the 2A12 antibody, which visualizes the tracheal lumen. A stage 15 embryo reveals the dorsal trunk, which is interrupted at several fusion points and therefore, contains gaps (arrows). In addition, the lateral trunk is disrupted at several positions (arrowheads).

In *trn*$^{28.4}$ mutant embryos approximately 1 kb of genomic sequence flanking 5'end of *trn*, the start sites of transcription and translation, and the nucleotide sequence 164-274 from 5' end of *trn* open reading frame are removed (Chang et al., 1993). Consequently, no Trn protein could be detected. These lack of *trn* function embryos were stained with the 2A12 antibody to visualize the tracheal lumen. Similarly as in *caps*$^{65.2}$ mutant embryos, the dorsal trunks are interrupted at several positions and as a result, discontinuous dorsal trunks are formed (**Figure 2.14**). However, in contrast to *caps*$^{65.2}$ mutant embryos, which demonstrate almost normal lateral trunk development, *trn*$^{28.4}$ mutant embryos have frequent interruptions in the lateral trunks.

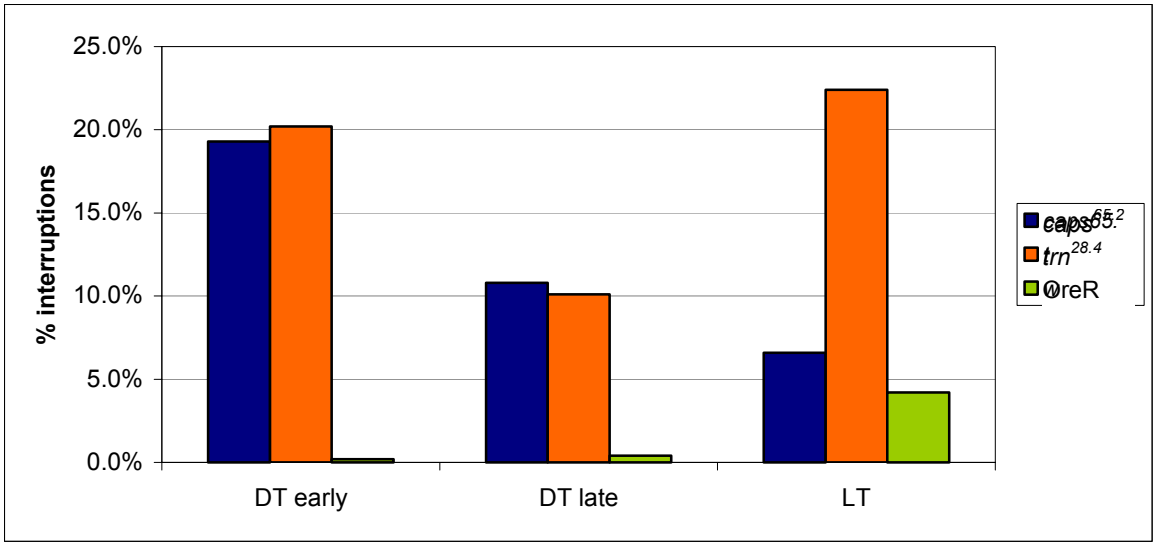

Figure 2.15. Chart showing percentage of interruptions in tracheal branches of *trn*$^{28.4}$ mutant embryos.
Interruptions of fusion points were counted for the dorsal trunks in embryos at early and late stages and for the lateral trunks.
DT early = dorsal trunk in early stage embryos; DT late = dorsal trunk in late stage embryos; LT = lateral trunk.
For homozygous *caps*$^{65.2}$ mutant embryos, the values are as following: DT early = 19.3% (N=1278), DT late = 10.8 % (N=1782), LT = 6.6% (N=684)
For homozygous *trn*$^{28.4}$ mutant embryos, the values are as following: DT early = 20.2% (N=810), DT late = 10.1% (N=1476), LT = 22.4% (N=684)
For OreR wild-type embryos, the values are as following: DT early = 0.2% (N=1260), DT late = 0.4% (N=1224), LT=4.2% (N=936)
N = total number of fusion points counted.

In order to compare the tracheal phenotypes in *caps*$^{65.2}$ and *trn*$^{28.4}$ mutant embryos more accurately, interruptions in the dorsal trunks and the lateral trunks were counted. Frequency of interruptions in the dorsal trunk is similar between *caps*$^{65.2}$ and *trn*$^{28.4}$ mutant embryos (**Figure 2.15**). However, interruption rates in the lateral trunks are strikingly divergent; while lateral trunks in *trn*$^{28.4}$ show 22.4% breaks, lateral trunks in *caps*$^{65.2}$ reveal

only 6.6% breaks, which is not significantly more than in wild-type. These phenotypic similarity on one hand and disparity on the other hand between *caps*$^{65.2}$ and *trn*$^{28.4}$ already suggest that Caps and Trn may not function in a redundant manner during the tracheal development as they do during the wing imaginal disc morphogenesis.

2.2.2 *trn* is expressed in the mesodermal cells but not in the bridge-cells.

Previous work described that *trn* is expressed in segmentally repeated patterns that correspond in position to the developing ventral, lateral and dorsal clusters of peripheral sense organs (Chang et al., 1993). However, this work did not provide information as to where *trn* is expressed in regard to the tracheal system. In order to gain more insight into why the development of dorsal trunk and lateral trunk is affected when *trn* is lacking, the wild-type expression pattern of *trn* was investigated in more detail during early stages of tracheal development. In contrast to *caps*, which is expressed specifically in few single cells including the bridge-cells, *trn* is induced more broadly during early stages (compare **Figure 2.1.A** and **Figure 2.16.A**). Double fluorescent labeling of *trn* and tracheal cells in *1-eve-1* embryos reveal that *trn* is expressed in the metamerically repeated clusters of mesodermal cells located laterally between the tracheal metameres (**Figure 2.16.B**). Notably, *trn* is induced in small groups of cells located ventrally from LTa and LTp, which appear to be in direct contact with those cells expressing *trn*.

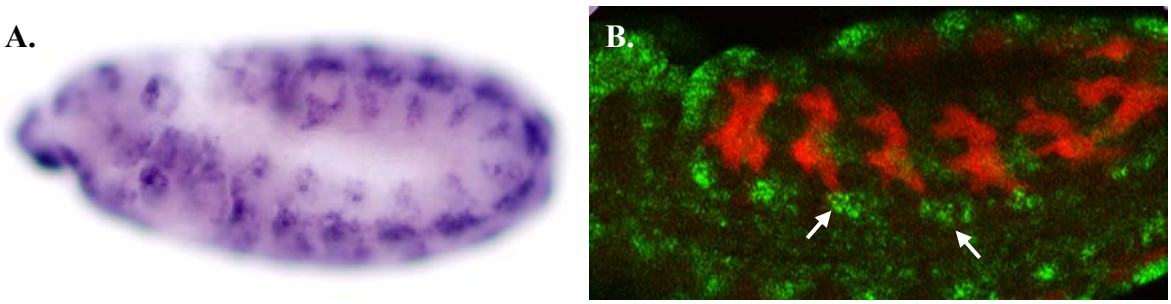

Figure 2.16. *trn* is expressed broadly in the mesodermal cells surrounding the tracheal cells.
A. OreR wild-type embryos were hybridized *in situ* with *trn* antisense RNA probes to label endogenous *trn* expression. A whole-mount embryo at stage 10 reveals metamerically repeated groups of mesodermal cells expressing *trn*.
B. *1-eve-1* embryos were hybridized *in situ* with *trn* antisense RNA probes to fluorescently label *trn* expression and then stained with anti-β-Gal antibody to fluorescently label the tracheal cells. A whole-mount embryo at stage 12 shows that *trn* is induced in the mesodermal cells between the tracheal metameres. LTa and LTp cells (arrows) appear to be in direct contact with clusters of cells expressing *trn*.

During outgrowth of primary branches, *trn* is induced dynamically in broad groups of mesodermal cells adjacent to the tracheal cells. Do these *trn* expressing mesodermal cells

include the bridge-cells? In order to determine whether the bridge-cells contain *trn* or not, the bridge-cells and *trn* expression were both labeled fluorescently in *trn-lacZ* enhancer trap line embryos that expresses nuclear *lacZ* in endogenous *trn* pattern (Chang et al., 1993). Even though the mesodermal cells directly adjoining the bridge-cells reveal *trn* expression, the bridge-cells do not contain *trn* expression (**Figure 2.17**).

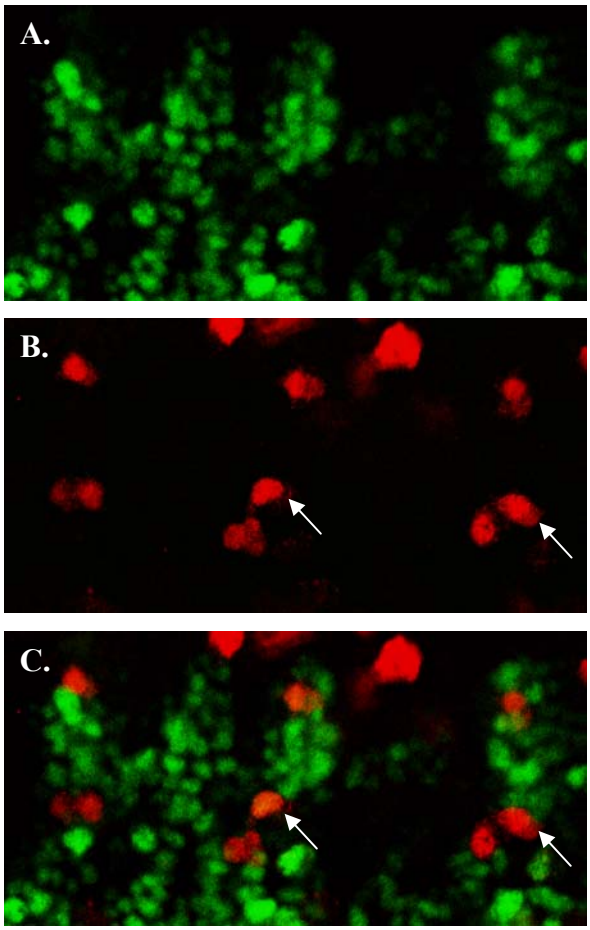

Figure 2.17. *trn* is expressed in the mesodermal cells but not in the bridge-cells.
trn-lacZ enhancer trap line embryos were stained fluorescently with anti-β-Gal (green) and anti-Hb (red) antibodies.
A. A whole-mount embryo at stage 11 shows *trn* expression in large number of mesodermal cells.
B. The same embryo reveals *hb* expression in the bridge-cells (arrows).
C. However, no co-expression of *trn* and *hb* can be observed in the bridge-cells (arrows).

Recent work demonstrated that Caps and Trn share redundant function during wing disc development and are expressed in identical pattern (Milan et al., 2001). Thus, it was speculated if *caps* and *trn* would be induced likewise during tracheal morphogenesis. Quite surprisingly, *caps* and *trn* are in fact expressed in non-overlapping patterns. Whereas *trn* is localized in the mesodermal cells but not in the bridge-cells, *caps* is found exclusively in the bridge-cells (compare **Figure 2.17** with **Figure 2.2**). This prominent distinction in expression patterns suggests that Caps and Trn play different roles during outgrowth of dorsal trunk cells.

2.2.3 Hb represses *trn* expression in the mesodermal cells.

As it was shown in **Figure 2.3**, *caps* is ectopically induced in the mesodermal cells upon ectopic induction of *hb*. This observation indicates that *hb* is one of the transcriptional activators of *caps*. The contrasting expression pattern of *trn*, which is expressed in most mesodermal cells except the bridge-cells, led to the postulation that Hb might be a transcriptional repressor of *trn.* In order to investigate whether *trn* is repressed by *hb*, *trn* expression was analyzed under ectopic overexpression of *hb* in the mesodermal cells.

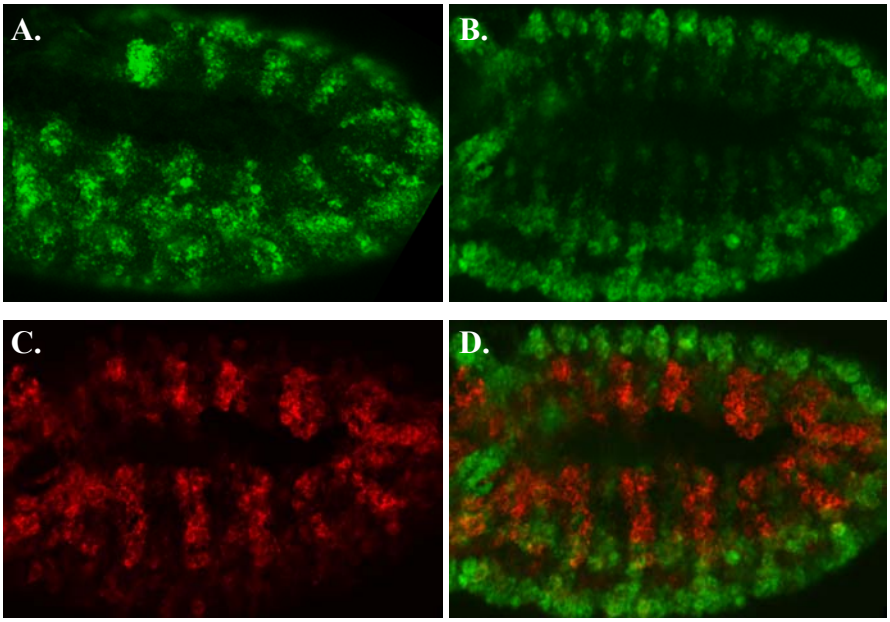

Figure 2.18. Ectopic *hb* in the mesodermal cells represses endogenous *trn*.
OreR wild-type embryos were hybridized *in situ* with *trn* antisense RNA probes (green) to label endogenous *trn* expression (**A**). Embryos carrying *twi-GAL4* driver and *UAS-hb* (**B-D**) were double labeled for endogenous *trn* expression and ectopic *hb* expression through i*n situ* hybridization with *trn* antisense RNA probes (green) and *hb* antisense RNA probes (red).
A. A stage 10 OreR wild-type embryo reveals endogenous *trn* expression in large groups of mesodermal cells on the lateral side.
B. A stage 10 embryo bearing *twi-GAL4* and *UAS-hb* shows that only vestige of *trn* expression remains in the mesodermal cells upon ectopic overexpression of *hb*.
C. In the same embryo as in (**B**), the mesodermal cells show clearly ectopic expression of *hb*.
D. Overlay of *trn* and *hb* expression reveals that there is no co-localization of *hb* and *trn* in the lateral mesodermal cells.

Interestingly, endogenous expression of *trn* in the lateral mesodermal cells almost disappears when *hb* is ectopically expressed in those cells (**Figure 2.18**). Compared to the wild-type embryo, the embryo with ectopic *hb* reveals a much weaker *trn* expression in the mesodermal cells on the lateral side of the embryos (compare **Figure 2.18.A** with **B**). Simultaneous labeling of *hb* and *trn* expression demonstrates that *trn* cannot be detected

anymore in the mesodermal cells, which normally express *trn*, when those cells contain ectopic *hb*. Induction of *trn* can be observed only in the cells that lack *hb* (**Figure 2.18.D**). Thus, ectopic *hb* appears to restrict endogenous *trn* expression. This result indicates that Hb functions as a transcriptional repressor of *trn* in the mesodermal cells when ectopically expressed.

2.2.4 Mesodermal overexpression of *trn* does not affect tracheal development.

As it was described in **Section 2.1.5**, dorsal trunks and lateral trunks become interrupted at several positions when *caps* is misexpressed in other mesodermal cells besides the bridge-cells. This observation suggests that *caps* expression must be restricted to the bridge-cell for proper function of Caps during tracheal development. In addition, misexpression of *caps* deletion constructs revealed that Caps requires the extracellular as well as the intracellular domain for its ectopic function (**Section 2.1.7**). What would happen if *trn*, which is normally expressed in many mesodermal cells except the bridge-cells, is overexpressed in mesoderm? Would ectopic Trn interfere with the outgrowth of dorsal and lateral trunk cells? Would Trn require its intracellular domain to carry out its function? Using the *twi-GAL4* driver, *trn* and a *trn* deletion construct, *UAS-trn*^{Ed} (Milan et al., 2002), were ectopically overexpressed in the mesodermal cells.

Overexpression of *trn* in the mesodermal cells through the *twi-GAL4* driver does not affect the formation of dorsal or lateral trunks. For example, interruptions observed in the embryos misexpressing *trn* occur as frequently as in the embryos misexpressing *lacZ* (**Figure 2.19**). In addition, deleting the intracellular domain of Trn did not affect the formation of normal dorsal trunks significantly, suggesting that Trn may not require its intracellular domain for its function during dorsal trunk formation. However, more interruptions in the lateral trunks were observed in the embryos expressing the truncated form of Trn (Trn^{Ed}) than in the embryos expressing complete Trn; 10.1% compared to 5.3% (**Figure 2.19**). This result suggests that the truncated form of Trn may slightly interfere with the endogenous Trn in the mesodermal cells during lateral trunk development.

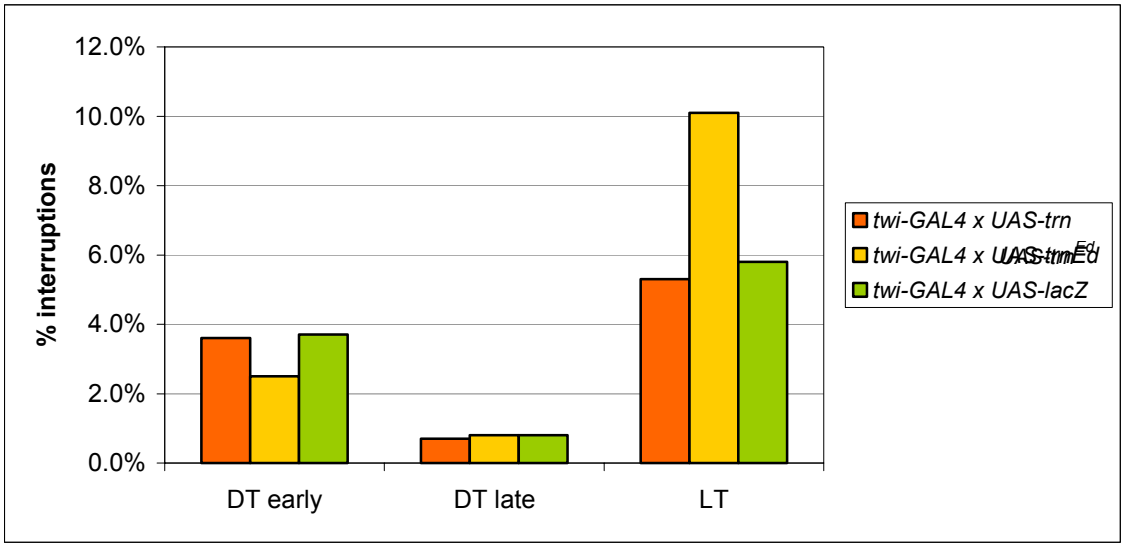

Figure 2.19. Chart showing percentage of interruptions in dorsal and lateral trunks of embryos misexpressing *trn* and *trn* deletion constructs.
Interruptions of fusion points were counted for the dorsal trunks in embryos at early and late stages and for the lateral trunks.
DT early = dorsal trunk in early stage embryos; DT late = dorsal trunk in late stage embryos; LT = lateral trunk.
For embryos carrying *twi-GAL4* and *UAS-trn*, the values are as following: DT early = 3.6% (N=972), DT late = 0.7% (N=918), LT=5.3% (N=918)
For embryos carrying *twi-GAL4* and *UAS-trn*^{Ed}, the values are as following: DT early = 2.5% (N=846), DT late = 0.8 % (N=900), LT = 10.1% (N=666)
For embryos carrying *twi-GAL4* and *UAS-lacZ*, the values are as following: DT early = 3.7% (N=990), DT late = 0.8 % (N=900), LT = 5.8% (N=900)
N = total number of fusion points counted.

2.2.5 Restoring *trn* expression rescues the *trn* tracheal phenotype.

Since overexpression of *trn* through *twi-GAL4* did not influence normal function of *trn*, it might be able to rescue the tracheal defects in *trn*$^{28.4}$ mutants. The rescue of this phenotype would ascertain that the discontinuous dorsal and lateral trunks are indeed due to lack of *trn* in the mesodermal cells. Thus, embryos that are mutant for *trn* and carry *twi-GAL4* as well as *UAS-trn* were generated. The embryos were then stained with the 2A12 antibody to visualize the tracheal lumen. As expected, the tracheal defects could be rescued by expressing *trn* in the mesodermal cells. Finally, the breaks in the dorsal and lateral trunks were counted to determine the effectiveness of the rescue.

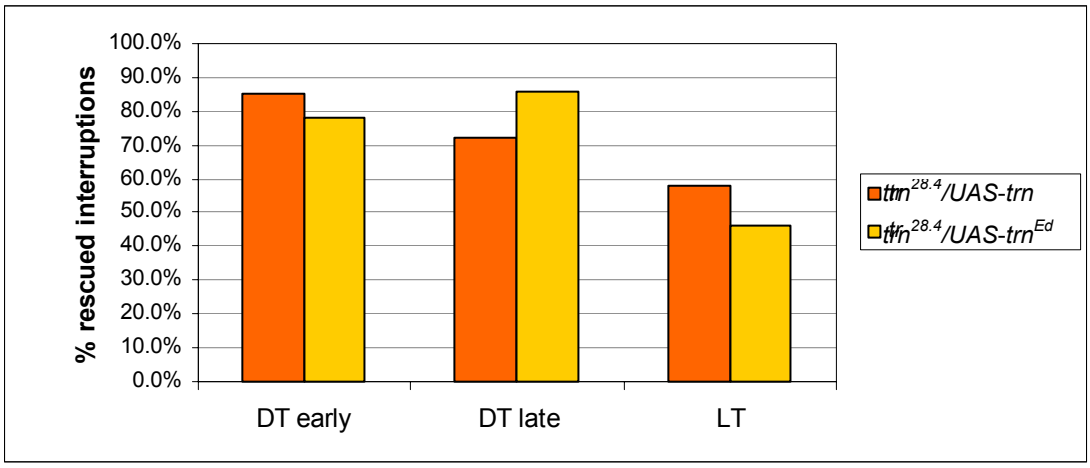

Figure 2.20. Chart showing percentage of rescued interruptions in dorsal and lateral trunks of *trn*$^{28.4}$ mutant embryos expressing *trn* and *trn*^{Ed} deletion construct.
Interruptions of fusion points were counted for the dorsal trunks in embryos at early and late stages and for the lateral trunks. Then, the values were nominalized against the percentage of interruptions in *trn*$^{28.4}$ mutant embryos (20.2%). Finally, the nominalized values were converted into percentage of rescued interruptions.
DT early = dorsal trunk in early stage embryos; DT late = dorsal trunk in late stage embryos; LT = lateral trunk.
For *trn*$^{28.4}$ embryos bearing *twi-GAL4* and *UAS-trn*, the values are as following: DT early = 85% (N=1224), DT late = 72% (N=972), LT=58% (N=900)
For *trn*$^{28.4}$ embryos bearing *twi-GAL4* and *UAS-trn*^{Ed}, the values are as following: DT early = 78% (N=846), DT late = 86 % (N=900), LT = 46% (N=900)
N = total number of fusion points counted.

Expression of *UAS-trn* in the mesodermal cells can effectively rescue the interruptions in dorsal trunks observed in *trn*$^{28.4}$ mutant embryos (**Figure 2.20**). Since the tracheal defect in lack of *trn* embryos can be reversed by restoring *trn* expression, this rescue experiment confirms that a lack of *trn* in the mesodermal cells causes formation of discontinuous tracheal branches. The tracheal phenotype in *trn*$^{28.4}$ mutant embryos can be also effectively rescued by expressing only the extracellular domain of Trn; 78% rescued interruptions in embryos carrying *UAS-trn*^{Ed} compared to 85% rescued interruptions in embryos carrying *UAS-trn* (**Figure 2.20**). This result implies that the intracellular domain of Trn is not essential for Trn function during tracheal morphogenesis.

2.2.6 Extracellular domain of Caps can rescue *trn*$^{28.4}$ tracheal phenotype.

Alignment of Caps against Trn revealed that they share astoundingly similar extracellular domain sequences (**Figure 2.13**). While overexpression of whole Caps in the mesodermal cells resulted in disrupted dorsal and lateral trunks, overexpression of only the extracellular domain of Caps did not affect the tracheal system at all. Since Trn seemed to require merely its extracellular domain, which is highly similar in sequence and structure to the

extracellular domain of Caps, it was investigated whether the tracheal defects in *trn*$^{28.4}$ mutant embryos could be rescued by expressing the extracellular domain of Caps. In addition, what would happen if only the intracellular domain of Caps or whole Caps was expressed in *trn*$^{28.4}$ mutant embryos? To answer this question, various *caps* constructs were expressed through *twi-GAL4* driver in *trn*$^{28.4}$ mutant embryos.

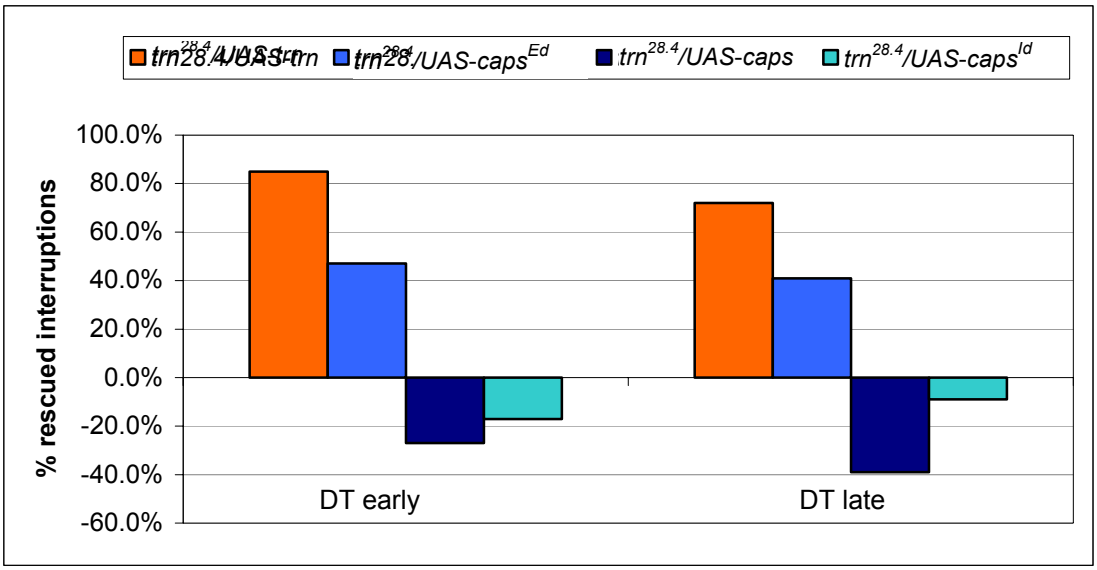

Figure 2.21. Chart showing percentage of rescued interruptions in dorsal and lateral trunks of *trn*$^{28.4}$ mutant embryos expressing *caps*, *caps*^{Ed} or *caps*^{Id}.
Interruptions of fusion points were counted for the dorsal trunks in early and late stage embryos and for the lateral trunks. Then, the values were nominalized against the percentage of interruptions in *trn*$^{28.4}$ mutant embryos (20.2%). Finally, the nominalized values were converted into percentage of rescued interruptions.
DT early = dorsal trunk in early stage embryos; DT late = dorsal trunk in late stage embryos; LT = lateral trunk.
For *trn*$^{28.4}$ embryos bearing *twi-GAL4* and *UAS-trn*, the values are as following: DT early = 85% (N=1224), DT late = 72% (N=972), LT=58% (N=900)
For *trn*$^{28.4}$ embryos bearing *twi-GAL4* and *UAS-caps*^{Ed}, the values are as following: DT early = 47% (N=1206), DT late = 41% (N=1206), LT= -96% (N=1116)
For *trn*$^{28.4}$ embryos bearing *twi-GAL4* and *UAS-caps*, the values are as following: DT early = -27% (N=576), DT late = -39 % (N=576), LT = -15% (N=504)
For *trn*$^{28.4}$ embryos bearing *twi-GAL4* and *UAS-caps*^{Id}, the values are as following: DT early = -17% (N=1062), DT late = -9 % (N=1080), LT = -21% (N=954)
N = total number of fusion points counted.

Surprisingly, by expressing only the extracellular domain of Caps (*UAS-caps*^{Ed}), the dorsal trunk defects could be partially rescued; 47% rescue compared to 85% rescue when *UAS-trn* is expressed (**Figure 2.21**). This astounding result implies that Caps extracellular domain is able to substitute for the extracellular domain of Trn, albeit not completely. In contrast, when whole *caps* was expressed in *trn*$^{28.4}$ mutant embryos, then the defects in dorsal trunks could not be rescued but became even more severe. For example,

interruptions in dorsal trunks of $trn^{28.4}$ embryos carrying *UAS-caps* increased by 27%. Similarly, when only the intracellular domain of *caps* was expressed in $trn^{28.4}$ mutant embryos, the tracheal defects also became more severe: $trn^{28.4}$ embryos carrying *UAS-*$caps^{Id}$ showed 17% more interruptions in the dorsal trunks. All these data suggest that the extracellular domain of Caps is sufficient to rescue $trn^{28.4}$ dorsal trunk phenotype.

2.3 Intracellular domains specify function of Capricious and Tartan.

The result, which showed that the extracellular domain of Caps could substitute for the extracellular domain of Trn, raised a central question regarding the functional specificity of Caps and Trn. If the tracheal cells are unable to distinguish between the extracellular domains of Caps and Trn at the cell surface, then, what makes these two proteins distinct from each other during tracheal development? The experimental data show clearly that the tracheal cells respond differently to Caps and Trn. For instance, the ectopic expression of *caps* causes formation of discontinuous dorsal and lateral trunks while the overexpression of *trn* has no effect on tracheal development (compare **Figure 2.10** and **Figure 2.19**). Since the difference obviously does not lie within the extracellular domains, it seems quite reasonable to presume that the functional specificity might be determined by the intracellular domain. In order to gain some insight into what dictates the functional identity of Caps and Trn, two different hybrid proteins were constructed.

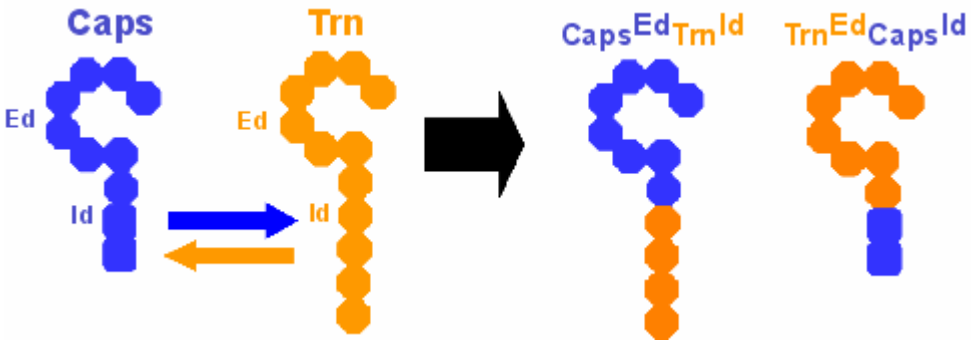

Figure 2.22. The intracellular domains of Caps and Trn were exchanged to generate hybrid proteins. Generation of hybrid proteins is schematically shown. The intracellular domain of Trn is fused to the extracellular domain of Caps to generate $Caps^{Ed}Trn^{Id}$ hybrid protein. Similarly, $Trn^{Ed}Caps^{Id}$ hybrid protein is generated by attaching the intracellular domain of Caps to the extracellular domain of Trn. Ed = extracellular domain; Id = intracellular domain.

$Caps^{Ed}Trn^{Id}$ hybrid protein consists of the extracellular domain of Caps but the intracellular domain of Trn (**Figure 2.22**). On the other hand, $Trn^{Ed}Caps^{Id}$ hybrid protein contains the

extracellular domain of Trn but the intracellular domain of Caps. How would these hybrid proteins function? Would their functions depend on the extracellular domain or rather on the intracellular domain or on both domains? Since ectopic expressions of *caps* and *trn* have contrasting effects on the tracheal system, the functional identity of hybrid proteins can be determined by studying their overexpression phenotypes.

2.3.1 Intracellular domain of hybrid protein determines tracheal phenotype.

As it has been shown so far, misexpression of *caps* results in discontinuous tracheal branches whereas overexpression of *trn* has no effect on tracheal morphogenesis (compare **Figure 2.10** and **Figure 2.19**). Therefore, depending on how the tracheal branches develop, it can be determined whether the hybrid protein functions as Caps or Trn. If $Caps^{Ed}Trn^{Id}$ functions like Caps, then its misexpression would result in discontinuous tracheal branches. On the other hand, if $Caps^{Ed}Trn^{Id}$ functions rather as Trn, then the tracheal system would appear normal. Finally, neither would be the case and $Caps^{Ed}Trn^{Id}$ would affect the tracheal development in an independent mechanism of its own. To determine how $Caps^{Ed}Trn^{Id}$ and $Trn^{Ed}Caps^{Id}$ affect the tracheal development, both hybrid proteins were misexpressed in the mesodermal cells through *twi-GAL4* driver and the resulting tracheal phenotypes were analyzed.

The phenotypic analysis of embryos misexpressing the hybrid proteins indicates that the $Trn^{Ed}Caps^{Id}$ hybrid protein functions similarly as Caps while the $Caps^{Ed}Trn^{Id}$ hybrid protein behaves more like Trn (**Figure 2.23**). For example, there were 15% interruptions in the dorsal trunks of embryos bearing *UAS-trn^{Ed}caps^{Id}*. This rate is much closer to the rate of interruptions found in embryos carrying *UAS-caps* (21%) than in embryos carrying *UAS-trn* (4%). In contrast, merely 4.3% interruptions were observed in the dorsal trunks of early stage embryos with *UAS-caps^{Ed}trn^{Id}*.

First, these data suggest that the extracellular domain of Trn can substitute for the extracellular domain of Caps. Second, they suggest that the functional specificity of Caps is dictated by its intracellular rather than its extracellular domain. While the interruption rates observed in the embryos carrying either *UAS-caps* or *UAS-trn^{Ed}caps^{Id}* are close to each other, the rates for the embryos bearing either *UAS-trn* or *UAS-caps^{Ed}trn^{Id}* are comparable (**Figure 2.23**). Thus, it seems that $Trn^{Ed}Caps^{Id}$ containing the intracellular domain of Caps operates as Caps whereas $Caps^{Ed}Trn^{Id}$ containing the intracellular domain of Trn functions as Trn. These comparisons between the tracheal defects found in the

embryos containing the hybrid proteins, Caps, or Trn strongly suggest that the intracellular domain specifies how Caps functions during tracheal morphogenesis.

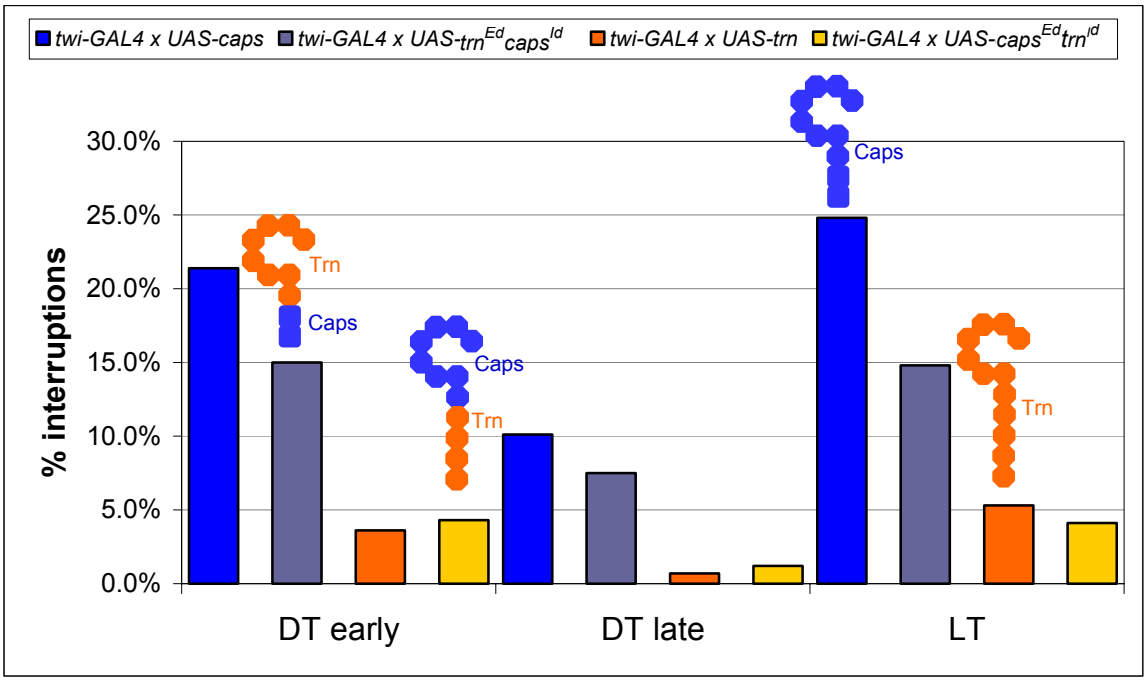

Figure 2.23. Chart showing percentage of interruptions in dorsal and lateral trunks of embryos misexpressing Caps^{Ed}Trn^{Id} and Trn^{Ed}Caps^{Id} hybrid proteins.
Interruptions of fusion points were counted for the dorsal trunks in embryos at early and late stage and for the lateral trunks.
DT early = dorsal trunk in early stage embryos; DT late = dorsal trunk in late stage embryos; LT = lateral trunk.
For embryos carrying *twi-GAL4* and *UAS-caps*, the values are as following: DT early = 21.4% (N=990), DT late = 10.1% (N=1170), LT=24.8% (N=954)
For embryos carrying *twi-GAL4* and *UAS-trn^{Ed}caps^{Id}*, the values are as following: DT early = 15.0% (N=936), DT late = 7.5 % (N=1026), LT = 14.8% (N=1008)
For embryos carrying *twi-GAL4* and *UAS-trn*, the values are as following: DT early = 3.6% (N=972), DT late = 0.7 % (N=918), LT = 5.3% (N=918)
For embryos carrying *twi-GAL4* and *UAS-caps^{Ed}trn^{Id}*, the values are as following: DT early = 4.3% (N=954), DT late = 1.2 % (N=936), LT = 4.1% (N=954)
N = total number of fusion points counted.

2.3.2 Caps^{Ed}Trn^{Id} hybrid protein can rescue *trn$^{28.4}$* tracheal phenotypes.

The overexpression studies with the hybrid proteins indicated that the function of hybrid proteins depends on which intracellular domains they contain. If Caps^{Ed}Trn^{Id} hybrid protein indeed functions as Trn, then it should be able to rescue the tracheal defects in *trn$^{28.4}$* mutant embryos. On the other hand, Trn^{Ed}Caps^{Id} hybrid protein, which operates like Caps, would be unable to restore continuous dorsal and lateral trunks in *trn$^{28.4}$* mutants. Thus, the tracheal lumens in *trn$^{28.4}$* embryos carrying *twi-GAL4* driver and the hybrid

protein constructs were visualized through the 2A12 antibody and the interruptions in the dorsal and lateral trunks were quantified.

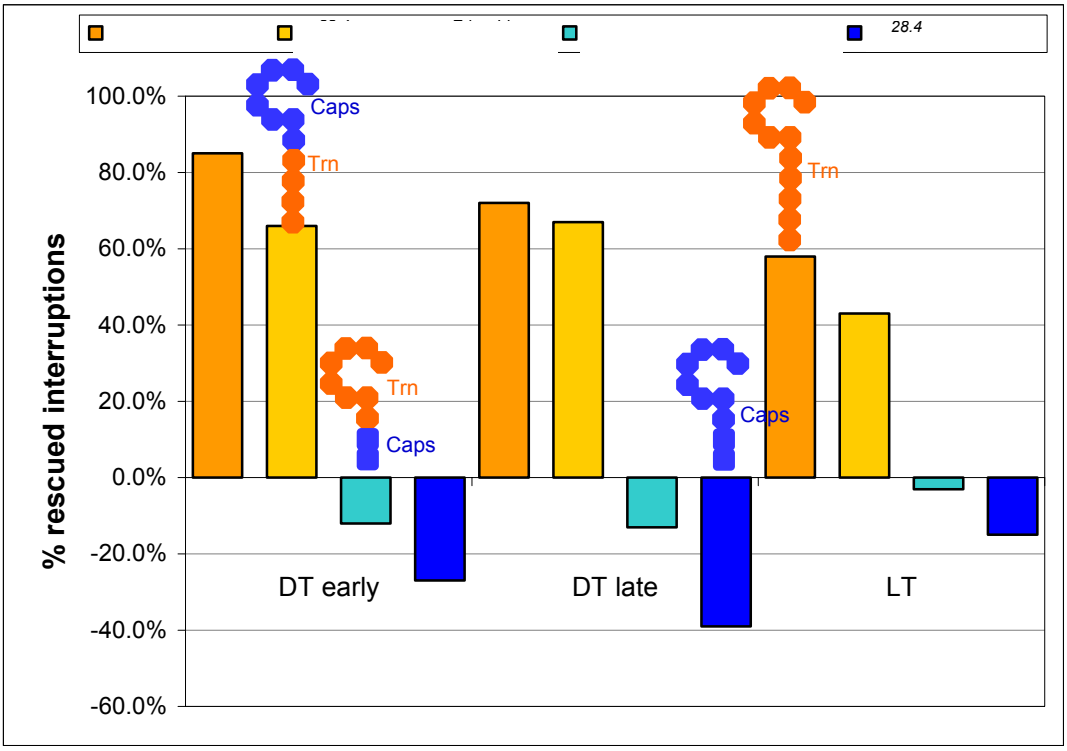

Figure 2.24. Chart showing percentage of rescued interruptions in dorsal and lateral trunks of $trn^{28.4}$ embryos expressing *trn*, $caps^{Ed}trn^{Id}$, $trn^{Ed}caps^{Id}$ or *caps*.
Interruptions of fusion points were counted for the dorsal trunks in embryos at early and late stages and for the lateral trunks. Then, the values were nominalized against the percentage of interruptions in $trn^{28.4}$ mutant embryos (20.2%). Finally, the nominalized values were converted into percentage of rescued interruptions.
DT early = dorsal trunk in early stage embryos; DT late = dorsal trunk in late stage embryos; LT = lateral trunk.
For $trn^{28.4}$ embryos carrying *twi-GAL4* and *UAS-trn*, the values are as following: DT early = 85% (N=1224), DT late = 72% (N=972), LT=58% (N=900)
For $trn^{28.4}$ embryos carrying *twi-GAL4* and *UAS-*$caps^{Ed}trn^{Id}$, the values are as following: DT early = 66% (N=810), DT late = 67% (N=900), LT= 43% (N=900)
For $trn^{28.4}$ embryos carrying *twi-GAL4* and *UAS-*$trn^{Ed}caps^{Id}$, the values are as following: DT early = -12% (N=1044), DT late = -13% (N=1350), LT= -3% (N=1026)
For $trn^{28.4}$ embryos carrying *twi-GAL4* and *UAS-caps*, the values are as following: DT early = -27% (N=576), DT late = -39 % (N=576), LT = -15% (N=504)
N = total number of fusion points counted.

As expected, $Caps^{Ed}Trn^{Id}$ hybrid protein can complement the lack of *trn* expression in $trn^{28.4}$ mutants so that the tracheal system can develop almost normally. 66% of interruptions observed in the dorsal trunks of $trn^{28.4}$ embryos at early stages could be rescued by expressing $caps^{Ed}trn^{Id}$ (**Figure 2.24**). This value does not diverge greatly from the rate of rescued interruptions in the embryos with *UAS-trn*, which show 85% rescued interruptions in dorsal trunks. This result demonstrates on one hand that the $Caps^{Ed}Trn^{Id}$

hybrid protein is functional and on the other hand that the extracellular domain of Caps can replace the extracellular domain of Trn for its role during tracheal morphogenesis.

In contrast, the interruptions in *trn*$^{28.4}$ mutants could not be rescued by expressing *trn*^{Ed}*caps*^{Id}. Rather, the defects in tracheal system became worse. For example, there were 12% more interruptions in the dorsal trunks of *trn*$^{28.4}$ embryos carrying *UAS-trn*^{Ed}*caps*^{Id} (**Figure 2.24**). Comparably, *trn*$^{28.4}$ embryos expressing *UAS-caps* exhibited 27% more interruptions in the dorsal trunks. **Figure 2.21** reveals that the expression of the extracellular domain alone is sufficient to efficiently rescue the tracheal defects in *trn*$^{28.4}$ mutants. Even though the Trn^{Ed}Caps^{Id} hybrid protein contains the complete extracellular domain of Trn, it not only fails to rescue the deficiencies in tracheal development, it even aggravates the effect, just like Caps. Again, these data demonstrate that the Trn^{Ed}Caps^{Id} hybrid protein functions analogously as Caps.

Analyses of the overexpression and the rescue experiments with the hybrid proteins indicate on one hand that the extracellular domains of Caps and Trn are redundant in their functions and on the other hand that the intracellular domain specifies the functional identity for Caps and Trn.

2.4 RHR motif in Caps intracellular domain is functionally essential.

Although Caps and Trn are both cell adhesion molecules expressed at cell surface and play roles in the formation of trachea, they operate in very divergent mechanisms. So far, the results demonstrate clearly that Trn does not require its intracellular domain for its role during outgrowth of dorsal trunk cells, whereas Caps needs its intracellular domain for proper functioning. Moreover, it is the intracellular domain that enables the cells to distinguish between Caps and Trn and respond accordingly. Therefore, it was of great interest to investigate why the intracellular domain is so essential for Caps function. Perhaps, the intracellular domain interacts with other membrane or cytosolic proteins. On the other hand, it may relay signals from an activated extracellular domain to another component of a signal pathway, similarly as other receptor proteins. Unfortunately, pattern and profile searches using programs available at the ExPASy (the Expert Protein Analysis System) World Wide Web server (http://www.expasy.org) did not reveal any specific information regarding the Caps intracellular domain (Gasteiger et al., 2003). Therefore, the

function of intracellular domain could not be simply deduced through comparative analysis.

By searching for any proteins that contain similar amino acid sequences as the intracellular domain of Caps using the blastp program at NCBI (Altschul et al., 1990), an *Anopheles gambiae* gene *agCP14407* was identified. This *Anopheles* gene has not been cloned yet, and therefore, there is no specific information regarding its expression pattern or function. Only its annotated sequence is available.

2.4.1 Three motifs are conserved between *Anopheles* and *Drosophila* Caps.

The alignment using the lalign program (Myers and Miller, 1989) shows 40% identity in overall sequences of Caps and agCP14407 (**Figure 2.25**). The REP search program (Andrade et al., 2000), which searches for any repeats in the protein, predicted that agCP14407 contains 14 LRR motifs, exactly as Caps. In addition, the TMHMM program (http://www.cbs.dtu.dk/services/TMHMM-2.0/), which searches for putative transmembrane domain, calculated that agCP14407 most likely includes a signal peptide at amino-terminal and a single transmembrane domain (aa439-461) with its C-terminal in cytoplasm. This topology matches precisely the orientation of Caps, which also contains single transmembrane domain (aa454-476). The high similarity in sequence and secondary structure suggests that agCP14407 (AgaCaps) is probably the *Anopheles* homolog of *Drosophila* Caps (DmeCaps).

Identifying a homolog of Caps in related species opened new possibilities for approaching the question: how does the intracellular domain of Caps mediate its function? For example, by investigating which sequences or motifs are particularly conserved between the intracellular domains of DmeCaps and AgaCaps, it might be possible to identify at least which amino acids are essential for the function of both proteins. This knowledge, then, might further elucidate the mechanisms by which Caps may operate.

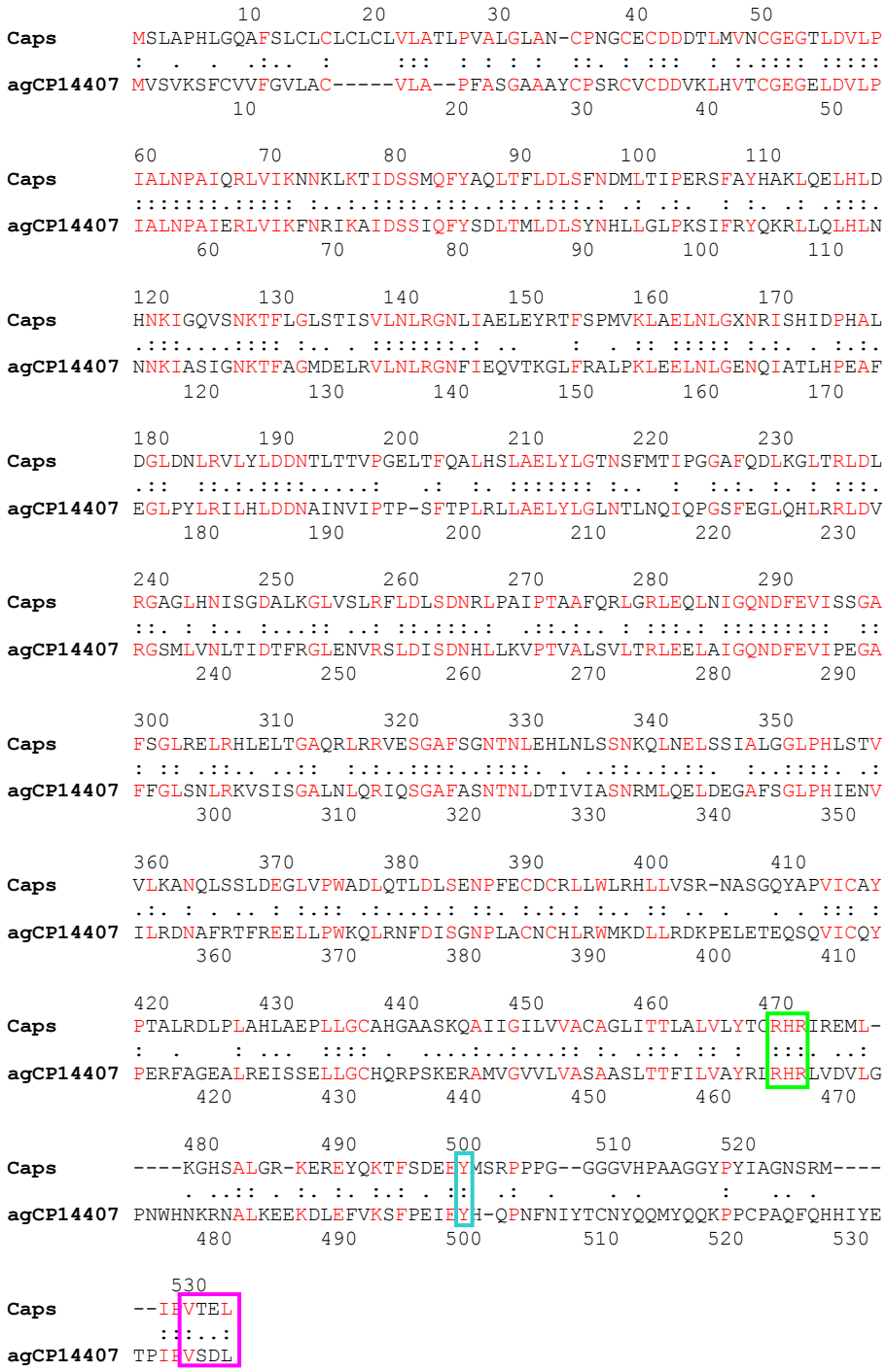

Figure 2.25. Three motifs are highly conserved in Caps and agCP14407, an *Anopheles* homolog of Caps.
Caps protein sequence (aa1-540) was aligned against agCP14407 protein sequence (aa1-539) using the lalign program (Myers and Miller, 1989). Single letter code was used for the amino acid residues. Red letters represent identical residues between Caps and agCP14407. **:** describes highly conserved residues whereas **.** describes lowly conserved residues. There is 42.9% identity among 539 residues between Caps and agCP14407 proteins. The boxed residues represent three motifs that are conserved most: RHR motif (green), putative tyrosine phosphorylation site (blue) and putative PDZ binding motif (pink).

Closer analysis of the alignment between the intracellular domains of DmeCaps and

AgaCaps identified three motifs that were predominantly conserved: an RHR motif immediately after the transmembrane domain, a putative tyrosine phosphorylation site, and finally a putative PDZ binding motif (**Figure 2.25**). Following the transmembrane domain, a stretch of 8 amino acids, RHRIREML in DmeCaps or RHRLVDVL in AgaCaps, are especially conserved. Particularly, the first three amino acids, RHR, are identical in both proteins. The well-known protein data sets neither recognized RHR motif as a specific motif nor revealed any information regarding its specific function. Perhaps, this unusual stretch of amino acids containing bulky side chains might play structural role in keeping certain conformation of Caps.

Program NetPhos2.0 predicts putative phosphorylation sites for threonine, serine and tyrosine residues (Blom et al., 1999). Both DmeCaps and AgaCaps contain two putative phosphorylation sites at tyrosine residues, Y498 and Y507 for DmeCaps and Y499 and Y507 for AgaCaps. Interestingly, alignment of DmeCaps protein to AgaCaps reveals that DmeCaps Y507 is conserved in AgaCaps. The conservation of Y507 might imply that this putative tyrosine phosphorylation site is essential for the function of Caps.

The last four amino acids at the C-terminal of Caps match one of the binding motifs found to interact with PDZ (PSD-95, Discs-large, ZO-1) domains (Woods and Bryant, 1991; Kennedy 1995; Kornau et al., 1995). The structure of the PDZ domain is designed for binding to a free carboxylate group at the end of peptide and therefore, prefers peptide sequences at C-terminal rather than the internal peptide sequence (Sheng and Sala, 2001). Interestingly, even though the last four amino acids in AgaCaps and DmeCaps are not identical, both match one of the consensus C-terminal peptide sequences recognized by PDZ domains: **X-S/T-X-L**, where X is unspecified amino acid. The C-terminal residues **V-T-E-L** of DmeCaps and **V-S-D-L** of AgaCaps match the specific PDZ binding motif and might, therefore, be putative targets of PDZ domain proteins.

2.4.2 RHR motif is essential for ectopic function of Caps.

How could it be tested if the three conserved motifs are indeed essential for the function of Caps? One of the widely accepted methods is to mutate the amino acid residues within the motifs and analyze whether the function is affected. Thus, point mutations leading to amino acid substitution were introduced into *caps* cDNA sequence through site-directed mutagenesis (**Figure 2.26**). While RH478-479 as well as Y507 was substituted for small and neutral glycine residues, the PDZ binding motif at C-terminal was deleted. The

resulting mutagenized Caps constructs were termed Caps$^{\Delta RH}$, Caps$^{\Delta Y}$ and Caps$^{\Delta PDZ}$, respectively.

It has been shown throughout this thesis that misexpression of *caps* results in discontinuous tracheal tubes. If the RHR motif, putative tyrosine phosphorylation site or the putative PDZ binding motif were in fact essential for the proper function of Caps, then mutations of these motifs would affect the functional efficiency of Caps and consequently, the outgrowth of tracheal cells. Thus, examination of the tracheal phenotypes in embryos misexpressing mutated *caps* in the mesodermal cells would provide some insights into the functional relevance of the three motifs. Through staining with the 2A12 antibody, tracheal lumens were visualized in embryos carrying *twi-GAL4* mesodermal driver and either *UAS-caps*$^{\Delta RH}$, *UAS-caps*$^{\Delta Y}$, or *UAS-caps*$^{\Delta PDZ}$ mutagenized *caps* constructs and the interruptions in dorsal and lateral trunks were counted.

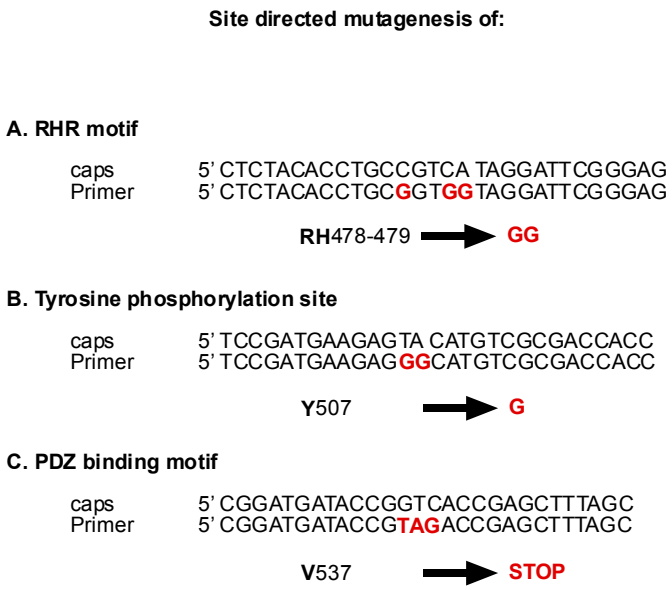

Figure 2.26. Site-directed mutagenesis of the three conserved peptide motifs in Caps.
The QuickChange site-directed mutagenesis kit (Stratagene) was used to make amino acid substitutions in RHR motif, tyrosine phosphorylation site and PDZ binding motif.
A. For mutation of RHR motif: RH478-479 was substituted with GG residues using the indicated primer.
B. For mutation of tyrosine phosphorylation site: Y507 was substituted with G residue using the indicated primer.
C. For deletion of PDZ binding motif: V537 was substituted with stop codon.
Mismatch nucleotides leading to amino acid substitutions are highlighted in red.

The most dramatic effect could be observed in the embryos misexpressing Caps$^{\Delta RH}$ mutagenized construct, which contains RH478-479 to GG substitution. Surprisingly, this mutation of RHR motif seems to render Caps almost non-functional, as the tracheal tubes appear to be normal under ectopic expression of Caps$^{\Delta RH}$. The rates of interruptions in the

embryos misexpressing *UAS-caps*$^{\Delta RH}$ or *UAS*-lacZ are very close to each other (**Figure 2.27**). For instance, the embryos carrying *UAS-caps*$^{\Delta RH}$ show merely 5.3% interruptions in the dorsal trunks while the embryos carrying *UAS-lacZ* show 3.7% interruptions. It seems that ectopic Caps cannot impair tracheal development anymore when the RHR motif is mutated. This result clearly demonstrates that the RHR motif in Caps is functionally essential during the formation of tracheal tubes.

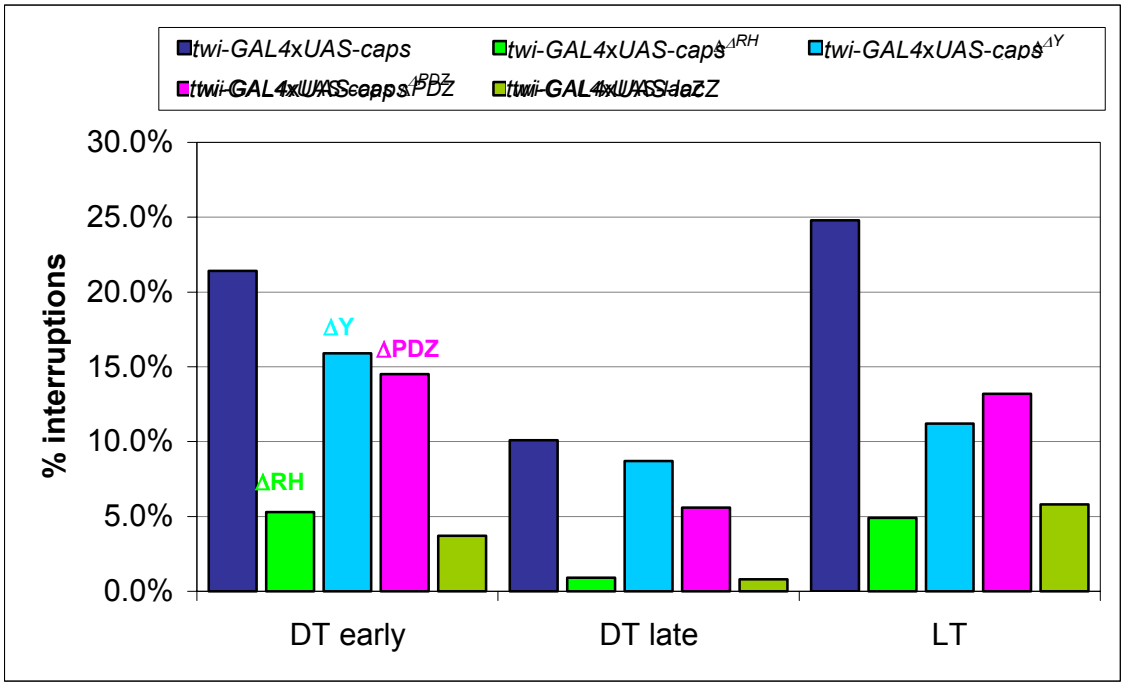

Figure 2.27. Chart showing percentage of interruptions in dorsal and lateral trunks of embryos misexpressing mutagenized *caps* constructs.
Interruptions of fusion points were counted for the dorsal trunks in embryos at early and late stages and for the lateral trunks.
DT early = dorsal trunk in early stage embryos; DT late = dorsal trunk in late stage embryos; LT = lateral trunk.
For embryos carrying *twi-GAL4* and *UAS-caps*, the values are as following: DT early = 21.4% (N=990), DT late = 10.1% (N=1170), LT=24.8% (N=954)
For embryos carrying *twi-GAL4* and *UAS-caps*$^{\Delta RH}$, the values are as following: DT early = 5.3% (N=918), DT late = 0.9% (N=936), LT = 4.9% (N=936)
For embryos carrying *twi-GAL4* and *UAS-caps*$^{\Delta Y}$, the values are as following: DT early = 15.9% (N=900), DT late = 8.7% (N=900), LT = 11.2% (N=900)
For embryos carrying *twi-GAL4* and *UAS-caps*$^{\Delta PDZ}$, the values are as following: DT early = 14.5% (N=918), DT late = 5.6 % (N=936), LT = 13.2% (N=900)
For embryos carrying *twi-GAL4* and *UAS-lacZ*, the values are as following: DT early = 3.7% (N=990), DT late = 0.8 % (N=900), LT = 5.8% (N=900)
N = total number of fusion points counted.

Only slight reductions in interruption rates can be observed in embryos misexpressing either *UAS-caps*$^{\Delta Y}$ or *UAS-caps*$^{\Delta PDZ}$. Whereas embryos carrying *UAS-caps*$^{\Delta Y}$, which

contains an Y507 to G507 substitution, show 16% interruptions in dorsal trunks, embryos bearing normal *caps* reveal 21% interruptions (**Figure 2.27**). Similarly, embryos carrying *UAS-caps*$^{\Delta PDZ}$, the mutagenized construct lacking the PDZ binding motif, exhibit 15% interruptions in dorsal trunks. These observations suggest that mutation of Y507 or deletion of the PDZ binding motif does not adversely affect the function of ectopic Caps during tracheal morphogenesis. Despite the predictions, Y507 may not be phosphorylated and/or Caps may not interact with PDZ proteins. Alternatively, phosphorylated tyrosine residue and/or interaction with PDZ proteins may be unnecessary for Caps function but important for the stability of Caps.

2.5 Caps intracellular domain interacts with Ras64B.

The results have demonstrated that the intracellular domain is essential for Caps to function properly and that the RHR motif within this domain is required. Unfortunately, there is no specific information available for this particular RHR motif found in the Caps intracellular domain. Possibly, it is involved in protein-protein interactions as found for many known motifs. Most likely, Caps interacts with other proteins in the cytoplasm through its intracellular domain to mediate its function. Identifying such interaction partners would help to elucidate which mechanisms underlie Caps function.

2.5.1 Putative interactors are found through yeast two-hybrid screening.

One of the widely used methods to search for protein interaction partners is yeast two-hybrid screening (Fields and Song, 1989), which usually involves a protein or domain of interest fused to yeast protein (bait protein) that interacts specifically with another yeast protein attached to unknown random proteins (target proteins). It also includes a reporter system such as β-Gal activity to facilitate easy visual detection when the bait protein interacts with the target proteins. Thus, the yeast two hybrid system allows screening of large number of target proteins (in the magnitude of 10^6) within reasonable period of time.
In order to identify putative interaction partners for Caps, the CytoTrap® two-hybrid system from Stratagene was used. In contrast to the conventional yeast two-hybrid system, which involves protein interaction in the nucleus and transcriptional activation of reporter gene for detection, the CytoTrap® system is based on the protein interaction in the cytoplasm that induces cell growth (Aronheim et al., 1997). Therefore, proteins that are

associated with the membrane or require post-translational modification in the cytoplasm can be successfully used as bait proteins. The CytoTrap® system utilizes the yeast temperature-sensitive mutant strain *cdc25H*, which can grow at permissive temperature (25°C) but not at restrictive temperature (37°C) because activation of Ras signaling pathway is defective (Petitjean et al., 1990). Human Sos (hSos), a human homolog of yeast Cdc25, can complement the function of yeast Cdc25 in activating the Ras signaling pathway when it is recruited to the cell membrane. Through the interaction between bait protein and target protein, hSos can be recruited to the membrane and activate the Ras signaling pathway. Consequently, *cdc25H* mutant strain can grow at 37°C.

Using Caps intracellular domain ($Caps^{Id}$) as the bait protein in the CytoTrap® yeast two-hybrid system, 1.7 x 10^6 colonies containing a *Drosophila* cDNA library were screened for putative interaction with $Caps^{Id}$. After 10 days of incubation at the restrictive temperature of 37°C, more than 400 *cdc25H* colonies containing $Caps^{Id}$ and random target proteins showed viability. These colonies were subsequently put through two rounds of interaction tests (described in **Section 4.2.6**) in order to verify their growth at the restrictive temperature. Finally, 60 *cdc25H* colonies indicating putative interaction between $Caps^{Id}$ and target proteins were selected.

Colony No.	Gene Name	Gene function
42	CG8418 (*ric*)	Ras which interacts with Calmodulin
51	CG1167 (*ras64B*)	Ras small monomeric GTPase
52	CG2945 (*cin*)	molybdenum cofactor biosynthesis protein
79	CG6791	C2H2 zinc finger protein
83	CG11426	phosphatidate phosphatase
90	CG1433 (*atu*)	transcription unit
92	CG8414	unknown
125	CG13388 (*akap200*)	protein kinase A anchoring protein
143	U13637 (*yolkless*)	vitellogenin receptor
159	CG15442 (*rpL27A*)	ribosomal protein
166	CG1167 (*ras64B*)	Ras small monomeric GTPase
167	CG8418 (*ric*)	Ras which interacts with Calmodulin
169	CG1167 (*ras64B*)	Ras small monomeric GTPase
170	CG1167 (*ras64B*)	Ras small monomeric GTPase
171	CG8173	Serine/threonine kinase
172	CG8418 (*ric*)	Ras which interacts with Calmodulin
173	CG4087 (*rpP2*)	structural constituent of ribosome
174	CG8416 (*rho1*)	Rho monomeric GTPase
177	CG8418 (*ric*)	Ras which interacts with Calmodulin
178	CG8418 (*ric*)	Ras which interacts with Calmodulin
180	CG6803	unknown
184	CG6791	C2H2 zinc finger protein

Colony No.	Gene Name	Gene function
186	CG4087 (*rpP2*)	structural constituent of ribosome
187	CG4769	electron transporter within CoQH2-cytochrome C reductase complex
188	CG8416 (*rho1*)	Rho monomeric GTPase
191	CG8418 (*ric*)	Ras which interacts with Calmodulin
200	CG8418 (*ric*)	Ras which interacts with Calmodulin
201	CG8418 (*ric*)	Ras which interacts with Calmodulin
203	CG8418 (*ric*)	Ras which interacts with Calmodulin
204	CG8418 (*ric*)	Ras which interacts with Calmodulin
206	CG8418 (*ric*)	Ras which interacts with Calmodulin
213	CG4087 (*rpP2*)	structural constituent of ribosome
214	CG8418 (*ric*)	Ras which interacts with Calmodulin
240	CG8418 (*ric*)	Ras which interacts with Calmodulin
247	CG8418 (*ric*)	Ras which interacts with Calmodulin
257	CG4087 (*rpP2*)	structural constituent of ribosome
260	CG8418 (*ric*)	Ras which interacts with Calmodulin
261	CG8418 (*ric*)	Ras which interacts with Calmodulin
264	CG11807	PX (Bem1/NCF1/PI3K) domain
268	CG3849	SH3 domain
270	CG8418 (*ric*)	Ras which interacts with Calmodulin
285	CG8418 (*ric*)	Ras which interacts with Calmodulin
289	CG9066	unknown
298	CG8416 (*rho1*)	Rho monomeric GTPase
300	CG8418 (*ric*)	Ras which interacts with Calmodulin
301	CG12157 (*tom40*)	component of mitochondrial outer membrane translocase complex
302	CG4087 (*rpP2*)	structural constituent of ribosome
304	CG8418 (*ric*)	Ras which interacts with Calmodulin
307	CG8418 (*ric*)	Ras which interacts with Calmodulin
311	CG1167 (*ras64B*)	Ras small monomeric GTPase
347	RE25555	zimbabwe 53 mitochondrion
349	CG8418 (*ric*)	Ras which interacts with Calmodulin
355	CG8416 (*rho1*)	Rho monomeric GTPase
400	CG1167 (*ras64B*)	Ras small monomeric GTPase
411	CG5639	pancreatic trypsin inhibitor (Kunitz) family domain, Elafin-like domain
414	CG9429 (*crc*)	calcium ion binding
415	CG18543	SAM/pointed domain
419	CG8418 (*ric*)	Ras which interacts with Calmodulin
439	CG8416 (*rho1*)	Rho monomeric GTPase
444	CG4087 (*rpP2*)	structural constituent of ribosome

Table 2.1. Putative interactors of Caps^{Id} were identified through CytoTrap yeast two-hybrid screening. The first column (**Colony No**.) describes the colony number of *cdc25H* transformants that were selected after two rounds of interaction test, which determines growth of colonies at the restrictive temperature of 37°C. The second column (**Gene name**) describes annotations of *Drosophila* gene sequences that are expressed in *cdc25H* transformants. In addition, gene names are indicated when the genes are already cloned or known. The third column (**Gene function**) describes either known functions or functional motifs of proteins encoded by the corresponding genes.

To obtain information regarding which *Drosophila* genes these yeast colonies were expressing, the target cDNA was either amplified through PCR or isolated through plasmid purification from yeast cells. By sequencing the obtained PCR product or plasmid, *Drosophila* genes that were inserted into target plasmids could be identified. Since numerous colonies were identified to contain the same *Drosophila* gene, the final number of genes encoding putative interactors was less than 60 (**Table 2.1**).

Notably, some genes were more strongly represented than others. For example, gene encoding Ric (Ras which interacts with Calmodulin) was found in 23 different colonies. Since Ric was found as a putative interaction partner during other CytoTrap® screenings using unrelated baits, it seemed possible that Ric activates the Ras signaling pathway independently of the bait proteins in *cdc25H* yeast cells (M. Behr, personal communication). Thus, no further experiments were done to verify the interaction between $Caps^{Id}$ and Ric. In addition, it seemed less likely that ribosomal or mitochondrial proteins affect tracheal development by directly interacting with $Caps^{Id}$ and therefore, their putative interactions with $Caps^{Id}$ were not analyzed further. On the other hand, it seemed quite plausible that Caps mediates its function by associating with a Ras GTPase, which is well known to participate in diverse developmental processes (de Celis and Garcia-Bellido, 1994; Brand and Perrimon, 1993). Therefore, additional *in vivo* and *in vitro* experiments were done to determine whether Ras64B indeed binds to $Caps^{Id}$.

2.5.2 Ras64B interacts specifically with $Caps^{Id}$ in *cdc25H* yeast strain.

In order to verify that the growth of *cdc25H* yeast strain at the restrictive temperature of 37°C is dependent specifically on coexpression of $caps^{Id}$ and *ras64B*, either $caps^{Id}$ and *ras64B* or *colI* and *ras64B* were cotransformed into *cdc25H* cells. *colI* encodes murine 72kDa type IV collagenase (Reponen et al., 1992), which would very unlikely interact with any *Drosophila* protein. Thus, transformants carrying *colI* and *ras64B* should be unable to grow on galactose medium at 37°C. In addition, target and bait plasmids containing full length *MAFB* gene were transformed into *cdc25H* cells as a positive control since MAFBs were shown to interact with each other (Kataoka et al., 1994). Finally, *cdc25H* transformants carrying *colI* and *MAFB* were used as a negative control because the two proteins do not interact with each other at all. Although the control *cdc25H* transformants carrying *colI* and *ras64B* are unable to grow properly on the galactose medium at 37°C, *cdc25H* cells cotransformed with $caps^{Id}$ and *ras64B* reveal comparably strong growth as

the positive control (**Figure 2.28.A**). In contrast, the viability of transformants bearing *caps*^{Id} and *ras64B* is distinctively weaker on the glucose medium (**Figure 2.28.B**), which represses the expression of *ras64B*, than on the galactose medium. Thus, *cdc25H* temperature sensitive mutant strain is fully viable at the restrictive temperature exclusively when *caps*^{Id} and *ras64B* are coexpressed. These results suggest that Ras64B interacts specifically with Caps^{Id} in the *cdc25H* yeast strain.

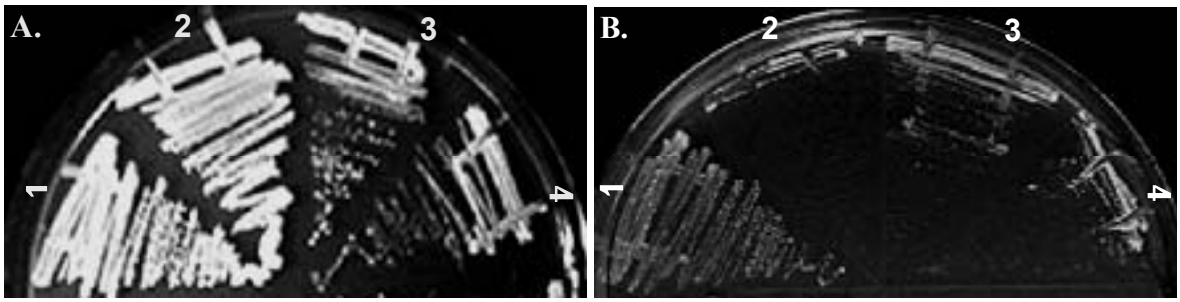

Figure 2.28. *cdc25H* transformants coexpressing *caps*^{Id} and *ras64B* show specific growth at 37°C.
cdc25H yeast strain was cotransformed with either *caps*^{Id} and *ras64B* or *colI* and *ras64B*. The transformants were streaked on either galactose or glucose medium and incubated at the restrictive temperature of 37°C for 4 days. *cdc25H* cells transformed with *MAFB* were used as positive control whereas transformants carrying *MAFB* and *colI* served as negative control. The numbers 1-4 indicate *cdc25H* yeast strains cotransformed with; 1 = *caps*^{Id} and *ras64B*; 2 = positive control; 3 = *colI* and *ras64B*; 4 = negative control.
A. *cdc25H* transformants carrying *caps*^{Id} and *ras64B* (1) are as viable as positive control (2) on galactose medium at 37°C. In contrast, *cdc25H* cells cotransformed with *colI* and *ras64B* (3) as well as the negative control (4) are nearly inviable.
B. All transformants show no (2) or only very weak growth (1, 3 and 4) on glucose medium, which represses expression of target plasmids, at 37°C. Notably, *cdc25H* cells cotransformed with *caps*^{Id} and *ras64B* (1) show slightly stronger growth than other transformants.

2.5.3 Ras64B binds directly to Caps intracellular domain *in vitro*.

Although the yeast two-hybrid system provides strong implication for possible protein-protein interaction, the physical presence of interaction often needs to be confirmed through other *in vitro* methods such as a GST pull-down assay (Beller et al., 2002). Thus, a fusion protein containing N-terminal GST and C-terminal Caps^{Id} was constructed (see **Section 4.2.7.1**). Ras proteins in active form containing GTP may demonstrate different binding affinities from inactive Ras proteins containing GDP. Therefore, both forms of ^{35}S-labeled Ras64B were generated through *in vitro* translation in order to analyze whether Caps binds preferentially active or inactive Ras64B. Then, same amounts of GST and GST-Caps^{Id} fusion protein were incubated with either active or inactive Ras64B. Finally, the bound protein fractions were separated by SDS-PAGE and visualized by fluorography.

Staining with Coomassie blue reveals that same amounts of GST and GST-Caps^{Id} fusion protein were incubated with either active or inactive Ras64B (**Figure 2.29.A**). Prominent bands of 32kDa in lane **3** and **4** show that GST-Caps^{Id} fusion protein is correctly expressed. Weak multiple bands below the 32kDa band probably correspond to degradation products of GST-Caps^{Id} fusion protein. Through fluorography, ^{35}S-labeled Ras64B binding to GST-Caps^{Id} fusion protein is visualized (**Figure 2.29.B**). Whereas neither active nor inactive Ras64B is found in control GST protein fraction (lanes **1** and **2**), single bands are detected in GST-Caps^{Id} fusion protein fraction (lane **3** and **4**). This result indicates that Caps^{Id} directly binds Ras64B *in vitro*. Interestingly, GST-Caps^{Id} incubated with inactive Ras64B shows significantly stronger band than GST-Caps^{Id} incubated with active Ras64B (compare lane **4** and **3** in **Figure 2.29.B**). This result indicates that Caps^{Id} preferentially binds inactive Ras64B containing GDP rather than active Ras64B containing GTP and suggests that inactive Ras64B binds directly to the intracellular domain of Caps and may become activated.

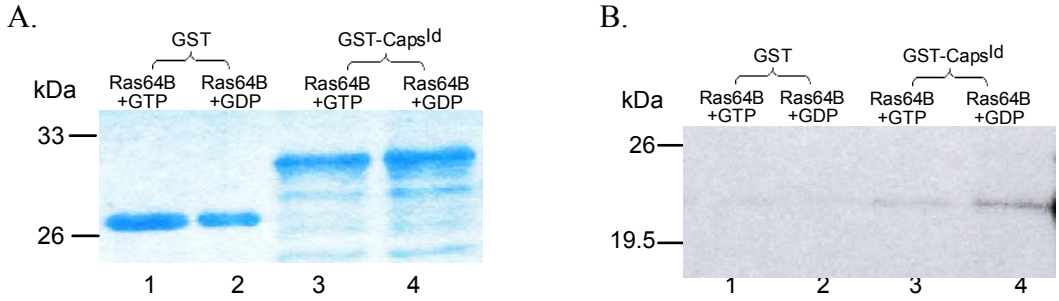

Figure 2.29. GST pull-down assay indicates direct interaction between Caps^{Id} and Ras64B.
^{35}S-labeled Ras64B in either active form containing GTP or inactive form containing GDP was generated through *in vitro* translation. Same amounts of GST and GST-Caps^{Id} fusion protein were immobilized to glutathione coupled beads and subsequently incubated with either Ras64B+GTP or Ras64B+GDP. After extensive washing, the bound protein fractions were separated by 12% SDS-PAGE and visualized by fluorography. Lane **1** and **2**: as a control, GST was incubated with Ras64B containing either GTP or GDP; lane **3** and **4**: GST-Caps^{Id} fusion protein was incubated with Ras64B containing either GTP or GDP.
A. Staining of SDS-polyacrylamide gel with Coomassie blue reveals that same amounts of GST (land **1** and **2**) and GST-Caps^{Id} fusion protein (lane **3** and **4**) were loaded.
B. Fluorography reveals single band corresponding to active or inactive Ras64B bound by GST-Caps^{Id} fusion protein (lane **3** and **4**). In contrast, GST control lanes do not show any bands.

2.5.4 Misexpression of *ras64B* results in discontinuous tracheal tubes.

Although the growth assay of the *cdc25H* yeast strain and the *in vitro* GST pull-down assay indicated strongly that Ras64B interacts specifically with Caps^{Id}, they could not provide information regarding in which cells this interaction may occur. Since Caps plays a

role not only during the outgrowth of tracheal cells but also during the formation of the affinity boundary within wing disc, it is possible that Caps associates with Ras64B only during the wing disc morphogenesis. Capability of ectopic Caps in the mesodermal cells to misguide the outgrowing tracheal cells imply that the downstream components, which mediate Caps function, are presumably also located in the mesodermal cells. Thus, if Ras64B binds to Caps^{Id} and indeed mediates Caps function in guiding the extending dorsal trunk cells, then *ras64B* would be expressed in the mesodermal cells including the bridge-cells.

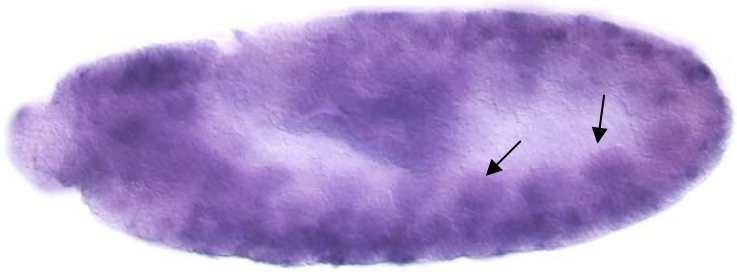

Figure 2.30. *ras64B* is expressed broadly in the mesodermal cells during early embryogenesis.
OreR wild-type embryos were hybridized *in situ* with *ras64B* antisense RNA probes. A whole-mount embryo at stage 11 reveals broad expression of *ras64B* in the mesodermal cells (arrows).

In order to analyze the expression pattern of *ras64B* during early embryogenesis, OreR wild-type embryos were hybridized *in situ* with *ras64B* antisense RNA probes. As expected, *ras64B* is not expressed exclusively in the bridge-cells like *caps* but rather broadly in the mesodermal cells (**Figure 2.30**). Concurrent expressions of *ras64B* and *caps* during the same developmental stages support further the implication that Caps^{Id} interacts with Ras64B to achieve its function as a guidance molecule.

It was shown in this thesis that discontinuous tracheal tubes are formed when *caps* is misexpressed in the mesodermal cells (**Figure 2.9**). If Ras64B indeed mediates Caps function, then the ectopic expression of *ras64B* would affect the tracheal development similarly as the misexpression of *caps* and disconnected dorsal and lateral trunks would be formed. Notably, the GST pull-down assay suggests that the inactive Ras64B binds directly to the Caps intracellular domain and presumably become activated (**Figure 2.29**). When ectopic *caps* is lacking in the mesodermal cells, Ras64B may remain inactive. Consequently, misexpression of *ras64B* would have no effect on the tracheal

morphogenesis. This problem can be circumvented by misexpressing constitutively active *ras64B*^{V12}, whose activation should be independent of Caps function. In order to investigate how ectopic Ras64B affects the outgrowth of tracheal cells, constitutively active *ras64B*^{V12} was misexpressed in the mesodermal cells using the *twi-GAL4* driver. The tracheal lumens were visualized through staining with the 2A12 antibody and the interruptions in the dorsal and lateral trunks were quantified.

A.

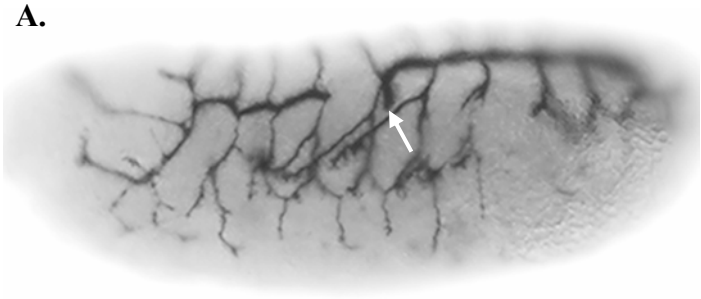

B.

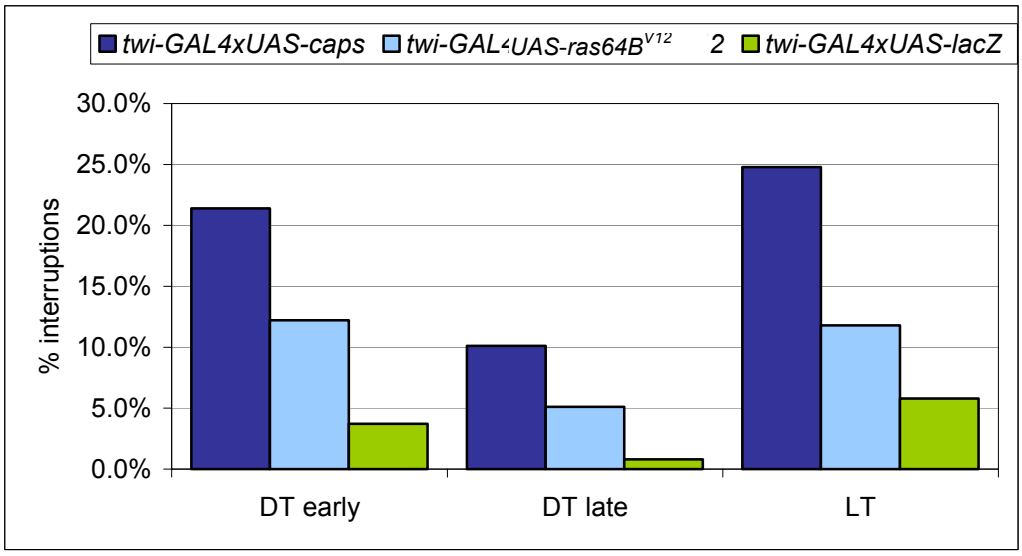

Figure 2.31. Misexpression of constitutively active *ras64B*^{V12} results in discontinuous tracheal tubes.
Embryos carrying *twi-GAL4* mesodermal driver and *UAS-ras64B*^{V12} were stained with the 2A12 antibody to visualize the tracheal lumen and the interruptions in the dorsal and lateral trunks were counted.
A. A whole-mount embryo at stage 14 reveals that the dorsal trunk as well as the lateral trunk is discontinuous. Moreover, some dorsal trunk cells extend in the wrong direction (arrow) instead of anterior-posteriorly.
B. A chart describing percentage of interruptions in the dorsal and lateral trunks of embryos misexpressing either *UAS-caps*, *UAS-ras64B*^{V12}, or *UAS-lacZ* is shown here. Interruptions of fusion points were counted for the dorsal trunks in embryos at early and late stages and for the lateral trunks.
DT early = dorsal trunk in early stage embryos; DT late = dorsal trunk in late stage embryos; LT = lateral trunk.
For embryos carrying *twi-GAL4* and *UAS-caps*, the values are as following: DT early = 21.4% (N=990), DT late = 10.1% (N=1170), LT=24.8% (N=954)
For embryos carrying *twi-GAL4* and *UAS-ras64B*^{V12}, the values are as following: DT early = 12.2% (N=900), DT late = 5.1% (N=900), LT = 11.8% (N=900)
For embryos carrying *twi-GAL4* and *UAS-lacZ*, the values are as following: DT early = 3.7% (N=990), DT late = 0.8 % (N=900), LT = 5.8% (N=900)
N = total number of fusion points counted.

As expected, embryos misexpressing constitutively active *ras64B*^{V12} reveal discontinuous dorsal and lateral trunks, similar to those embryos expressing ectopic *caps*. Moreover, some dorsal trunk cells extend in abnormal directions (compare **Figure 2.31.A** and **Figure 2.9**). However, the tracheal defect is less severe in the embryos carrying *UAS-ras64B*^{V12} than in the embryos carrying *UAS-caps*. This variation is demonstrated further in the chart comparing the interruption rates of embryos carrying either *UAS-caps*, *UAS-ras64B*^{V12} or *UAS-lacZ* (**Figure 2.31.B**). Although the embryos misexpressing constitutively active *ras64B*^{V12} demonstrate lower interruption rates than the embryos misexpressing *caps*, they show significantly higher rates than the embryos misexpressing *lacZ*. This result indicates that ectopic expression of constitutively active *ras64B*^{V12} evidently inhibits the formation of continuous dorsal and lateral trunks. Analogous tracheal deficiencies observed in the embryos misexpressing *caps* and constitutively active *ras64B*^{V12} suggest once more that Caps may mediate the guidance function of bridge-cells through the small GTPase Ras64B.

3 Discussion

3.1 Caps mediates guidance function of bridge-cell.

The guidance provided by FGF signaling is not sufficient for the formation of continuous dorsal trunk, the only multicellular tube in *Drosophila* tracheal system, (Lee et al., 1996; Sutherland et al., 1996). Single mesodermal cells called bridge-cells are required to provide supplementary local guidance for the outgrowing dorsal trunk cells (Wolf and Schuh, 2000). Identification of *caps*, which is specifically expressed in the bridge-cells, reveal that the bridge-cells require at least one cell surface molecule for its guidance function during outgrowth of dorsal trunk cells.

Interestingly, in contrast to *hb*, which is expressed in the bridge-cells as well as their sibling cells called anchor-cells, *caps* is expressed exclusively in the bridge-cells (**Figure 2.2**). This clear distinction in the expression patterns suggests on one hand, that *caps* can be used as even more specific marker for the bridge-cells than *hb*, and on the other hand, that the transcription factor Hb alone cannot activate the expression of *caps*. Ectopic expression of *hb* in the ectodermal tracheal cells fails to induce any ectopic *caps* expression. In contrast, ectopic activation of *hb* in the mesodermal cells does in fact result in ectopic induction of *caps* (**Figure 2.3**). Thus, it seems that another transcriptional activator localized in mesodermal cells including the bridge-cells regulates expression of *caps* in concert with Hb. Which transcription factor restricts *caps* expression to the bridge-cells remains to be identified. It is rather intriguing that two daughter cells arising from single cell division display such contrasting gene expressions. Interestingly, muscle progenitor cells are known to undergo such asymmetric cell divisions (Rhyu et al., 1994; Carmena et al., 1995; Spana et al., 1995; Ruiz-Gomez et al., 1997). Since bridge-cell is presumably one of the muscle progenitor cells (C. Wolf, personal communication), it is possible that the same mechanisms regulating the asymmetric cell division drive disproportionate expression of *caps*.

Earlier observations already demonstrated that the bridge-cells but not the anchor-cells stretch posteriorly towards the adjacent dorsal trunk cells and interconnect them (Wolf and Schuh, 2000). Thus, the equal expression of *hb* in the bridge-cells as well as the anchor-cells is unlikely to be solely responsible for the specific modification of cell shape or the function of bridge-cells. The distinctive expression of *caps* in the bridge-cells implies that

Caps is one of the distinguishing factors that mark the bridge-cells apart from the anchor-cells for recognition by the tracheal cells.

As observed with *hb* mutants, embryos lacking *caps* reveal disrupted dorsal trunks whereas development of other tracheal branches is not affected (**Figure 2.4**). However, in contrast to hb^{FB} mutants, which lack the bridge-cells, $caps^{65.2}$ mutants reveal viable bridge-cells (**Figure 2.6**). Thus, the interruptions in dorsal trunks of $caps^{65.2}$ embryos cannot be due to the absence of bridge-cells. Why is the directed outgrowth of dorsal trunk cells disrupted when *caps* is lacking? One reason could be that Caps plays important role in inducing the bridge-cells to stretch posteriorly to the neighboring dorsal trunk cells. When *caps* is absent, the bridge-cells frequently fail to extend towards the tracheal cells and remain round instead (**Figure 2.7**). As the bridge-cells fail to interconnect the juxtaposing tracheal metameres, the dorsal trunk cells cannot extend along the surface of bridge-cells towards their targets and consequently, gaps arise within dorsal trunk.

In addition, Caps might be involved in directly mediating communication between the bridge-cells and the tracheal cells, as it is a transmembrane protein with 14 Leucine Rich Repeats (LRR) in the extracellular domain. The crystal structure of a ribonuclease inhibitor containing 15 LRRs revealed that the LRRs are arranged consecutively and parallel to a common axis so that the conformation resembles a horseshoe (Kobe and Deisenhofer, 1995a). Such a structure provides an extensive binding area for other proteins or ligands and therefore, is ideal for cell-cell interactions (Kobe and Deisenhofer, 1995b). Possibly, the extracellular domain of Caps assumes the horseshoe-like conformation as well and binds other cell surface molecules on the tracheal cells. Thus, Caps may provide an essential link between the guiding bridge-cells and the outgrowing tracheal cells.

Caps role in the bridge-cells could be further elucidated through misexpression studies. When *caps* is ectopically expressed in other mesodermal cells through *twi-GAL4* driver, discontinuous dorsal trunks as well as lateral trunks are formed (**Figure 2.9**). Moreover, some dorsal trunk cells grow dorsally or ventrally rather than anteriorly towards their adjacent targets. Why does ectopic expression of *caps* disrupt directed outgrowth of tracheal cells? Closer analysis of embryos misexpressing *caps* reveals that some tracheal cells become misguided by ectopic sources of *caps* and extend in abnormal directions (**Figure 2.11**). Consequently, the misguided tracheal cells cannot connect to their correct targets and interruptions arise within dorsal and lateral trunks. These observations imply that ectopic expression of *caps* in the mesodermal cells can render them to become like the

bridge-cells and guide the extending tracheal cells. Presumably, ectopic Caps on the surface of mesodermal cells can bind its interactors on the surface of tracheal cells and thereby direct the outgrowth of tracheal cells. This ability of ectopic Caps to misguide the tracheal cells suggests that Caps, which is distinctively expressed in the bridge-cells, provides specific local guidance for the outgrowing dorsal trunk cells by directly interacting with them.

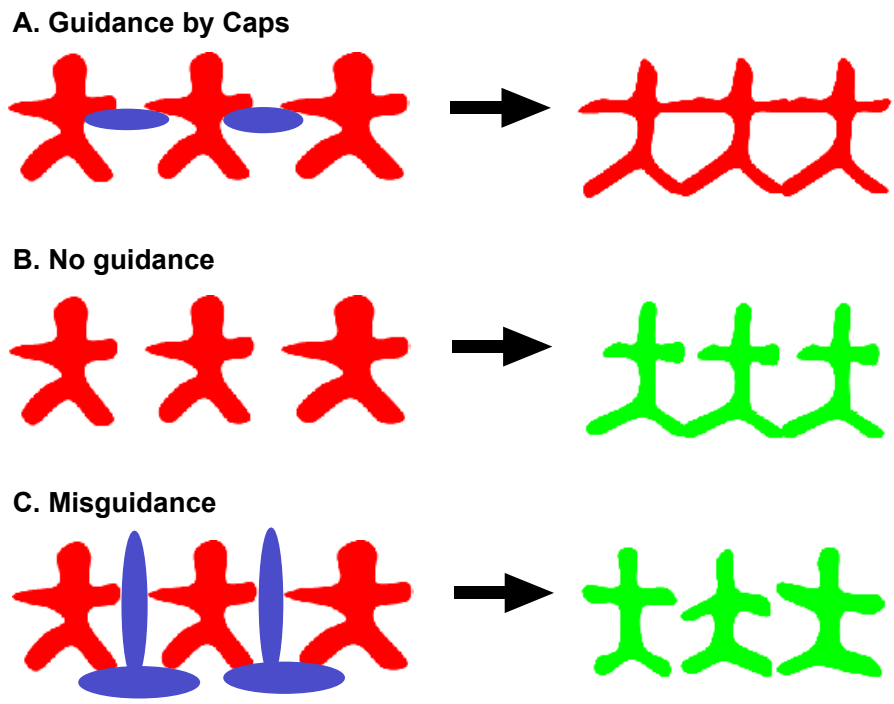

Figure 3.1. A model for Caps mediating the guidance function of bridge-cells.
A. Schematic diagram shows wild-type expression of *caps* (blue) in bridge-cells, which interconnect juxtaposing dorsal trunk cells (red). Through Caps, bridge-cells are able to interact directly with tracheal cells and guide them towards their proper targets. As a result, continuous dorsal trunk is formed.
B. When *caps* is lacking in bridge-cells, guidance function cannot be mediated properly and dorsal trunk cells fail to find their targets efficiently. Consequently, discontinuous dorsal trunk (green) is generated.
C. When *caps* is misexpressed in other mesodermal cells (blue) besides the bridge-cells, the outgrowing dorsal trunk cells become misguided by ectopic source of *caps* and extend in abnormal directions. Thus, an interrupted dorsal trunk is formed.

Based on the experimental results shown throughout this thesis, the following model proposes that Caps specifically mediates the guidance function of bridge-cells (**Figure 3.1**). In wild-type embryos, *caps* is distinctively expressed in the bridge-cells and induces elongation of the bridge-cells towards the juxtaposing dorsal trunk cells. Localized at the surface, Caps binds to cell surface molecules on the tracheal cells and enables the tracheal cells to extend along the bridge-cells towards the adjacent targets (**Figure 3.1.A**).

Subsequently, a continuous dorsal trunk is formed. When *caps* is lacking, the bridge-cells can neither interconnect the neighboring dorsal trunk cells properly nor interact with the tracheal cells and therefore, cannot direct the outgrowing dorsal trunk cells towards each other (**Figure 3.1.B**). As a result, a discontinuous dorsal trunk is formed. Finally, mesodermal cells misexpressing *caps* attain bridge-cell like identity and acquire the guidance function mediated by Caps (**Figure 3.1.C**). The tracheal cells become misguided by these ectopic sources of *caps* and consequently, tracheal branches with interruptions are generated.

$caps^{65.2}$ mutants at late stages demonstrate considerably less interruptions in dorsal trunks than the mutants at early stages (**Figure 2.5**). This reduction in interruption rates suggests that the outgrowth of dorsal trunk cells may be significantly delayed rather than completely inhibited when *caps* is lacking in the bridge-cells. Without Caps guiding them, the dorsal trunk cells may locate and extend towards their correct targets considerably more slowly than when Caps is present. Nevertheless, some dorsal trunk cells would eventually reach the adjacent targets and fuse with them. Therefore, some interruptions observed in dorsal trunks of $caps^{65.2}$ mutants at early stages would no longer be found during late stages.

If *caps* were the only downstream target of *hb* mediating the guidance function, then lack of *caps* would mimic closely lack of *hb*. However, detailed investigation reveals that lack of *caps* results in a less severe tracheal defect than lack of *hb*. This observation suggests that Caps is not the only cell surface molecule mediating the guidance function of bridge-cells. Presumably, a complex of cell adhesion molecules are involved in guiding the tracheal cell extensions along the surface of bridge-cells. Further screening for genes specifically expressed in the bridge-cells will elucidate which other cell surface molecules are required for the cell-cell interaction.

3.2 Caps functions as a cell adhesion molecule and a receptor.

Previous results demonstrated that Caps plays essential role during pathfinding of motorneurons and boundary formation in wing imaginal disc (Shishido et al., 1998; Milan et al., 2001). Normally, *caps* is expressed in a subset of CNS neurons including aCC, RP2, and RP5 (Shishido et al., 1998). When *caps* is overexpressed in all neurons, then the axons of muscle 12 motorneurons (MNs) become misrouted in 29% of segments (Taniguchi et al., 2000). Similarly, when $Caps^{Ed}$ containing only the extracellular domain is

misexpressed, then the axons of muscle 12 MNs still extend along the wrong path. However, when Caps^{Id} containing only the intracellular domain is misexpressed, no defects can be observed in pathfinding of muscle 12 MNs. These results clearly indicate that the extracellular domain of Caps is essential for misrouting of muscle 12 MNs whereas the intracellular domain is not. During boundary formation in the wing disc, cells incorrectly specified for their position undergo apoptosis because they fail to express Caps (Milan et al., 2002). Again, expression of the Caps extracellular domain alone is sufficient to prevent apoptosis of misspecified cells. During these developmental events, Caps may function as a cell adhesion molecule providing specific affinity between two different cells and thus, may require only its extracellular domain.

On the other hand, establishment of aberrant synapses of muscle 12 MNs under ectopic expression in all muscles occurs only when the whole *caps* is overexpressed (Taniguchi et al., 2000). Similarly, only embryos misexpressing the whole *caps* reveal interruptions in dorsal and lateral trunks (**Figure 2.12**). Thus, the intracellular domain is essential for ectopic Caps function. These results suggest that Caps requires its intracellular domain for its function during establishment of synapse or tracheal morphogenesis. Previously, it was postulated that Caps may interact with receptors on specific motorneurons via its extracellular domain and transmit the signal into muscles via its intracellular domain (Taniguchi et al., 2000). Likewise, Caps may function as a signal transmitter between the tracheal cells and the bridge-cells. Interestingly, proteins containing LRRs are predicted to undergo conformation change upon binding the ligand or other proteins. This change does not involve the usual movement of separate domains relative to each other, but rather an elastic alteration of the entire structure (Kobe and Deisenhofer, 1995b). Such conformational change may subsequently induce Caps to interact with other intracellular proteins involved in signaling pathways or regulation of cytoskeletal structures. It appears that depending on which functions to fulfill, Caps may act as a cell adhesion molecule or as a receptor that relays signals from the outside to the inside of cells.

3.3 Trn mediates the matrix function of mesodermal cells.

During boundary formation in wing disc development, *trn*, the gene most similar to *caps*, is expressed identically as *caps* and plays a redundant role. Whereas single mutants of *caps* or *trn* do not reveal any defects, double mutants of *caps* and *trn* demonstrate

disturbances in the affinity boundary (Milan et al., 2001). However, during tracheal morphogenesis, *trn* is expressed in non-overlapping pattern and contributes independently to the formation of continuous anterior-posterior tracheal branches. Whereas *caps* is expressed specifically in the bridge-cells but not in other mesodermal cells, *trn* is detected in the mesodermal cells but not in the bridge-cells (compare **Figure 2.2** and **Figure 2.17**). How are these contrasting expression patterns of *caps* and *trn* established? One of the transcriptional activators that can induce *caps* expression is Hb. Upon ectopic expression of *hb* in the mesodermal cells, *caps* become induced ectopically (**Figure 2.3**). On the other hand, ectopic *hb* in the mesodermal cells represses endogenous *trn* in those cells (**Figure 2.18**). Thus, Hb seems to function as a transcriptional repressor of *trn* in the mesodermal cells and may downregulate *trn* in the bridge-cells.

Possibly, *trn* expression in the bridge-cells is deliberately inhibited. What would happen when *trn* is misexpressed in the bridge-cells? Trn may disturb the guidance function of bridge-cell by competing against Caps. The extracellular domain of Trn may bind to the cell surface molecules on tracheal cells but would be unable to relay the signal to the downstream cytosolic proteins in the bridge-cells since its intracellular domain is different from Caps intracellular domain. Thus, even though the contact between the tracheal cells and the bridge-cells is established, the guidance function cannot be mediated properly. Misexpression of *trn* explicitly in the bridge-cells would elucidate whether Trn interferes with the guidance function of Caps when both proteins are co-expressed. Unfortunately, such misexpression analysis could not be done because a bridge-cell specific driver line is yet unavailable.

In embryos lacking *trn*, not only the dorsal trunk but also the lateral trunk contains gaps where the outgrowth of tracheal cells was deferred (**Figure 2.14**). These tracheal defects in $trn^{28.4}$ mutants could be efficiently rescued by restoring *trn* expression in the mesodermal cells through the *twi-GAL4* driver (**Figure 2.20**). These observations indicate that Trn plays an essential role during tracheal morphogenesis. Interestingly, the Trn extracellular domain alone is sufficient to rescue the interruptions in dorsal and lateral trunks of $trn^{28.4}$ mutants (**Figure 2.20**). Thus, Trn does not seem to need the intracellular domain for its function during tracheal development. In contrast, Caps requires both extracellular and intracellular domains for its guidance function during outgrowth of tracheal cells. In addition, misexpression of *trn* in the mesodermal cells has no effect on tracheal development, whereas ectopic expression of *caps* in the mesodermal cells results in

discontinuous tracheal branches (compare **Figure 2.10** and **Figure 2.19**). These results suggest that Trn plays a different role from Caps during tracheal development. In contrast to Caps, which may provide a guidance cue for the outgrowing tracheal cells, Trn may serve as a matrix that simply allows the tracheal cells to move along. The following model proposes that Trn presumably functions as a matrix molecule in the mesodermal cells, which allow the tracheal cells to navigate efficiently towards the targets (**Figure 3.2**).

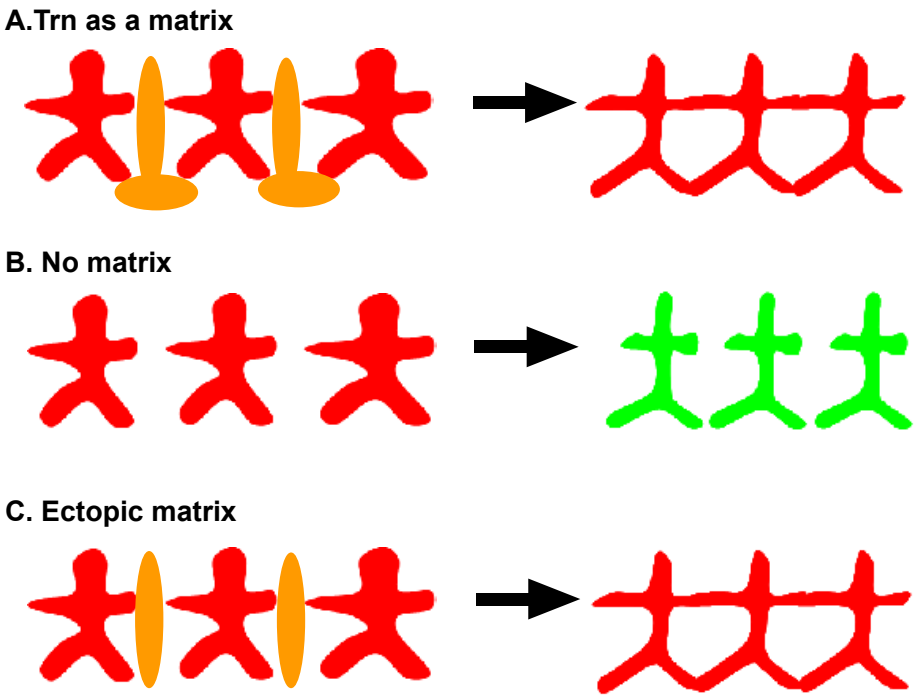

Figure 3.2. A model for Trn mediating the matrix function of mesodermal cells.
A. Schematic diagram shows wild-type expression of *trn* (orange) in mesodermal cells located laterally between dorsal trunks and ventrally from lateral trunks. The tracheal cells may use the surrounding mesodermal cells as a matrix to determine their positions and migrate towards their targets. Expressed on the surface of mesodermal cells, Trn may interact directly with other cell surface molecules on tracheal cells and thereby mediate the matrix function of mesodermal cells. As a result, continuous tracheal branches are formed.
B. When *trn* is lacking in mesodermal cells, the matrix function cannot be mediated properly and tracheal cells fail to find their targets efficiently within specified period of time. Consequently, discontinuous tracheal branches (green) are generated.
C. Ectopic overexpression of *trn* in mesodermal cells (orange) mimic closely the endogenous *trn* expression in wild-type embryos. Since Trn functions as a matrix molecule rather than as a guidance molecule, ectopic Trn allows the outgrowing tracheal cells to navigate normally through mesodermal cells and connect to their targets.

Previous studies had already indicated that the mesodermal cells help the tracheal cells to follow their migratory paths (Franch-Marro and Casanova, 2000). The mesodermal cells may serve as a matrix enabling the tracheal cells to find their ways efficiently towards the targets within specified period of time. Such cell-cell interaction most likely involves

extracellular proteins such as Trn. Localized at the surface of mesodermal cells, Trn may interact directly with other cell surface molecules on the tracheal cells and thereby mediate the matrix function of mesodermal cells (**Figure 3.2.A**). When *trn* is absent, the outgrowing tracheal cells cannot easily navigate through their migratory paths and therefore, fail to connect to their targets (**Figure 3.2.B**). Consequently, discontinuous tracheal branches are generated. On the other hand, misexpression of *trn* in the mesodermal cells is analogous to endogenous *trn* expression in wild-type embryos. Ectopic Trn allows the outgrowing tracheal cells to navigate normally through the matrix of mesodermal cells and find their targets (**Figure 3.2C**). As a result, continuous tracheal branches arise. Such a role as a matrix would require only the extracellular domain of Trn for cell-to-cell interaction. The rescue of tracheal defects in $trn^{28.4}$ mutants by expression of the Trn extracellular domain alone indicates that Trn indeed does not require its intracellular domain for the function as a matrix.

3.4 Caps intracellular domain dictates the functional specificity.

Overexpression of *trn* or extracellular domain of *trn* rescues effectively tracheal defects in $trn^{28.4}$ mutants (**Figure 2.20**). Surprisingly, interruptions in dorsal trunks can be sufficiently rescued when only the extracellular domain of Caps is expressed in $trn^{28.4}$ embryos (**Figure 2.21**). In addition, Caps and Trn share redundant functions during boundary formation in the wing disc where only the extracellular domains are required (Milan et al., 2002). These observations suggest that Caps and Trn can substitute for each other during developmental events that require only their extracellular domains. Interestingly, the primary sequences of extracellular and transmembrane domains in Caps and Trn are remarkably similar to each other (**Figure 2.13**). As the extracellular domains in both proteins contain same number of LRRs, which are also of same length, their three-dimensional structures are presumably almost identical. Thus, the extracellular domains of Caps and Trn may appear indistinguishable to the interactors on the surface of tracheal cells or wing disc cells. Another morphological process that requires only the extracellular domain of Caps is pathfinding of motorneuron 12 (Taniguchi et al., 2000). It would be interesting to find out whether the Trn extracellular domain could replace the function of the Caps extracellular domain during migration of MN12 as well. Panneural expression of

the Trn extracellular domain may reveal whether it can play a role similar to that of the Caps extracellular domain during development of motorneurons.

It has been shown so far that the extracellular domains of Caps and Trn appear to share redundant functions. However, Caps and Trn play significantly different roles during tracheal morphogenesis. Caps mediates the guidance function of bridge-cells to direct the outgrowth of tracheal cells whereas Trn contributes to the matrix function of mesodermal cells. What renders Caps functionally distinct from Trn? Since the extracellular domains of Caps and Trn seem to be redundant, it is plausible to assume that the intracellular domain dictates the functional specificity of Caps. Consistent with this presumption, the hybrid protein $Trn^{Ed}Caps^{Id}$, which contains Caps intracellular domain, functions like Caps rather than like Trn. Misexpression of $Trn^{Ed}Caps^{Id}$ in the mesodermal cells results in discontinuous tracheal branches (**Figure 2.23**). Moreover, expression of the $Trn^{Ed}Caps^{Id}$ hybrid protein aggravates the tracheal defects in $trn^{28.4}$ mutants (**Figure 2.24**). These observations suggest that the $Trn^{Ed}Caps^{Id}$ hybrid protein can guide the outgrowing tracheal cells similarly as Caps even though it contains only the intracellular domain of Caps. Thus, it is the intracellular domain and not the extracellular domain that differentiates Caps functionally from Trn during tracheal morphogenesis. Is this determination of functional specificity by the intracellular domain a special case of Caps or does it apply to other cell surface molecules in general? Future investigations of cell surface molecules including a comprehensive analysis of their extracellular domains separately from their intracellular domains may elucidate how the specification of their function is established.

3.5 Caps interacts with small GTPase protein Ras64B.

The unique intracellular domain of Caps is essential for Caps function as a guidance molecule in the bridge-cells for the outgrowing tracheal cells. Moreover, it is the intracellular domain that dictates the functional identity of Caps. How does the intracellular domain mediate Caps function? Alignment of DmeCaps against AgaCaps revealed conservation of three putative motifs within the intracellular domain: the RHR motif, the putative tyrosine phosphorylation site and the PDZ binding motif (**Figure 2.25**). Site-directed mutagenesis of these putative functional motifs suggests that only the RHR motif is essential for Caps function during tube formation. Misexpression of Caps containing mutated the tyrosine phosphorylation site or Caps lacking the PDZ binding

motif resulted in the formation of disrupted tracheal branches (**Figure 2.8**). In contrast, ectopic expression of Caps with mutated RHR motif had no effect on tubular structure. This RHR motif is not yet recognized as a functional motif by existing protein data bases available at ExPASy server (Gasteiger et al., 2003). Therefore, no information regarding other proteins containing such a motif or prediction about its putative function is known. Located immediately after the transmembrane domain, the RHR motif may interact with small membrane-associated proteins that bind the components of signaling pathways or the cytoskeleton. Identification of other proteins containing the RHR motif would help to elucidate its specific function.

One of the putative interaction partners of Caps was identified through a yeast two-hybrid screening using the Caps intracellular domain as a bait protein. The temperature sensitive mutant strain *cdc25H* can grow at the restrictive temperature when $caps^{Id}$ and *ras64B* are coexpressed (**Figure 2.28**). In addition, a GST pull-down assay with immobilized GST-$Caps^{Id}$ fusion protein reveals that Ras64B binds specifically to $Caps^{Id}$ (**Figure 2.29**). These *in vivo* and *in vitro* results suggest that $Caps^{Id}$ interacts specifically with Ras64B. Interestingly, inactive Ras64B containing GDP demonstrates significantly stronger binding affinity to $Caps^{Id}$ than active Ras64B (**Figure 2.29**). This observation suggests that Ras64B in its inactive form binds to the intracellular domain of Caps and become presumably activated. Thus, Caps may mediate the guidance function of bridge-cells through the Ras64B GTPase, which is known to interact with transmembrane receptors and to be a crucial component of signaling pathways (de Celis and Garcia-Bellido, 1994; Glise and Noselli, 1997).

When *caps* is ectopically expressed in the mesodermal cells, then the mesodermal cells seem to acquire the guidance function of bridge-cells and misguide the outgrowing tracheal cells. Consequently, discontinuous tracheal branches, which grow frequently in abnormal directions, are formed (**Figure 2.9**). This observation already suggested that the downstream targets of Caps must be expressed in those mesodermal cells as well as the bridge-cells. Thus, if Caps mediates the guidance function through Ras64B, then Ras64B should be localized in the mesodermal cells. Furthermore, misexpression of constitutively active $ras64B^{V12}$ in the mesodermal cells would mimic misexpression of *caps* and would cause formation of disconnected tracheal branches. As expected, analysis of the *ras64B* expression pattern during early embryogenesis reveals that *ras64B* is expressed broadly in the mesodermal cells (**Figure 2.30**). Moreover, embryos expressing constitutively active

ras64B^{V12} ectopically in the mesodermal cells reveal discontinuous tracheal tubes similarly as embryos misexpressing *caps* (**Figure 2.31**). These results from diverse *in vitro* and *in vivo* experiments investigating the interaction between Caps and Ras64B suggest consistently that Ras64B presumably binds to the Caps intracellular domain and thereby mediates Caps function as a guidance molecule.

Notably, in addition to Ras64B, Rho1 and other proteins containing predicted functional domains have been identified as putative interaction partners of Caps^{Id} through the yeast two-hybrid screening (**Table 2.1**). One of the important future experiments would be to confirm the association between Caps^{Id} and other putative interactors similarly as it was verified for Ras64B. As more and more interactors of Caps become known, deeper understanding of the underlying mechanisms that regulate the guidance function in the bridge-cells can be obtained.

So far, the results have shown that Caps requires both extracellular and intracellular domains for its ectopic function during outgrowth of tracheal cells. Various observations indicate that Caps associates with a small GTPase, Ras64B, through its intracellular domain. Usually, receptor molecules need an extracellular as well as an intracellular domain for their function as they receive signal from outside via their extracellular domains and transmit the signal to other cytosolic proteins via their intracellular domains. Although Caps is previously known as a cell adhesion molecule, these novel understandings of its mechanism suggest that it functions more like a receptor molecule in the bridge-cell. Caps may bind cell surface molecules on the tracheal cells through its extracellular domain and subsequently undergo a conformational change that induces the interaction between Caps and signal pathway components such as Ras64B. The functional analysis of Caps implies that mechanisms underlying cell surface molecules may be more complex. Depending on the developmental context, the cell surface molecules may operate as cell adhesion molecules or as receptor molecules. To function as cell adhesion molecules, the cell surface molecules require only their extracellular domains to mediate direct cell-to-cell contact. However, as the signal from outside is received via their extracellular domains and transmitted to other cytosolic proteins via their intracellular domains, the cell surface molecules need extracellular as well as intracellular domains to function as receptors.

4 Materials and methods

4.1 Source of materials

4.1.1 Standard chemicals and kits

- Gel extraction and purification kit: Quiagen (Hilden)
- Maxi- midi- and mini-plasmid preparation kit: Quiagen (Hilden)
- TOPO® PCR Cloning Kit: Invitrogen (Karlsruhe)
- Y-DER® Yeast DNA Extraction Reagent Kit: Pierce (Bonn)
- TSA™ Fluorescence or Biotin Systems: PerkinElmer (Jügesheim)
- TNT® T7 Coupled Reticulocyte Lysate System: Promega (Mannheim)
- Dig or fluorescein RNA labeling mix: Boehringer (Mannheim)
- Vectastain® ABC-AP and ABC elite kit: Vector Laboratories (Grünberg)
- QuikChange® Site-Directed Mutagenesis Kit: Stratagene (Heidelberg)
- Advantage® 2 PCR Enzyme System: Clontech (Heidelberg)
- Glutathione Sepharose 4B beads: Amersham (Braunschweig)
- CH Sepharose 4B beads: Amersham (Braunschweig)
- Agarose, formamide, phenol, LB-medium and -agar, BBL-agar: Gibco-BRL (Eggenstein)
- Binding-silan, repel-silan: Pharmacia (Freiburg)
- Chemicals (in p.A. quality): Serva (Heidelberg), Sigma (München), Merck (Darmstadt)
- ^{35}S-methionine (1000 Ci/mmol): Amersham (Braunschweig)
- DNA-modifying enzymes and restriction endonucleases: Amersham (Braunschweig), Boehringer (Mannheim), Pharmacia (Freiburg), Gibco-BRL (Eggenstein) and Biolabs (Schwalbach)
- RNase A, DNase I, lysozyme: Sigma (München)
- 1 kb Ladder: MBI Fermentas (St.Leon-Rot)
- Prestained protein molecular weight marker: MBI Fermentas (St.Leon-Rot)
- Glutathione Sepharose 4B: Amersham (Freiburg)
- *Drosophila* EST (expressed sequence tag): Invitrogen (Karlsruhe)

4.1.2 Equipments

- Centriprep®: Millipore (Eschborn)
- Ultra centrifuge tubes: Beckman (München)
- Plastic microfuge tubes: Eppendorf (München)
- Plastic ware: Greiner (Nürtingen)
- General laboratory techware: Schütt (Göttingen)
- Spectrophotometer: Pharmacia (Freiburg)
- Binocular: Stemi SV 11, Zeiss (Göttingen)
- Electroporation device: Bio-Rad (München)
- Photomicroscope: Zeiss Axiophot (Göttingen)
- Table centrifuge: Heraeus (Hanau)
- Centrifuge: Sorvall (Langenselbold)
- Slab Gel Dryer: Pharmacia (Freiburg)
- X-Ray Automatic Processor Optimax TR: MS-Laborgeräte (Wiesloch)

4.1.3 Reagents and buffers

Generally, all solutions were prepared using double deionized and autoclaved water. For electrophoresis, normal distilled water was used. Concentration factor of concentrated solutions are indicated in parenthesis. Solutions that need to be autoclaved (121°C, 45 min) or sterile filtered before use are marked by "*" and "**", respectively. Storing temperatures for solutions, which are not kept at room temperature, are shown in parenthesis. All percentages are indicated as weight/volume relation.

- Alkaline phosphatase buffer*:
  100 mM Tris-HCl (pH 9.5)
  100 mM NaCl
  50 mM $MgCl_2$
- Ampicillin solution (-20°C)**:
  100 mg/ml
- DNA loading buffer (6 x):
  0.1 % bromophenolblue
  0.1 % xylene cyanol FF
  15 % ficoll 400
- BBS (10x, -20°C):
  100 mM Tris
  550 mM NaCl
  400 mM KCl

	70 mM $MgCl_2$ 50 mM $CaCl_2$ 200 mM D(+)-glucose 500 mM saccharose pH 6.95
♦ BBT (4°C):	BBS (1X) 0.1% BSA 0.1% Tween 20
♦ binding buffer	20 mM Tris-HCl (pH 7.5) 150 mM NaCl
♦ Calcium chloride**:	100 mM
♦ Carbonate buffer (2x):	120 mM Na_2CO_3 80 mM $NaHCO_3$ (pH 10.2)
♦ Chloramphenicol (-20°C)	25mg/ml
♦ Coupling buffer	0.1M $NaHCO_3$ (pH 8) 0.5M NaCl
♦ DAB (Diaminobenzidine) solution:	10 mg/ml in 50 mM Tris-HCl (pH 7.5)
♦ DNase I-solution (-20°C):	10 mg/ml in water/glycerol: 1/1
♦ DTT**:	0.1 M dithiotreitol
♦ EDTA*:	0.5 M (pH 8.0)
♦ Elution buffer	100 mM glycine (pH2.5)
♦ Ethidium bromide solution: (4°C, protect from light)	10 mg/ml
♦ FastRed buffer	0.1 M Tris-Cl (pH 8.2) 0.1% Tween 20
♦ Fixative (for embryos used for antibody staining or *in situ* hybridization, 4°C)	10% paraformaldehyde 50 mM EGTA in 1X PBS (pH 7)
♦ Glucose**:	1 M
♦ HEPES solution**:	100 mM HEPES (pH 6.9) 2 mM $MgSO_4$ 1 mM EGTA

♦ Hybridization solution: (for RNA *in situ* hybridization with digoxigenin or fluorescein labeled probes) (-20°C)	50 % formamide (deionized) 0.1 % Tween 20 50 µg/ml heparin 100 µg/ml sonicated, denatured Salmon sperm DNA
♦ Hybridization solution B:	50% formamide and 5x SSC in water
♦ Calcium chloride**:	100 mM
♦ 50% Clorox-solution:	equivalent to 2.5% sodium hypochloride solution
♦ IPTG-solution (-20°C)**:	1 M
♦ Levamisol solution (4°C):	50 mM
♦ Ligation buffer (10 x, -20°C):	500 mM Tris-HCl (pH 7.5) 100 mM $MgCl_2$ 20 mM DTT 20 mM spermidine 10 mM ATP
♦ LiSORB	100mM LiOAc 10mM Tris-HCl (pH8.0) 1mM EDTA 1M sorbitol
♦ Lithium chloride**:	4 M
♦ lysis buffer (4°C)	25mM Hepes/KOH (pH7.6) 0.1mM EDTA (pH8.0) 12.5mM $MgCl_2$ 10% glycerol 0.5M NaCl 0.1% NP-40 add 1 tablet of protease inhibitor (EDTA free from Roche) per 25ml
♦ Magnesium chloride*:	1 M $MgCl_2$
♦ Magnesium sulfate*:	1 M $MgSO_4$
♦ β-mercapthoethanol	1.4M
♦ PEG/LiOAc	10 mM Tris-HCl (pH8.0) 1 mM EDTA (pH8.0) 100 mM LiOAc (pH7.5)

- Salmon sperm DNA (-20°C): 20 mg/ml
- Sodium acetate*: 3 M NaOAc (adjust pH with acetic acid to 6.0–7.0)
- PBS (10 x)*: 1.3 M NaCl
  100 mM Na-PO_4 buffer (pH 7.4)
- PBT: 1 x PBS
  0.1 % Triton-X-100
- Restriction enzymes buffers (10x, -20°C):
  A-buffer: 33 mM Tris-acetate (pH 7.9)
  10 mM magnesium acetate
  66 mM potassium acetate
  0.5 mM dithiothreitol (DTT)

  B-buffer: 10 mM Tris-acetate (pH 8)
  5 mM magnesium chloride
  100 mM NaCl
  1 mM 2-mercaptoethanol

  H-buffer: 500 mM Tris-HCl (pH 7.5)
  100 mM $MgCl_2$
  1 M NaCl
  10 mM DTT

  L-buffer: 100 mM Tris-HCl (pH 7.5)
  100 mM $MgCl_2$
  10 mM DTT

  M-buffer: 100 mM Tris-HCl (pH 7.5)
  100 mM $MgCl_2$
  500 mM NaCl
  10 mM DTT

  One-Phor-All buffer PLUS: 100 mM Tris-acetate
  100 mM magnesium acetate
  100 mM potassium acetate

  Not I - buffer: H-Puffer
  0.01% Triton X-100
- RNase A solution (-20°C): 20 mg/ml
- SDS-polyacrylamide gel (12%):
  Running Gel: 6.6 ml H_2O
  8.0 ml 30% acrylamide
  5.0 ml 1.5M Tris (pH8.8)

	0.2 ml 10% SDS 0.1 ml 20% APS 8 µl TEMED
Stacking gel:	1.835 ml H_2O 2.51 ml 0.25M Tris (pH 6.8) 0.2% SDS 650 µl 30% acrylamide 25 µl APS 5 µl TEMED
♦ 6x SDS loading buffer (-20°C)	0.35M Tris-HCl (pH 6.8) 10.28% SDS 35% glycerol 5% β-mercaptoethanol 0.1% bromphenolblue
♦ SSC (20 x)*:	3 M NaCl 0.3 M sodium citrate (pH 7.0)
♦ TAE-buffer (50 x):	2 M Tris-Base 50 mM EDTA adjust pH to 8.0 with acetic acid
♦ TBE-buffer (10 x):	800 mM Tris-Base (pH 8.2) 800 mM boric acid 20 mM EDTA
♦ TE*:	10 mM Tris-HCl (pH 8.0) 1 mM EDTA
♦ TELT:	50 mM Tris-HCl (pH7.5) 62.5 mM EDTA 2.5 M LiCl 0.4% Triton-X-100
♦ Tris-HCl*:	1 M (pH 9.5)
♦ wash buffer 2:	25mM Hepes/KOH (pH 7.6) 0.1mM EDTA (pH 8.0) 12.5mM $MgCl_2$ 10% glycerol 0.5M NaCl 0.01% NP-40 add 1 tablet of protease inhibitor (EDTA free from Roche) per 25ml
♦ wash buffer 3:	25mM Hepes/KOH (pH 7.6)

	0.1mM EDTA pH8.0 12.5mM $MgCl_2$ 10% glycerol 0.1M NaCl 0.01% NP-40 add 1 tablet of protease inhibitor (EDTA free from Roche) per 25ml
♦ X-Gal solution or BCIP (-20°C):	8 % in DMSO

4.1.4 Mediums for *E. coli*

The LB medium and agar are autoclaved (45 min, 121°C) before use.

♦ LB medium (Luria-Bertani medium):	10 g bacto-tryptone 5 g bacto-yeast extract 10 g NaCl add 950 ml deionized water Adjust pH to 7.0 with 5N NaOH
♦ LB agar:	LB medium with 15 g agar-agar

4.1.5 Mediums for *S. cerevisiae*

The YPAD medium and agar are autoclaved (15 min, 121°C) before use.

♦ YPAD medium	6.0 g bacto-yeast extract 12.0 g peptone 12.0 g glucose 60 mg adenine hemisulphate 600 ml distilled water
♦ YPAD agar	YPAD medium with 2% agar
♦ Synthetic glucose minimal medium	1.7 g yeast nitrogen base without amino acids 5 g ammonium sulfate 20 g glucose 900 ml distilled water autoclave at 121°C for 15 min cool to 55°C add 100 ml drop-out solution (10x)
♦ Synthetic galactose minimal medium	1.7 g yeast nitrogen base without amino acids 5 g ammonium sulfate 20 g galactose 10 g raffinose

900 ml distilled water
autoclave at 121°C for 15 min
cool to 55°C
add 100 ml drop-out solution (10x)

- Synthetic minimal plates: 1 l synthetic minimal medium, 17 g Bacto agar

4.1.6 Mediums for *D. melanogaster*

- Fly food: 8 g agar, 18 g inactive dry yeast, 10 g soy bean powder, 80 g cornmeal, 7 g light corn syrup, 80 g malt extract, 6.3 ml propionic acid, add 1 l tap water
- Apple juice agar: 1 l apple juice, 100 g sugar, 95 g agar, 40 ml 15 % Nipagin (in 95 % ethanol), add 3 l tap water
- Baker's yeast: baker's yeast mixed and stirred with proper amount of tap water until soft and sticky but not watery

4.1.7 Plasmids used

- *caps* cDNA: Shishido et al., 1998
- *trn* cDNA: EST GH10871
- *hb* cDNA: EST LD34229
- *btl* cDNA: Glazer and Shilo, 1991
- pCR®II-TOPO®: Invitrogen (Karlsruhe)
- pUAST: Brand and Perrimon, 1993
- pSos: Stratagene (Heidelberg)
- pMyr: Stratagene (Heidelberg)
- pGEX-4T-3: Amersham (Braunschweig)
- pcDNA3.1/His B: Invitrogen (Karlsruhe)

4.1.8 Antibodies used

Table 4.1 Primary antibodies used

Primary Antibody	mono- / polyclonal	Company / Donor	Working Concentration
2A12, mouse IgM	Monoclonal	Hybridoma Bank	1:5
anti-β–Galactosidase, mouse IgG	Monoclonal	Promega	1:600 – 1:1000
anti–β–Galactosidase, rabbit IgG	Polyclonal	Cappel	1:1000
anti-Capricious, rabbit IgG	polyclonal	this thesis	1:100
anti-Hunchback, guinea pig IgG	polyclonal	La Rosée[1]	1:400
anti-digoxigenin-AP	Fab fragment	Roche	1:1000
anti-fluorescein-AP	Fab fragment	Roche	1:1000
anti-digoxigenin-POD	Fab fragment	Roche	1:400
anti-fluorescein-POD	Fab fragment	Roche	1:400

[1] Wolf and Schuh, 1998

Table 4.2 Secondary antibodies used

Conjugated Secondary Antibody (monoclonal)	Company	Working concentration
biotinylated goat anti-mouse IgM	Jackson	1:600
biotinylated horse anti-mouse IgG	Vector	1:250
biotinylated goat anti-rabbit IgG	Vector	1:250
AP coupled goat anti-rabbit IgG	Vector	1:250
goat anti-mouse IgG-Cy3	Molecular Probes	1:1000
goat anti-rabbit IgG-Cy3	Molecular Probes	1:1000
goat anti-mouse IgG-Cy2	Molecular Probes	1:300
goat anti-rabbit IgG-Cy2	Molecular Probes	1:300
goat anti-guinea pig-Cy3	Molecular Probes	1:200

4.1.9 *E. coli* and *S. cerevisiae* strains used

- XL1-Blue:(Bullock et al., 1987; Stratagene)

  *sup*E44 *hsd*R17 *rec*A1 *end*A1 *gyr*A46 *thi rel*A1 *lac*$^-$ F' [*pro*AB$^+$ *lac*I^q *lacZ*ΔM15 Tn*10*(*tet*^{r})]

- DH5-α: (Hanahan, 1983)

  *sup*E44 ΔlacU169 (ϕ80 *lacZ*ΔM15) *hsd*R17 *rec*A1 *end*A1 *gyr*A96 *thi*-1 *rel*A1

- BL21-CodonPlus®(DE3)-RIL Competent Cells (Jerpseth et al., 1998; Stratagene)
  E. coli B F^- *ompT hsdS*(rB^- mB^-) dcm^+ Tetr *gal* λ(DE3) *endA* Hte [*argU ileY leuW* Cam^r]

- *cdc25H* (Petitjean et al., 1990; Stratagene)
  MATα *ura3-52 his3-200 ade2-101 lys2-801 trp1-901 leu2-3 112 cdc25-2* Gal^+

4.1.10 *D. melanogaster* strains used

- *btl-GAL4*: Shiga et al., 1996
- *twi-GAL4*: Greig and Akam, 1993
- *UAS-caps*: Shishido et al., 1998
- *UAS-caps*^{Ed}: Taniguchi et al., 2000
- *UAS-caps*^{Id}: Taniguchi et al., 2000
- *UAS-caps*^{Ed}*trn*^{Id}: this thesis
- *UAS-trn*^{Ed}*caps*^{Id}: this thesis
- *UAS-caps*$^{\Delta RH}$: this thesis
- *UAS-caps*$^{\Delta Y}$: this thesis
- *UAS-caps*$^{\Delta PDZ}$: this thesis
- *UAS-trn*: Milan et al., 2001
- *UAS-trn*^{Ed}: Milan et al., 2002
- *UAS-hb*: Wimmer et al., 2000
- *UAS-ras64B*^{V14}: Brand and Perrimon, 1993
- *UAS-GFPNlacZ*: Shiga et al., 1996
- *caps*$^{65.2}$: Shishido et al., 1998
- *trn*$^{28.4}$: Chang et al., 1993

4.2 Molecular Biology

4.2.1 Cultivation of *E. coli* and *S. cerevisiae*

E. coli cells are grown in liquid LB medium containing appropriate antibiotics at 37°C with vigorous shaking (250 rpm) for overnight. Alternatively, the cells are streaked on agar plates containing appropriate antibiotics and incubated at 37°C for overnight. *S. cerevisiae* cells are grown either in YEPD or in synthetic minimal medium at 25°C for overnight.

4.2.2 Cloning methods

4.2.2.1 Measuring DNA concentration using UV spectrophotometer

The amount of DNA in solution, either double-stranded (ds) or single-stranded (ss), can be measured by their absorbance value at 260nm (OD_{260}) using UV light calculated by the following formula:

$$1\ OD_{260} = 50\ g\ dsDNA/ml$$

$$1\ OD_{260} = 40\ \mu g\ ssDNA/ml$$

4.2.2.2 Purification of DNA

1. Phenol-chloroform extraction

   Add an equal volume of phenol:chloroform to the DNA sample. Mix the contents of the tube until an emulsion forms. Centrifuge the mixture at 12,000g for 15 seconds in a microfuge at room temperature. Check if the organic and aqueous phases are well separated. If not, repeat centrifugation. Transfer the aqueous phase to a new tube. Repeat these steps until no protein is visible at the interface between the organic and aqueous phase. Add an equal volume of chloroform and repeat the extraction steps. Recover the DNA by precipitation with ethanol as described below.

2. Ethanol precipitation

   Estimate the volume of DNA solution. Add an equal volume of TE or H_2O to dilute the DNA concentration. Add 2 volumes of ice-cold 100% ethanol and 1/10 volume of 3M NaOAc and mix the solution well. Centrifuge at 15,000g for 20 minutes at 4°C. Prolong the centrifugation if DNA amount is less than 0.1μg/ml. Remove carefully the supernatant and fill half of the tube with 70% ethanol to wash the DNA. Recentrifuge at 15,000g for 15 minutes at 4°C. Remove the supernatant and air-dry. Resuspend the DNA pellet in the desired volume of TE or H_2O.

3. Isopropanol precipitation

   The principle is similar to ethanol precipitation. Add 1/10 of 3M NaOAC and 0.7 volume of isopropanol to the 1:1 DNA-H_2O solution. Mix well, incubate for 15 minutes at room temperature and then centrifuge at 15,000g for 15 minutes at 4°C.

The washing and evaporation steps are as described in ethanol precipitation. Resuspend the DNA pellet in the desired volume of TE or H_2O.

4.2.2.3 PCR (polymerase chain reaction)

Advantage®2 PCR enzyme system (Clontech) was used to amplify the DNA fragments encoding the intracellular domains of Caps and Trn. Such amplified DNA fragments were then inserted into appropriate vector plasmids to generate *caps*^{Ed}*trn*^{Id} and *trn*^{Ed}*caps*^{Id} hybrid constructs, p*Sos-caps*^{Id} bait construct, and finally *GST-caps*^{Id} fusion protein construct. In addition, *ras64B* cDNA was also amplified for cloning into pcDNA3.1/HisB vector. The primers were designed to contain appropriate restriction sites so that the amplified fragments can be inserted into the corresponding vectors in frame (**Table 4.3**). As DNA templates, *caps* cDNA (Shishido et al., 1998), *trn* cDNA (GH10871) or *ras64B* cDNA (RE36103) was used.

Table 4.3. Primers used in PCR or site-directed mutagenesis.

Primer name	Primer sequence
caps^{Id} forward	5' GAGCGCGAATACCAGAAGACCTTCTCCG
caps^{Id} reverse	5' TATCCCGGTTCAGACATCGCATCACACG
trn^{Id} forward	5' TGGCTTTGGTTCTGTACACCTGCCGTC
trn^{Id} reverse	5' CGCGTAATACGACTCACTATAGG
pSos-caps forward	5' CGCGGATCCACACCTGCCGTCATAG
pSos-caps reverse	5'ATAAGAATGCGGCCGCCGCTGGCGGTGCTGG
pGEX-caps forward	5'CGTGGATCCACCTGCCGTCATAGGATTC
ras64B forward	5'GGAATTCTATGCAGATGCAAACGTACA
ras64B reverse	5'GCTCTAGACGGCATTCAGGAGATTCTC
RH mut upper	5' CTCTACACCTGCGGTGGTAGGATTCGGGAG
RH mut lower	5' CTCCCGAATCCTACCACCGCAGGTGTAGAG
Y mut upper	5' TCCGATGAAGAGGGCATGTCGCGACCACC
Y mut lower	5' GGTGGTCGCGACATGCCCTCTTCATCGGA
PDZ del upper	5' CGGATGATACCGTAGACCGAGCTTTAGC
PDZ del lower	5' GCTAAAGCTCGGTCTACGGTATCATCCG

In general, the reaction was performed according to the user manual provided by Clontech (Protocol #PT3281-1). Each PCR reaction (50µl) contained the following reagents:

template DNA:	100ng
50x dNTP Mix (10mM each)	1µl
forward primer (10µM)	2.5µl
reverse primer (10µM)	2.5µl
10x Advantage 2 PCR buffer	5µl
50x Advantage 2 Polymerase Mix	1µl
ad 50µl with PCR-Grade water	

Cycling was done following the parameters described in the user manual by Clontech (Protocol #PT3281-1) using the PerkinElmer thermocycler. Generally, the cycling parameter was:

95°C 1 min;

25cycles { 95°C 30 sec
68°C 1 min (for amplification of fragments < 1 kb)
or 3 min (for amplification of 1-3 kb fragments)

68°C 1 min

72°C 10 min

4.2.2.4 Agarose gel electrophoresis

DNA fragments are separated according to their molecular size in agarose gels of different concentrations (usually 0.5 -1.5 %). To prepare the agarose gel, the desired amount of agarose powder is dissolved in 0.5 x TAE or 0.5 x TBE buffer and the solution is boiled until it is clear and homogenized. Before pouring the gel, ethidium bromide (EtBr) solution is added to end concentration of 40µg/100ml in order to examine the gel by ultraviolet light during the run. The agarose-EtBr mixture is poured into a plaxiglass plate, which is sealed with tapes and inserted with a comb that generates the desired number of wells and sizes. After the gel is completely set (30-45 minutes at room temperature or 15 minutes at 4°C), the comb and the tapes are carefully removed and transferred to the electrophoresis tank. The volume of the electrophoresis buffer (0.5 x TAE or 0.5 x TBE buffer) should cover the gel to a depth of about 1mm. The sample DNA with the desired gel-loading buffer (Sambrook et al., 1989) is carefully pipetted into the wells of submerged gel using a disposable micropipette. The voltage used to run the gel ranges from 20-150 volt and

depends on the percentage of the gel. For preparative gels, the voltage can be set at a maximum of 7V/cm of gel length. A molecular weight marker, the 1 kb-Ladder, is used and loaded in a separate well. The DNA fragments are visualized with a UV-transilluminator at 366 nm. To document the gel, the image captured by Polaroid camera is printed onto a thermopaper.

4.2.2.5 DNA extraction from agarose gel

To recover the DNA from TAE or TBE agarose gels, the desired DNA fragments are cut out with a clean, sterilized scalpel. Following the procedures described in Gel Extraction Kit Handbook (Quiagen), the DNA in agarose is incubated with solvent and glass milk, which serves as a substrate for DNA. The DNA-glass milk complex is washed several times to get rid of excessive salt, dye and agarose. Subsequently, the DNA is eluted from the glass milk. The elution is dissolved in adequate amount of TE or H_2O. As a control, an adequate amount of eluted DNA is loaded on an agarose gel

4.2.2.6 Restriction of DNA

Restriction endonucleases are used to characterize, isolate and linearize DNA.

For analytical purpose, 1µg of phage or plasmid DNA is incubated with restriction enzyme(s) in a final volume of 20-40µl for 1h (depending on the enzyme) at 37°C or at the enzyme-specific temperature. For DNA preparation, adequate amount of DNA is incubated with proper units of restriction enzyme(s) for prolonged time span (2-5h) at the temperature as described above. The salt concentration for optimal restriction digest is adjusted by enzyme-specific restriction buffers (e.g., L-, M-, H- A-, B- buffer) added in the digest reaction.

For DNA double digest, two kinds of enzymes working with a similar or the same salt concentration can be added in the same reaction. Otherwise, the enzyme working at a lower salt concentration than the other one should be added first for reaction before the second digest is performed. Before continuing the second digest, the salt concentration should be adjusted to match the optimal working condition of second enzyme.

4.2.2.7 Dephosphorylation of restricted DNA

During the ligation reaction, the foreign DNA and the plasmid carrying identical termini (either blunt-ended or protruding) have the capacity to circularize and form tandem oligomers. Removal of 5'-phosphate groups with alkaline phosphatase is frequently used

to suppress self-ligation and recircularization of plasmid DNA. To dephosphorylate, the restricted DNA is incubated for 30 minutes at 37°C with appropriate amount of dephosphorylation buffer and alkaline phosphatase (1µl CIP, Boehringer Mannheim). At the end of incubation, the dephosphorylated DNA is precipitated with ethanol. The DNA is resuspended in TE or H_2O.

4.2.2.8 DNA Ligation

50 ng to 1 µg of restricted and dephosphorylated vector DNA is incubated with 2-3 molar excess of isolated DNA fragments. In addition, the ligation mixture contains ligation buffer and 1unit of T4-DNA ligase in a total volume of 15 to 20 µl. Subsequently, the ligation mixture is incubated for 6-18 h at 16°C or 4h at room temperature. To enhance the ligation reaction and the efficiency of ligation (e.g., in the case of blunt end ligation), 5 % PEG 6000 (5 x Ligation buffer) can be used as an alternative. The incubation is performed at room temperature for 4-8 h. PCR products are generally ligated directly into pCR®II-TOPO® vector following the procedures described in the instruction manual by Invitrogen (Karlsruhe)

4.2.2.9 Preparation of *E. coli* electrocompetent cells

50 ml LB-Medium with tetracycline (10µg/ml) is inoculated with 1 well-isolated colony of DH5-α or XL1-Blue cells and grown overnight at 37°C. On the next day, 1l of LB-tetracycline$^+$ medium is inoculated with 20 ml of the fresh overnight culture and grown to an OD_{600} of 0.5 to 0.6 at 37°C. From now on, all steps are performed on ice. The cells are spinned down at 4,000g for 10 minutes at 4°C and the pellet is resuspended in 1l cold, sterilized water (4°C). The suspension and centrifugation steps are repeated twice at the same conditions. Then, the pellet is resuspended in 0.5l ice cold 10% sterilized glycerol and spinned down at 4,000g for 10 minutes at 4°C. The pellet is resuspended in 1 pellet volume of ice cold 10% sterilized glycerol. The suspension aliquots of 80µl are pipetted into microfuge tubes, submerged into liquid N_2 and stored at -80°C.

4.2.2.10 Transformation using electroporation

40µl frozen competent *E. coli* XL1-Blue or DH5-α cells are thawed on ice and then mixed with 1 to 2µl of plasmid DNA. The mixture is pipetted with care (avoid producing bubbles) into cooled electroporation cuvette, which is placed into the cooled slot of

electroporation machine ("Pulse-Generator/Capacitor" adjusted to 250 µFD, 1,8 kV, 200 W). After applying the current (a pulse duration between 3.5 and 4.2 ms usually yields high efficiency of transformation), 250µl LB without antibiotics is pipetted immediately into the cuvette and mixed thoroughly with the cells. The cells are than incubated for 60 minutes on a shaker at 37°C. 100 to 250 µl of the bacterial suspension is plated out on agar plates with the appropriate antibiotics and incubated overnight at 37°C. As a control, a transformation without DNA is performed.

4.2.2.11 Plasmid DNA purification

1. TELT: (Wilmzig, 1985)

A well-isolated bacterial colony is inoculated in 4 ml LB medium and the culture is incubated (shaking) overnight (but not longer than 14h) at 37°C. 1.5 ml of overnight culture is pipetted into a microfuge tube, which is centrifuged at 15,000g for 3 minutes. The supernatant is removed and the pellet is resuspended in 150µl TELT with 25µl lysozyme (10 mg/ml, to break down the cell wall) on the shaker for 5 minutes. The resuspended bacteria are left unstirred at room temperature for 5 minutes. The solution is then boiled for 2 minutes in a water bath and submerged immediately into ice-water for 30 seconds. The solution is then centrifuged down at 15,000g for 8 minutes. The bacterial debris is removed and the DNA is precipitated with isopropanol and finally resuspended in 20µl TE or H_2O with 0.5µl RNAseA solution (10 mg/ml).

2. Qiagen Kit

A well-isolated colony is inoculated in appropriate volume of LB medium with the desired antibiotics and grown overnight at 37°C. The cells are spinned down at 6,000g for 10 minutes at 4°C in Sorvall GS3 rotor. The rest of the preparation steps are performed according to the procedures described in QUIAGEN® Plasmid Purification Handbook.

4.2.3 Automatic DNA sequencing

DNA sequencing of all clones in this work was performed using the automatic sequencing machine of the Applied Biosystem. The principle is modified after the dideoxy-mediated chain termination method described in Sanger et al. (1977). For each of the four reactions (G, A, T, C), the primers are labeled with different non-radioactive fluorophors. The four individual reactions are then loaded in a common gel slot. At the bottom of the gel, a laser

beam scans the fluorophor property of the running-out DNA, the information of which is saved by a computer program and transformed into nucleic acid sequences.

4.2.4 Construction of hybrid proteins

$Caps^{Ed}Trn^{Id}$ and $Trn^{Ed}Caps^{Id}$ hybrid proteins were generated by the following procedures. To generate *UAS-caps^{Ed}trn^{Id}* hybrid construct, the intracellular domain of *caps* was removed from *caps* cDNA by cutting out a 660bp *Bsp*MI-*Not*I fragment. Then, the intracellular domain (aa 469-737) of *trn* was amplified through PCR using primers "trn^{Id} forward" and "trn^{Id} reverse" (**Table 4.3**). Subsequently, TOPO PCR Cloning Kit (Invitrogen) was used to ligate and transform the PCR products following the procedures in the instruction manual (Invitrogen). The pCR®II-TOPO + *trn^{Id}* plasmid was isolated and digested with *Bsp*MI and *Not*I. The resulting fragment containing *trn* intracellular domain was ligated in frame into the previously digested *caps* cDNA vector lacking the intracellular domain. Finally, the hybrid DNA fragment containing *caps* extracellular domain and *trn* intracellular domain (*caps^{Ed}trn^{Id}*) was cloned into *Eco*RI site of p*UAST* vector.

Similarly, for the construction of $Trn^{Ed}Caps^{Id}$ hybrid protein, an *Xmn*I-*Xho*I fragment (1871-3174bp) was cut out from *trn* cDNA (GH10871). The intracellular domain of *caps* containing 5' *Xmn*I and 3' *Xho*I was amplified using the primers "$caps^{Id}$ forward" and "$caps^{Id}$ reverse" (**Table 4.3**). Subsequently, *Xmn*I and *Xho*I fragment containing *caps^{Id}* was ligated in frame into the previously digested *trn* cDNA vector lacking the intracellular domain. Finally, the hybrid DNA fragment containing *trn* extracellular domain and *caps* intracellular domain (*trn^{Ed}caps^{Id}*) was cloned into *Eco*RI and *Xho*I site of p*UAST*. The sequences of hybrid plasmids were thoroughly verified.

4.2.5 Site-directed mutagenesis

QuikChange® Site-Directed Mutagenesis Kit (Stratagene) was used to introduce point mutations into *caps* cDNA following the procedures in the instruction manual (#200518). First, the primers that contain the desired mutations and are complementary to opposite strands of *caps* cDNA plasmid were generated (**Table 4.3**). Then, the primers were extended during temperature cycling. As a result, a mutated plasmid containing staggered nicks is generated. The *Dpn*I endonuclease digests only the parental vector leaving the

mutated plasmid intact. Finally, the mutated plasmid in transformed into XL1-Blue cells (Stratagene).

4.2.6 Yeast two-hybrid screening with CytoTrap® system (Stratagene)

Yeast two-hybrid screening with CytoTrap® system was performed by following the procedures described in the instruction manual (BN #832700-12) by Stratagene. To generate p*Sos-caps*^{Id} bait construct, DNA sequences encoding *caps* intracellular domain are amplified using primers "pSos-caps forward" and "pSos-caps reverse" (**Table 4.3)**. The amplified fragment is cloned into the p*Sos* vector at 5' *Bam*HI and 3' *Not*I sites. The sequence of the resulting fusion protein was thoroughly verified to ensure that there is no spontaneous point mutation that could render Caps^{Id} non-functional and also that Caps^{Id} is translated in frame with the Sos domain. Then, it was tested that Sos-Caps^{Id} bait protein does not interact with the myristylation signal of pMyr plasmid and therefore, is suitable for the CytoTrap® two-hybrid screen.

In parallel, pMyr target plasmids containing *Drosophila* cDNA library were isolated from XL10-Gold Kan competent cells (donated by M. Hoch). Then, p*Sos-Caps*^{Id} bait plasmid and p*Myr-cDNA* target plasmids were cotransformed in the yeast *cdc25H* cells. Subsequently, the transformants were spread on synthetic glucose minimal medium plates (glucose-UL), which contain glucose as carbon source and lack uracil (U) and leucine (L). The transformants were incubated at room temperature for two days, replica plated on galactose-UL plates (synthetic galactose minimal medium lacking uracil and leucine) and then incubated at 37°C to select for putative interactor candidates. After 10 days of incubation at 37°C, more than 400 colonies were selected. They were streaked onto the fresh glucose-UL plates and were grown at room temperature. These interactor candidate colonies were then put twice through the interaction tests.

Table 4.4 Interaction test

glucose-UL 25°C	glucose-UL 37°C	galactose-UL 37°C	
Yes	No	No	No interaction
Yes	Yes	Yes	Temperature revertant
Yes	**No**	**Yes**	**Positive interaction**

First row indicates growth medium (synthetic glucose or galactose minimal medium lacking uracil and leucine) and temperature for the colonies. Growth or no growth is indicated by Yes or No, respectively. Clones that show growth on galactose-UL plates but not on glucose-UL plates at 37°C reveal positive interaction and contain putative interactors of Caps^{Id}.

4.2.7 GST pull-down assay (Beller et al., 2002)

4.2.7.1 Expression of GST-Caps^{Id} fusion protein

First, the plasmid encoding GST-Caps^{Id} fusion protein was generated. *caps* intracellular domain was amplified through PCR using the primers "pGEX-caps forward" and "pSos-caps reverse" (**Table 4.3**). The amplified *caps^{Id}* was cloned in frame into pGEX-4T-3 (GST) vector at 5'*Bam*HI and 3'*Not*I sites. The sequence of *GST-caps^{Id}* fusion plasmid was thoroughly verified. Then, the *GST-caps^{Id}* fusion plasmid was transformed into BL21-CodonPlus®(DE3)-RIL Competent Cells (Stratagene) following the procedures described in the instruction manual (#230245). On the next day, single colony is picked and inoculated in 5ml fresh LB medium containing ampicillin and chloramphenicol (LB+Amp+Chl). After 8 hours of incubation with shaking at 37°C, the culture is diluted 1:750 in 30 ml LB+Amp+Chl. On the next day, the culture is diluted again 1:30 in 500ml LB+Amp+Chl and incubated at 37°C until OD_{600} 0.4 is reached. Then, IPTG is added to end concentration of 0.4mM and the culture is incubated at 37°C for another 2 hours.

To harvest the cells, the culture is centrifuged at 6,000 rpm (4°C, 15 min) and the pellet is washed with 100ml ice cold PBS. Then, the suspension is centrifuged at 4,000 rpm (4°C, 10 min) and the pellet is resuspended in 10ml lysis buffer. 100µl lysozyme (0.5g/10ml in lysis buffer) is added to the harvested cells, which are subsequently incubated for 30 min and then frozen in liquid N_2. Then, the cells are thawed again and lysed with sonicator. Finally, the cells are centrifuged at 15,000 rpm (4°C, 20min). The supernant is frozen in liquid N_2 and stored at -20°C.

4.2.7.2 Purification of GST-Caps^{Id} fusion protein

GST-Caps^{Id} fusion protein was purified from bacterial protein extract using Glutathione Sepharose 4B beads (Amersham). First, the Glutathione Sepharose 4B beads were washed 3x with 5-10 vol of lysis buffer. Then, crude bacterial lysate containing GST-Caps^{Id} fusion protein and lysis buffer (1:1) were added and incubated for 2 hours at 4°C with rotating to

allow binding of GST-Caps^{Id} fusion to the beads. The beads were washed 5x with 1ml lysis, 5x with 1ml wash buffer 2 and 5x with 1ml wash buffer 3. The Glutathione Sepharose 4B beads coupled with GST-Caps^{Id} fusion protein was stored at 4°C.

4.2.7.3 *In vitro* translation of *ras64B*

For efficient *in vitro* translation of *ras64B*, ORF of *ras64B* was first amplified through PCR using the primers "ras64B forward" and "ras64B reverse" (**Table 4.3**). Then, the amplified *ras64B* ORF was cloned in frame into pcDNA3.1/HisB (Invitrogen) at 5'*EcoR*I and 3'*Xba*I sites. The sequence of pcDNA3.1/HisB plasmid containing *ras64B* was thoroughly verified. Then, TNT® T7 Coupled Reticulocyte Lysate System (Promega) was used to produce radioactively labeled Ras64B protein *in vitro*. After ^{35}S-Ras64B was generated by following the procedures described in the instruction manual (#TB126; Promega), GTP or GDP was added to end concentration of 1mM to induce active or inactive form of ^{35}S-Ras64B, respectively. Then, the reaction mixtures were diluted to a final volume of 260µl in wash buffer 3 and centrifuged at 15,000 rpm (4°C, 15 min).

4.2.7.4 GST pull-down assay

The Glutathione Sepharose 4B beads coupled with GST-Caps^{Id} fusion protein were incubated separately with Ras64B containing either GTP or GDP for 2 hours at 4°C to allow binding of Ras64B to GST-Caps^{Id}. Then, the beads were washed 5x with lysis buffer, which is the same as a high stringency wash buffer, to remove unbound Ras64B. The beads were then resuspended in 100µl lysis buffer and SDS loading buffer was added. The suspension was then boiled for 5 min in water bath and cooled down to room temperature. Finally, the suspension was centrifuged at 15,000 rpm for 2 min and the supernatant containing GST-Caps^{Id} fusion protein and *in vitro* translated Ras64B was stored at -20°C.

4.2.7.5 SDS-PAGE (Laemmli, 1970)

The supernatants containing GST-Caps^{Id} fusion protein and *in vitro* translated Ras64B were loaded on 12% SDS-polyacrylamide gel and run at 50V until they reached the running gel. Then, they were run at 130V until the SDS loading buffer reached the edge of running gel. The SDS-polyacrylamide gel was washed 3x with water (5 min) and stained with GelCode Bluestain Reagent (Pierce). When the protein bands became clearly visible,

the SDS-polyacrylamide gel was washed again 3x with water (5 min) and dried at 65°C for 1hour using Slab Gel Dryer (Pharmacia)

4.2.7.6 Autoradiography

The dried SDS-polyacrylamide gel is wrapped in a plastic bag, which is covered by an X-ray film (X-OMAT™AR, 35 x 43 cm, Kodak) marked with a "dog-ear" folding for exposure. The exposure is performed in a cassette at –80°C for adequate amount of time, which is adjusted experimentally. To develop the X-ray film, the X-Ray Automatic Processor Optimax TR: (MS-Laborgeräte) is used.

4.2.8 Purification of anti-Capricious antibody

Antibody against Capricious was raised in rabbit using peptide sequences (Eurogentec): H_2N-CEYQKTFSDEEYMSRP-$CONH_2$ and H_2N-AAGGYPYIAGNSRMIPVTEL-COOH. To improve the quality of antibody signal, the antibody was purified using activated CH Sepharose 4B beads following the procedures described in the instruction manual (#71-7088-00; Amersham). The peptide sequences, which were used to generate anti-Caps antibody, were coupled to the activated CH Sepharose 4B beads as ligands to generate specific binding of anti-Caps antibody. OD_{280} was measured before and after coupling reaction to control how effective coupling of peptide to the activated CH Sepharose 4B beads was. To remove the unbound peptide, the coupled beads were washed 5vol with coupling buffer. Then, the beads were incubated with blocking buffer to block any remaining active CH group. Finally, the beads coupled with peptides were packed into column.

The crude blood samples containing anti-Caps antibody was thawed slowly at room temperature and then submerged into 56°C water bath for 30 sec to inactivate complements. Then, the samples were cooled on ice and centrifuged for 2 min to remove any debris. The clear supernatant was diluted 1:10 with binding buffer and applied to the prepacked column. The flow-through was collected and reapplied to the column (3x in total). After extensive washing, the bound antibody was eluted with elution buffer and collected in tubes containing 1M Tris-Base so that the end pH would be 7.5. This is important because acidic pH would denature the eluted antibody. Finally, the eluted antibody solution was concentrated using Centriprep following the procedures described in

the User Guide (#99320; Millipore). Thus concentrated anti-Caps antibody was aliquoted and stored at -80°C.

4.3 Embryology

4.3.1 Fly care and feeding

The care and feeding of *Drosophila melanogaster* is performed according to Ashburner (1989). Flies are kept in plastic vials of various sizes, which are filled with the fly food for ¼ of the vial volume and closed with raw cotton plugs. To prevent the pupals and adults from sticking in the food, a paper filter is inserted as a substrate. Depending on the desired development rate, flies can be kept at 18°C or 25°C. Every 2-4 weeks the flies are flipped into new vials for propagation.

4.3.2 Collecting embryos

To collect the embryos, the flies are transferred to a cage covered by an apple juice plate, on which baker's yeast is spread. The flies were stored at 25°C for embryo collection.

4.3.3 Fixation of embryos

The collected embryos are washed with water to get rid of the yeast and then dechorionated with 50% bleach (Clorox) for 3 minutes. To stop dechorionation, the embryos are rinsed several times with water. Subsequently, the embryos are shaken for 20 minutes in the fixing solution, which consists of 6 ml heptane and 1ml fixative. After fixation, the fixative (lower phase) is removed and 10 ml of methanol is added. Then, the embryos are shaken for 3 minutes to remove the vitelline membrane. The devitellinated embryos are washed several times with methanol and then kept in microfuge tube at -20°C for long term storage.

4.3.4 Whole-mount antibody staining of embryos

The fixed embryos were washed 3x 20 minutes with 1ml BBT and incubated with 300µl primary antibody-BBT mixture (see **Table 4.1** for various primary antibody working concentrations) overnight at 4°C (Ashburner, 1989). On the following day, the embryos

were washed 1x 20 minutes with 1ml BBT to get rid of unbound primary antibody. Then the embryos were washed 2x 20 minutes with 0.5 ml BBT-blocking serum solution (6% normal goat or 9% horse serum). Subsequently, the embryos were incubated with the secondary antibody-BBT-blocking serum mixture (see **Table 4.2** for various secondary antibody working concentrations) for at least 2 hours at room temperature. Then, the embryos were washed 4x 10 minutes with 1ml PBT to remove unbound secondary antibody.

For detection of biotinylated secondary antibodies, the embryos were preincubated with either a complex of avidin/biotinylated horseradish peroxidase (HRP) or alkaline phosphatase (AP) (Vectastain® ABC elite kit or ABC-AP kit) for at least 30 minutes. Then, the embryos were washed 4x 10 minutes with 1ml PBT to remove uncoupled complex. To detect HRP, one DAB and one H_2O_2 tablet (Sigma) were dissolved in 1ml water. Then, to start a chromogenic reaction, 150µl of DAB/ H_2O_2 solution was added to 850µl PBT containing embryos. Subsequently, dark brown, water- and alcohol insoluble precipitates form and the reaction is stopped by washing the embryos several times with PBT.

For detection of AP, the embryos were washed 2x 5 minutes with 1ml alkaline phosphatase buffer (pH 9) that is supplemented with 0.1% Tween20 and 1mM levamisol. Levamisol inhibits endogenous lysosomal phosphatase in embryos and should prevent unspecific staining.. To start a chromogenic reaction, 4.5µl NBT and 3.5µl BCIP was added to 1ml PBT containing the embryos. The chromogenic reaction was controlled under a binocular and stopped by washing the embryos several times with PBT.

To visualize staining with secondary antibodies conjugated with fluorophores, a confocal laser-scanning microscope (Zeiss Axiovert) was used.

4.3.5 Whole-mount *in situ* hybridization of embryos

The single and double *in situ* hybridizations of whole-mount embryos are modified after the procedures described by Klingler and Gergen (1993) and Hartmann et al. (1994), respectively.

The fixed embryos are washed with PBT:methanol (1:1) and then with PBT:fixative (1:1). The embryos are fixed with 1ml fixative for 20 minutes at room temperature. To stop fixation, embryos are washed 4x with 1ml PBT. Then, the embryos are washed with 500µl

PBT/hybridization B mixture (1:1), 250µl hybridization B and 250µl hybridization solution. Subsequently, the embryos are prehybridized at 60°C for at least 1h. After the hybridization solution is removed as much as possible, embryos are hybridized with 3-4µl (approximately 100ng/µl) of digoxigenin-dUTP or fluorescein-dUTP conjugated antisense RNA probe at 60°C for overnight.

On the following day, the embryos are washed 3x 20 minutes with 1ml PBT to remove antisense RNA probes that are not incorporated. Then, the embryos are incubated with anti-digoxygenin or anti-fluorescein antibodies, which are conjugated with either HRP or AP, for at least 2h at room temperature. See **Table 4.1** for various antibody working concentrations. The embryos are washed 4x 10 minutes with 1ml PBT to remove unbound antibody. For detection of HRP conjugated antibodies, the embryos are incubated with TSA-biotin (1:50) for 15 min and subsequently washed 4x 10 min with 1ml PBT. For chromogenic detection of TSA-biotin, the embryos are preincubated with a complex of avidin/biotinylated AP (Vectastain® ABC-AP kit) for at least 30 minutes. Then, the embryos are treated similarly as in the whole-mount antibody staining to detect AP (**Section 4.3.4**). Alternatively, for fluorescence detection of TSA-biotin, the embryos were incubated with streptavidin conjugated Cy2 for at least 1 hour. Then, the embryos are washed 4x 10 min with 1ml PBT. For detection of AP conjugated antibodies, the embryos were treated similarly as in the whole-mount antibody staining (**Section 4.3.4)**.

4.3.6 Signal amplification using TSA

To amplify weak signals of antibodies during whole-mount antibody stainings or *in situ* hybridization, either TSA™ Cy3 or Biotin System (PerkinElmer) is used. The TSA System technology uses HRP to catalyze the deposition of labeled (either with Cy3 or biotin) tyramide in the cells. Since one unit of HRP can catalyze numerous tyramide molecules, this technology provides significant amplification of signal. In addition, there is minimal loss in resolution as the added labels are deposited immediately next to the immobilized HRP.

TSA-Cy3 is visualized directly with confocal laser-scanning microscope (Zeiss Axiovert). On the other hand, TSA-biotin is detected by either chromogenic or fluorescence visualization techniques. For chromogenic detection, embryos are incubated with a complex of avidin/biotinylated AP (Vectastain® ABC-AP kit) for at least 30 minutes.

Then, the embryos are washed 4x 10 minutes with 1ml PBT to remove uncoupled complex. For detection of AP, the embryos are treated similarly as in the whole-mount antibody staining (**Section 4.3.4**). For fluorescence detection, the embryos are incubated with streptavidin-coupled Cy2 for 2 hours at room temperature.

4.3.7 Embedding of embryos

After stopping the chromogenic reaction, PBT is removed as much as possible from embryos in a staining dish. Then, 100% glycerol is added to the embryos. The dehydration steps are not necessary. Such embedded embryos can be stored for more than 3 years in staining dishes sealed with parafilm. For documentation of staining, embryos are transferred onto a glass slide covered with a slip with glass feet beneath. Alternatively, to mount the embryos incubated with the antibodies conjugated with fluorophores, PBT was removed as much as possible and fluorescence mounting medium (Vector Laboratories) was added. The embryos can be stored at 4°C up to 7 days for visualization with a confocal laser-scanning microscope (Zeiss Axiovert).

4.3.8 Light microscopy

Whole-mount embryos, which are immunostained or *in situ* hybridized, are mounted on slides and viewed with a Zeiss Axiophot compound microscope using differential interference contrast optics and light polarization.

4.3.9 Confocal laser scanning microscopy (LSM)

Zeiss Axiovert confocal microscope is used for fluorescence imaging. Cy3 and Cy2 are excited at 543 and 488 nm, respectively. The combining pass filter for Cy3 is at 575 nm and for Cy2 at 515 nm.

4.4 Genetics

4.4.1 P-Element mediated germline transformation

Transgenic flies are obtained by following the previously described protocol (Rubin and Spradling, 1982). Approximately 300 Df(1)w^{67C23} embryos at the appropriate pole cell

stage are injected with pUAST constructs (600ng/µl; Brand and Perrimon, 1993) and helper plasmid (150ng/µl; Laski et al., 1986) in water. The DNA and helper plasmid are prepared by the following procedures. First, the DNA is extracted with phenol, phenol-chloroform and chloroform/isoamyl alcohol (**Section 4.2.2.2**). Then, 6 µg of such purified DNA and 1-2µg of helper plasmid is mixed in a final volume of 100µl water, precipitated with ethanol and finally resuspended in 20µl water.

Each hatching fly is backcrossed to the original $Df(1)w^{67C23}$ strain. Progenies of such crosses showing red eye color (due to w^+ gene in pUAST plasmid) are the transformants. The transformed chromosomes are stabilized using balancer chromosome or through viability in homozygous state. At least two independent transgenic lines are established and analyzed for each construct.

4.4.2 Ectopic expression of genes induced by UAS/GAL4 system

In *Drosophila melanogaster*, ectopic induction of genes can be controlled spatially and temporally using UAS/GAL4 system. This powerful genetic tool utilizes yeast UAS (upstream activating sequence) and GAL4 protein (Brand and Perrimon, 1993). The system is based on a driver line, which carries a tissue specific enhancer sequence at upstream of yeast Gal4 gene, and an effector line, which carries a gene of interest at downstream of yeast UAS. When a driver line is crossed to an effector line, the GAL4 protein recognizes the UAS and drives the expression of linked gene ectopically in the cells that contain GAL4 protein.

5 Summary

The tubular structures, which transport essential gases, liquids, or cells from one site to another, are shared among various divergent organisms. These highly organized tubular networks include lung, kidney, vasculature and mammary gland in mammals as well as trachea and salivary gland in *Drosophila melanogaster*. Many questions regarding the tubular morphogenesis cannot be addressed sufficiently by investigating the mammalian organs because their structures are extremely complex and therefore, systematic analyses of genetic and cellular programs guiding the development is not possible. In contrast, the *Drosophila* tracheal development provides an excellent model system since many molecular markers and powerful tools for genetic manipulations are available.

Two mechanisms were shown to be important for the outgrowth of tracheal cells: the FGF signaling pathway and the interaction between the tracheal cells and the surrounding mesodermal cells. The Drosophila FGF ligand encoded by *branchless* (*bnl*) is localized in groups of cells near tracheal metameres. The tracheal cells expressing the FGF receptor *breathless* (*btl*) respond to these sources of FGF ligand and extend towards them. However, this FGF signaling pathway is not sufficient for the formation of continuous dorsal trunk, the only muticellular tube in tracheal system. Recently, it was found out that single mesodermal cells called bridge-cells are essential for the formation of continuous dorsal trunk as they direct the outgrowth of dorsal trunk cells towards the correct targets.

The results in this PhD thesis demonstrate that a cell adhesion molecule Capricious (Caps), which is specifically localized on the surface of bridge-cells, plays an essential role in guiding the outgrowing dorsal trunk cells towards their correct targets. When *caps* is lacking, some bridge-cells cannot stretch properly towards the adjacent posterior tracheal metameres and thus fail to interconnect the juxtaposing dorsal trunk cells. Consequently, discontinuous dorsal trunks containing interruptions at several positions are formed. On the other hand, when *caps* is ectopically expressed in the mesodermal cells through a *twi-GAL4* driver, these mesodermal cells acquire a guidance function through ectopic *caps* and misguide the outgrowing dorsal trunk cells in abnormal directions. As a result, disconnected dorsal trunks are formed. These loss- and gain-of-function studies suggest that Caps presumably establishes the cell-to-cell contact between the bridge-cells and the tracheal cells and thereby mediates directly the guidance function of bridge-cells.

The most similar protein known to Caps is another cell adhesion molecule called Tartan (Trn). Interestingly, *trn* is expressed in the mesodermal cells but not in the bridge-cells. When *trn* is lacking, the outgrowth of not only the dorsal trunks but also the lateral trunks are disrupted. However, in contrast to the ectopic expression of *caps*, the misexpression of *trn* does not affect tracheal development. Whereas Trn requires only its extracellular domain to mediate the matrix function, Caps requires both its extracellular and intracellular domains to function as a guidance molecule in the bridge-cells. These observations suggest that Trn functions differently from Caps during tracheal morphogenesis. Presumably, Trn mediates a matrix function of mesodermal cells, which support the tracheal cells to extend efficiently through the surrounding mesodermal tissue.

In order to determine which domains dictate the functional specificity of Caps, two hybrid proteins $Caps^{Ed}Trn^{Id}$, which contains the Caps extracellular domain and the Trn intracellular domain, and $Trn^{Ed}Caps^{Id}$, which consists of the Trn extracellular domain and the Caps intracellular domain, were constructed. Gain of function and rescue experiments with these hybrid proteins suggest on one hand that the extracellular domains of Caps and Trn are functionally redundant and on the other hand that the intracellular domain dictates the functional specificity of Caps.

Alignment of Caps against its *Anopheles* homolog revealed that their intracellular domains contain a highly conserved RHR motif, whose function is yet unknown. Mutagenesis of this RHR motif renders Caps non-functional. This result suggests that the RHR motif is essential for the Caps function. Possibly, Caps may interact with other proteins through the RHR motif. In order to identify putative interactors of Caps, yeast two-hybrid screening was performed. An *in vivo* interaction assay in yeast suggests that Ras64B interacts specifically with the Caps intracellular domain. In addition, an *in vitro* binding assay reveals a direct interaction between an inactive form of Ras64B and the Caps intracellular domain. *ras64B*, which encodes a small GTPase, is expressed in the mesodermal cells concurrently as *caps*. Finally, a gain-of-function study with the constitutively active Ras64B suggests that Ras64B presumably functions downstream of Caps. All these results suggest consistently that the small GTPase Ras64B binds specifically to the Caps intracellular domain and may thereby mediate the guidance function of Caps.

6 Zusammenfassung

Tubulär aufgebaute Organe, wie z.B. Lunge, Niere und das Blutgefäßsystem, sind in allen höheren tierischen Organismen anzutreffen. Sie dienen dem Transport und Austausch von Gasen, Nähr- und Exkretionsstoffen. Die Analyse solcher tubulären Organe ist in Vertebratensystemen sehr aufwendig und nur eingeschränkt möglich. Im Gegensatz dazu ist die embryonale Entwicklung des Tracheensystems der Fruchtfliege *Drosophila melanogaster* ein ideales Modellsystem, um die Ausbildung multizellulärer tubulärer Strukturen zu untersuchen. Fragen zur Organisation und Kontrolle der Zellmigration, der Zellmorphogenese, der Ausbildung intrazellulärer Lumina, der Zellfusion und der Zelldifferenzierung lassen sich dabei durch die vielfältigen Möglichkeiten der Molekularbiologie und der Genetik *in vivo* beantworten.

Besonders für das Auswachsen der Tracheenzellen gibt es zwei essentielle Mechanismen: zum einen die FGF-Signalkaskade und zum anderen die Interaktion zwischen den Tracheenzellen und den angrenzenden mesodermalen Zellen. Das Gen *branchless* (*bnl*) kodiert für einen putativen FGF-Liganden in *Drosophila* und wird in Zellgruppen außerhalb der trachealen Metamere exprimiert. Andererseits wird der FGF-Rezeptor Breathless (Btl) in den Tracheenzellen exprimiert. Bnl-Signale werden über Btl an das Tracheensystem vermittelt and induzieren dadurch das Auswachsen der Tracheenzellen in gezielte Richtungen. Jedoch ist die FGF-Signalkaskade nicht ausreichend für das Auswachsen des Dorsalstammes. Kürzlich wurde entdeckt, dass einzelne mesodermale Zellen unabhängig von der FGF-Signalkaskade räumliche Informationen spezifisch an die auswachsenden Tracheenzellen des Dorsalstammes vermitteln. Zu Beginn des Auswachsens verbinden diese mesodermalen Zellen die dorsalen Stammäste miteinander in Form einer Brücke. Deshalb werden diese Zellen als Brückenzellen bezeichnet. Entlang der Brückenzellen wachsen die dorsalen Stammäste von beiden Seiten aufeinander zu, kommen in Kontakt und fusionieren anschließend.

Der Transkriptionsfaktor Hunchback (Hb) wird sowohl in den Brückenzellen als auch in den ventral liegenden Ankerzellen exprimiert. Seine Expression ist für die Lebensfähigkeit der Brückenzellen essentiell. Welche Proteine knüpfen nun einen direkten Kontakt mit den Tracheenzellen und vermitteln dadurch die Funktion der Brückenzelle? In dieser Arbeit wurde das Zelloberflächeprotein Capricious (Caps) identifiziert, das spezifisch in der Brückenzelle lokalisiert ist und die Interaktion zwischen den Brückenzellen und den

Tracheenzellen vermittelt. Die Ergebnisse dieser Arbeit deuten darauf hin, dass Hb zusammen mit einem Kofaktor die gezielte Expression von *caps* in den Brückenzellen reguliert. Vermutlich ist dieser noch nicht identifizierte Transkriptionskofaktor spezifisch in mesodermalen Zellen lokalisiert.

Caps enthält in seiner extrazellulären Domäne 14 „Leucine Rich Repeat" (LRR)-Motive und ist in der Zellmembran lokalisiert. Es wurde bereits gezeigt, dass die LRR-Motive breite Bindungsoberflächen bilden und deshalb für Interaktion mit anderen Molekülen geeignet sind. Die Ergebnisse aus dieser Arbeit deuten darauf hin, dass Caps vermutlich durch seine extrazelluläre Domäne direkt mit den auswachsenden Tracheenzellen interagiert und erhaltene Signale zu anderen cytoplasmatischen Proteinen durch seine intrazelluläre Domäne weiterleitet. Dadurch vermittelt Caps die Führungsfunktion von Brückenzellen. Wenn *caps* fehlt, können sich manche Brückenzellen nicht richtig zu den benachbarten anterioren Dorsalstammzellen strecken und nicht mehr effektiv mit den auswachsenden Tracheenzellen verbinden. Dadurch kann die direkte Interaktion zwischen den Tracheenzellen und den Brückenzellen nicht stabil etabliert werden. Folglich werden gebrochene Dorsalstammäste gebildet. Wird andererseits die Expression von *caps* ektopisch in mesodermalen Zellen durch *twi-GAL4* getrieben, bekommen diese eine Brückenzellen-ähnliche Funktion durch das ektopische *caps* und leiten die auswachsenden Tracheenzellen in abnormale Richtungen. Statt anterior-posterior zu wachsen, wandern manche Dorsalstammäste dorsal oder ventral und dadurch entsteht ein gebrochener Dorsalstamm.

Ein Protein, das größte Ähnlichkeit zu Caps aufweist, ist Tartan (Trn). Wie Caps ist auch Trn in der Zellmembran lokalisiert. Es wurde gezeigt, dass *caps* und *trn* während der Flügelmorphogenese in den gleichen Zellen exprimiert werden und redundante Funktionen besitzen. Deshalb habe ich untersucht, ob *trn* ebenfalls in den Brückenzellen exprimiert wird und zusammen mit Caps die Funktion der Brückenzelle vermittelt. Überraschenderweise wird *trn* nicht in den Brückenzellen, sondern in mesodermalem Gewebe exprimiert. Interessanterweise deutet die Expressionsanalyse von *trn* unter ektopischem Hb an, dass Hb die endogene *trn*-Expression unterdrückt. Möglicherweise wird die Expression von *trn* durch Hb gezielt in den Brückenzellen reprimiert.

Ähnlich wie in *caps* Mutanten werden diskontinuierliche Dorsalstämme in *trn* Mutanten gebildet. Im Gegensatz zu den *caps* Mutanten sind jedoch auch die lateralen Stämme in *trn* Mutanten häufig unterbrochen. Während die Misexpression von *caps* in mesodermalen

Zellen die Entwicklung der kontinuierlichen Äste behindert, werden die normalen Tracheenstämme wie im Wildtyp in *trn* misexprimierenden Embryonen gebildet. Obwohl Caps sowohl die extrazelluläre als auch die intrazelluläre Domäne für seine Funktion während der Tracheenentwicklung benötigt, braucht Trn nur seine extrazelluläre Domäne. Diese gegensätzlichen Beobachtungen zeigen, dass Caps und Trn unterschiedliche Funktionen während der Tracheenmorphogenese haben. An der Oberfläche von Brückenzellen lokalisiert, vermittelt Caps direkt die Interaktion zwischen den Dorsalstammzellen und den Brückenzellen und führt dabei gezielt das Auswachsen der Dorsalstammzellen. Andererseits bildet Trn in mesodermalen Zellen möglicherweise eine Matrix, die Tracheenzellen beim Auswachsen durch die umgebenden mesodermalen Zellen unterstützt.

Durch die Wiederherstellung der Expression von *trn* in mesodermalen Zellen können die trachealen Defekte *trn* mutanter Embryonen gerettet werden. Erstaunlicherweise kann die Expression der extrazellulären Domäne von Caps ebenfalls den trachealen Phänotyp von *trn* Mutanten retten. Diese Ergebnisse deuten an, dass die extrazelluläre Domäne von Caps die Funktion von Trn in mesodermalen Zellen übernehmen kann. Sie weisen darüber hinaus darauf hin, dass der funktionelle Unterschied zwischen Caps und Trn vermutlich in der intrazellulären Domäne liegt.

Um zu analysieren welche Domäne die funktionelle Spezifität von Caps und Trn bestimmt, wurden die Hybridproteine $Caps^{Ed}Trn^{Id}$ und $Trn^{Ed}Caps^{Id}$ konstruiert. Das Hybridprotein $Caps^{Ed}Trn^{Id}$, das die extrazelluläre Domäne von Caps aber die intrazelluläre Domäne von Trn enthält, funktioniert ähnlich wie Trn. Auch kann das $Caps^{Ed}Trn^{Id}$ Hybridprotein den trachealen Phänotyp von *trn* Mutanten effizient retten. Im Gegensatz dazu verschlechtern sich die trachealen Defekte von *trn* Mutanten durch die Expression des $Trn^{Ed}Caps^{Id}$ Hybridproteins, das die extrazelluläre Domäne von Trn aber die intrazelluläre Domäne von Caps enthält. Dieses zeigt, dass das $Trn^{Ed}Caps^{Id}$ Hybridprotein ähnlich wie Caps das Auswachsen der Tracheenzellen beeinflusst. Diese Hybridproteinanalysen deuten einerseits darauf hin, dass die extrazellulären Domänen von Caps und Trn funktionell redundant sind und zeigen andererseits, dass die intrazelluläre Domäne von Caps die funktionelle Spezifität bestimmt.

Welche Mechanismen liegen der Funktion von Caps zugrunde? Die Identifikation funktioneller Motive und/oder Interaktionspartnern könnte Hinweise darüberliefern, wie die Funktion von Caps durch die intrazelluläre Domäne vermittelt wird. Die Mutagenese

und *in vivo*-Analyse des RHR-Motivs, das zwischen Caps und seinem *Anopheles*-Homologen hoch konserviert ist, deutet darauf hin, dass dieses Motiv für die Funktion von Caps essentiell ist. Wenn $caps^{\Delta RHR}$ in mesodermalen Zellen ektopisch exprimiert wird, wachsen die Tracheenäste wie im Wildtyp normal aus. Somit ist das RHR-Motiv für die Caps-Funktion essentiell und stellt möglicherweise eine Protein-Interaktionsdomäne dar.

Durch „yeast two-hybrid screening" wurden mehrere putative Interaktionspartner von Caps identifiziert. Eine davon ist die kleine GTPase Ras64B, die eine wichtige Rolle in verschiedenen Signalkaskaden spielt. Temperatursensitive *cdc25H* Hefemutanten können bei der restriktiven Temperatur wachsen, wenn die intrazelluläre Domäne von Caps und Ras64B koexprimiert werden. Dieses deutet auf eine Interaktion zwischen den beiden Proteinen hin. Außerdem zeigten *in vitro* „GST pull-down assays", dass Ras64B in der inaktiven Form direkt an die intrazelluläre Domäne von Caps bindet. *ras64B* wird in mesodermalen Zellen exprimiert. Embryonen, die ektopisch konstitutiv aktives *ras64B* in mesodermalen Zellen exprimieren, zeigen unterbrochene Tracheenäste ähnlich wie *caps* misexprimierende Embryonen. Diese *in vivo*- und *in vitro*- Ergebnisse deuten gemeinsam daraufhin, dass Ras64B vermutlich direkt an die intrazelluläre Domäne von Caps bindet und dadurch Caps-Funktion vermittelt.

In dieser Arbeit wurden die Funktionen zweier Zelladhäsionsproteine, Caps und Trn, für die Tracheenmorphogenese untersucht. Funktionsverlust- und Funktionsgewinnanalysen deuten darauf hin, dass Caps an der Oberfläche von Brückenzellen direkt mit den auswachsenden Tracheenzellen interagiert und sie dadurch entlang der Brückenzellen zu ihren Zielen leitet. Andererseits etabliert Trn an der Oberfläche von mesodermalen Zellen eine Matrix, die Tracheenzellen hilft, durch das sie umgebende Substrat von mesodermalen Zellen effizient auswachsen zu können.

7 References

Adryan, B., Decker, H.J., Papas, T.S. and Hsu, T. (2000) Tracheal development and the von Hippel-Lindau tumor suppressor homolog in Drosophila. *Oncogene*, **19**, 2803-11.

Affolter, M., Bellusci, S., Itoh, N., Shilo, B., Thiery, J.P. and Werb, Z. (2003) Tube or not tube: remodeling epithelial tissues by branching morphogenesis. *Dev Cell*, **4**, 11-8.

Affolter, M., Montagne, J., Walldorf, U., Groppe, J., Kloter, U., LaRosa, M. and Gehring, W.J. (1994a) The *Drosophila* SRF homolog is expressed in a subset of tracheal cells and maps within a genomic region required for tracheal development. *Development*, **120**, 743-753.

Affolter, M., Nellen, D., Nussbaumer, U. and Basler, K. (1994b) Multiple requirements for the receptor serine/threonine kinase *thick veins* reveal novel functions of TGFß homologs during *Drosophila* embryogenesis. *Development*, **120**, 3105-3117.

Affolter, M. and Shilo, B.Z. (2000) Genetic control of branching morphogenesis during Drosophila tracheal development. *Curr Opin Cell Biol*, **12**, 731-5.

Altschul, S.F., Gish, W., Miller, W., Myers, E.W. and Lipman, D.J. (1990) Basic local alignment search tool. *J Mol Biol*, **215**, 403-10.

Anderson, M.G., Certel, S.J., Certel, K.C., Lee, T., Montell, D.J. and Johnson, W.A. (1996) Function of the *Drosophila* POU domain transcription factor Drifter as an upstream regulator of Breathless receptor tyrosine kinase expression in developing trachea. *Development*, **122**, 4169-4178.

Anderson, M.G., Perkins, G.L., Chittick, P., Shrigley, R.J. and Johnson, W.A. (1995) *drifter*, a *Drosophila* POU-domain transcription factor, is required for the correct differentiation and migration of tracheal cells and midline glia. *Genes Dev.*, **9**, 123-137.

Andrade, M.A., Ponting, C.P., Gibson, T.J. and Bork, P. (2000) Homology-based method for identification of protein repeats using statistical significance estimates. *J Mol Biol*, **298**, 521-37.

Aronheim, A., Zandi, E., Hennemann, H., Elledge, S.J. and Karin, M. (1997) Isolation of an AP-1 repressor by a novel method for detecting protein-protein interactions. *Mol Cell Biol*, **17**, 3094-102.

Ashburner, M. (1989) *Drosophila: A Laboratory Handbook and Manual. Two volumes.* Cold Spring Harbor Laboratory Press, Cold Spring Harbor, New York.

Bard, J. (1990) *Morphogenesis*. Cambridge University Press, United Kingdom.

Baylies, M.K., Martinez Arias, A. and Bate, M. (1995) wingless is required for the formation of a subset of muscle founder cells during Drosophila embryogenesis. *Development*, **121**, 3829-37.

Beller, M., Blanke, S., Brentrup, D. and Jäckle, H. (2002) Identification and expression of Ima, a novel Ral-interacting Drosophila protein. *Mech Dev*, **119 Suppl 1**, S253-60.

Blom, N., Gammeltoft, S. and Brunak, S. (1999) Sequence and structure-based prediction of eukaryotic protein phosphorylation sites. *J Mol Biol*, **294**, 1351-62.

Boube, M., Llimargas, M. and Casanova, J. (2000) Cross-regulatory interactions among tracheal genes support a co-operative model for the induction of tracheal fates in the Drosophila embryo. *Mech Dev*, **91**, 271-8.

Boube, M., Martin-Bermudo, M.D., Brown, N.H. and Casanova, J. (2001) Specific tracheal migration is mediated by complementary expression of cell surface proteins. *Genes Dev*, **15**, 1554-62.

Boutros, M., Mihaly, J., Bouwmeester, T. and Mlodzik, M. (2000) Signaling specificity by Frizzled receptors in Drosophila. *Science*, **288**, 1825-8.

Bradley, P.L. and Andrew, D.J. (2001) ribbon encodes a novel BTB/POZ protein required for directed cell migration in Drosophila melanogaster. *Development*, **128**, 3001-15.

Brand, A.H. and Perrimon, N. (1993) Targeted gene expression as a means of altering cell fates and generating dominant phenotypes. *Development*, **118**, 401-15.

Brose, K., Bland, K.S., Wang, K.H., Arnott, D., Henzel, W., Goodman, C.S., Tessier-Lavigne, M. and Kidd, T. (1999) Slit proteins bind Robo receptors and have an evolutionarily conserved role in repulsive axon guidance. *Cell*, **96**, 795-806.

Brown, N.H. (2000) An integrin chicken and egg problem: which comes first, the extracellular matrix or the cytoskeleton? *Curr Opin Cell Biol*, **12**, 629-33.

Brown, S., Hu, N. and Hombria, J.C. (2001) Identification of the first invertebrate interleukin JAK/STAT receptor, the Drosophila gene domeless. *Curr Biol*, **11**, 1700-5.

Bruick, R.K. and McKnight, S.L. (2001) A conserved family of prolyl-4-hydroxylases that modify HIF. *Science*, **294**, 1337-40.

Bullock, W.O., Fernandez, J.M., and Short, J.M. (1987) XL1-Blue: A high efficiency plasmid transforming recA Escherichia coli strain with beta-galactosidase selection. *BioTechniques*, **5**, 376.

Campos-Ortega, J.A. and Hartenstein, V. (1985) *The embryonic development of Drosophila melanogaster*. Springer, Berlin.

Carmena, A., Bate, M. and Jimenez, F. (1995) Lethal of scute, a proneural gene, participates in the specification of muscle progenitors during Drosophila embryogenesis. *Genes Dev*, **9**, 2373-83.

Caron, E. and Hall, A. (1998) Identification of two distinct mechanisms of phagocytosis controlled by different Rho GTPases. *Science*, **282**, 1717-21.

Casci, T., Vinos, J. and Freeman, M. (1999) Sprouty, an intracellular inhibitor of Ras signaling. *Cell*, **96**, 655-65.

Chang, Z., Price, B.D., Bockheim, S., Boedigheimer, M.J., Smith, R. and Laughon, A. (1993) Molecular and genetic characterization of the Drosophila tartan gene. *Dev Biol*, **160**, 315-32.

Chen, C.K., Kuhnlein, R.P., Eulenberg, K.G., Vincent, S., Affolter, M. and Schuh, R. (1998) The transcription factors KNIRPS and KNIRPS RELATED control cell migration and branch morphogenesis during Drosophila tracheal development. *Development*, **125**, 4959-68.

Chen, H.W., Chen, X., Oh, S.W., Marinissen, M.J., Gutkind, J.S. and Hou, S.X. (2002) mom identifies a receptor for the Drosophila JAK/STAT signal transduction pathway and encodes a protein distantly related to the mammalian cytokine receptor family. *Genes Dev*, **16**, 388-98.

Chihara, T. and Hayashi, S. (2000) Control of tracheal tubulogenesis by Wingless signaling. *Development*, **127**, 4433-42.

Chuang, P.T. and McMahon, A.P. (2003) Branching morphogenesis of the lung: new molecular insights into an old problem. *Trends Cell Biol*, **13**, 86-91.

de Celis, J.F. and Garcia-Bellido, A. (1994) Roles of the Notch gene in Drosophila wing morphogenesis. *Mech Dev*, **46**, 109-22.

de Celis, J.F., Llimargas, M. and Casanova, J. (1995) *ventral veinless*, the gene encoding the Cf1a transcription factor, links positional information and cell differentiation during embryonic and imaginal development in *Drosophila melanogaster*. *Development*, **121**, 3405-3416.

Deak, P., Omar, M.M., Saunders, R.D., Pal, M., Komonyi, O., Szidonya, J., Maroy, P., Zhang, Y., Ashburner, M., Benos, P., Savakis, C., Siden-Kiamos, I., Louis, C., Bolshakov, V.N., Kafatos, F.C., Madueno, E., Modolell, J. and Glover, D.M. (1997) P-element insertion alleles of essential genes on the third chromosome of Drosophila melanogaster: correlation of physical and cytogenetic maps in chromosomal region 86E-87F. *Genetics*, **147**, 1697-722.

Dossenbach, C., Rock, S. and Affolter, M. (2001) Specificity of FGF signaling in cell migration in Drosophila. *Development*, **128**, 4563-72.

Englund, C., Steneberg, P., Falileeva, L., Xylourgidis, N. and Samakovlis, C. (2002) Attractive and repulsive functions of Slit are mediated by different receptors in the Drosophila trachea. *Development*, **129**, 4941-51.

Fields, S. and Song, O. (1989) A novel genetic system to detect protein-protein interactions. *Nature*, **340**, 245-6.

Franch-Marro, X. and Casanova, J. (2000) The alternative migratory pathways of the Drosophila tracheal cells are associated with distinct subsets of mesodermal cells. *Dev Biol*, **227**, 80-90.

Fullilove, S.L. and Jacobson, A.G. (1978) Embryonic development: Descriptive. In Ashburner, M. and Wright, T.R.F. (eds.), *The genetics and biology of Drosophila*. Academic Press, London, Vol. 2c, pp. 106-227.

Gasteiger, E., Gattiker, A., Hoogland, C., Ivanyi, I., Appel, R.D. and Bairoch, A. (2003) ExPASy: The proteomics server for in-depth protein knowledge and analysis. *Nucleic Acids Res*, **31**, 3784-8.

Glazer, L. and Shilo, B.-Z. (1991) The *Drosophila* FGF-R homolog is expressed in the embryonic tracheal system and appears to be required for directed tracheal cell extension. *Genes Dev.*, **5**, 697-705.

Glise, B. and Noselli, S. (1997) Coupling of Jun amino-terminal kinase and Decapentaplegic signaling pathways in Drosophila morphogenesis. *Genes Dev*, **11**, 1738-47.

Greig, S. and Akam, M. (1993) Homeotic genes autonomously specify one aspect of pattern in the *Drosophila* mesoderm. *Nature*, **362**, 630-632.

Guillemin, K., Groppe, J., Dücker, K., Treisman, R., Hafen, E., Affolter, M. and Krasnow, M.A. (1996) The *pruned* gene encodes the *Drosophila* Serum Response Factor and regulates cytoplasmic outgrowth during terminal branching of the tracheal system. *Development*, **122**, 1353-1362.

Gumbiner, B.M. (1992) Epithelial morphogenesis. *Cell*, **69**, 385-387.

Hacohen, N., Kramer, S., Sutherland, D., Hiromi, Y. and Krasnow, M.A. (1998) *sprouty* encodes a novel antagonist of FGF signaling that patterns apical branching of the *Drosophila* airways. *Cell*, **92**, 253-263.

Hanahan, D. (1983) Studies on transformation of Escherichia coli with plasmids. *J Mol Biol*, **166**, 557-80.

Hartmann, C., Taubert, H., Jaeckle, H. and Pankratz, M.J. (1994) A two-step mode of stripe formation in the Drosophila blastoderm requires interactions among primary pair rule genes. *Mech. Dev. (CODEN: MEDVE6)*, **45**, 3--13.

Hemphala, J., Uv, A., Cantera, R., Bray, S. and Samakovlis, C. (2003) Grainy head controls apical membrane growth and tube elongation in response to Branchless/FGF signalling. *Development*, **130**, 249-58.

Hogan, B.L., Grindley, J., Bellusci, S., Dunn, N.R., Emoto, H. and Itoh, N. (1997) Branching morphogenesis of the lung: new models for a classical problem. *Cold Spring Harb Symp Quant Biol*, **62**, 249-56.

Hülskamp, M., Pfeifle, C. and Tautz, D. (1990) A morphogenetic gradient of hunchback protein organizes the expression of the gap genes Kruppel and knirps in the early Drosophila embryo. *Nature*, **346**, 577-80.

Ikeya, T. and Hayashi, S. (1999) Interplay of Notch and FGF signaling restricts cell fate and MAPK activation in the Drosophila trachea. *Development*, **126**, 4455-63.

Imam, F., Sutherland, D., Huang, W. and Krasnow, M.A. (1999) stumps, a Drosophila gene required for fibroblast growth factor (FGF)-directed migrations of tracheal and mesodermal cells. *Genetics*, **152**, 307-18.

Isaac, D.D. and Andrew, D.J. (1996) Tubulogenesis in *Drosophila*: a requirement for the *trachealess* gene product. *Genes Dev.*, **10**, 103-117.

Jarecki, J., Johnson, E. and Krasnow, M.A. (1999) Oxygen regulation of airway branching in Drosophila is mediated by branchless FGF. *Cell*, **99**, 211-20.

Jerpseth, M., Jerpseth, B., Breister, L. and Greener, A. (1998) High-efficiency Derivatives of the BL21 Series for Protein Expression. *Strategies*, **11**, 3-4.

Kamimura, K., Fujise, M., Villa, F., Izumi, S., Habuchi, H., Kimata, K. and Nakato, H. (2001) Drosophila heparan sulfate 6-O-sulfotransferase (dHS6ST) gene. Structure, expression, and function in the formation of the tracheal system. *J Biol Chem*, **276**, 17014-21.

Kataoka, K., Fujiwara, K.T., Noda, M. and Nishizawa, M. (1994) MafB, a new Maf family transcription activator that can associate with Maf and Fos but not with Jun. *Mol Cell Biol*, **14**, 7581-91.

Kennedy, M.B. (1995) Origin of PDZ (DHR, GLGF) domains. *Trends Biochem Sci*, **20**, 350.

Kidd, T., Brose, K., Mitchell, K.J., Fetter, R.D., Tessier-Lavigne, M., Goodman, C.S. and Tear, G. (1998) Roundabout controls axon crossing of the CNS midline and defines a novel subfamily of evolutionarily conserved guidance receptors. *Cell*, **92**, 205-15.

Klämbt, C., Glazer, L. and Shilo, B.-Z. (1992) *breathless*, a *Drosophila* FGF receptor homolog, is essential for migration of tracheal and specific midline glial cells. *Genes Dev.*, **6**, 1668-1678.

Klingler, M. and Gergen, J.P. (1993) Regulation of runt transcription by *Drosophila* segmentation genes. *Mech. Dev. (CODEN: MEDVE6)*, **43**, 3-19.

Kobe, B. and Deisenhofer, J. (1994) The leucine-rich repeat: a versatile binding motif. *Trends Biochem Sci*, **19**, 415-21.

Kobe, B. and Deisenhofer, J. (1995) Proteins with leucine-rich repeats. *Curr Opin Struct Biol*, **5**, 409-16.

Kobe, B. and Deisenhofer, J. (1995) A structural basis of the interactions between leucine-rich repeats and protein ligands. *Nature*, **374**, 183-6.

Kornau, H.C., Schenker, L.T., Kennedy, M.B. and Seeburg, P.H. (1995) Domain interaction between NMDA receptor subunits and the postsynaptic density protein PSD-95. *Science*, **269**, 1737-40.

Kramer, S., Okabe, M., Hacohen, N., Krasnow, M.A. and Hiromi, Y. (1999) Sprouty: a common antagonist of FGF and EGF signaling pathways in Drosophila. *Development*, **126**, 2515-25.

Kühnlein, R.P. and Schuh, R. (1996) Dual function of the region specific homeotic gene *spalt* during *Drosophila* tracheal system development. *Development*, **122**, 2215-2223.

Laemmli, U.K. (1970) Cleavage of structural proteins during the assembly of the head of bacteriophage T4. *Nature*, **227**, 680-685.

Laski, F.A., Rio, D.C. and Rubin, G.M. (1986) Tissue specificity of Drosophila P element transposition is regulated at the level of mRNA splicing. *Cell*, **44**, 7-19.

Lavista-Llanos, S., Centanin, L., Irisarri, M., Russo, D.M., Gleadle, J.M., Bocca, S.N., Muzzopappa, M., Ratcliffe, P.J. and Wappner, P. (2002) Control of the hypoxic response in Drosophila melanogaster by the basic helix-loop-helix PAS protein similar. *Mol Cell Biol*, **22**, 6842-53.

Lee, S. and Kolodziej, P.A. (2002) The plakin Short Stop and the RhoA GTPase are required for E-cadherin-dependent apical surface remodeling during tracheal tube fusion. *Development*, **129**, 1509-20.

Lee, T., Hacohen, N., Krasnow, M.A. and Montell, D.J. (1996) Regulated Breathless receptor tyrosine kinase activity required to pattern cell migration and branching in the *Drosophila* tracheal system. *Genes Dev.*, **10**, 2912-2921.

Lin, X., Buff, E.M., Perrimon, N. and Michelson, A.M. (1999) Heparan sulfate proteoglycans are essential for FGF receptor signaling during Drosophila embryonic development. *Development*, **126**, 3715-23.

Llimargas, M. (2000) Wingless and its signalling pathway have common and separable functions during tracheal development. *Development*, **127**, 4407-17.

Llimargas, M. and Casanova, J. (1997) *ventral veinless*, a POU domain transcription factor, regulates different transduction pathways required for tracheal branching in *Drosophila*. *Development*, **124**, 3273-3281.

Llimargas, M. and Casanova, J. (1999) EGF signalling regulates cell invagination as well as cell migration during formation of tracheal system in Drosophila. *Dev Genes Evol*, **209**, 174-9.

Locke, M. (1958) The formation of tracheae and tracheoles in *Rhodnius prolixus*. *Q. J. Microsc. Sci.*, **99**, 29-46.

Lubarsky, B. and Krasnow, M.A. (2003) Tube morphogenesis: making and shaping biological tubes. *Cell*, **112**, 19-28.

Madhavan, M.M. and Schneiderman, H.A. (1977) Histological analysis of the dynamics of growth of imaginal discs and histoblast nests during the larval development of Drosophila melanogaster. *Wilhelm Roux's Arch. Dev. Biol.*, **183**, 269-305.

Manning, G. and Krasnow, M.A. (1993) *Development of the Drosophila tracheal system*. CSHL press, New York.

Metzger, R.J. and Krasnow, M.A. (1999) Genetic control of branching morphogenesis. *Science*, **284**, 1635-9.

Michelson, A.M., Gisselbrecht, S., Buff, E. and Skeath, J.B. (1998) Heartbroken is a specific downstream mediator of FGF receptor signalling in Drosophila. *Development*, **125**, 4379-89.

Milan, M., Perez, L. and Cohen, S.M. (2002) Short-range cell interactions and cell survival in the Drosophila wing. *Dev Cell*, **2**, 797-805.

Milan, M., Weihe, U., Perez, L. and Cohen, S.M. (2001) The LRR proteins capricious and Tartan mediate cell interactions during DV boundary formation in the Drosophila wing. *Cell*, **106**, 785-94.

Montagne, J., Groppe, J., Guillemin, K., Krasnow, M.A., Gehring, W.J. and Affolter, M. (1996) The Drosophila Serum Response Factor gene is required for the formation of intervein tissue of the wing and is allelic to blistered. *Development*, **122**, 2589-97.

Myers, E.W. and Miller, W. (1989) Approximate matching of regular expressions. *Bull Math Biol*, **51**, 5-37.

Nagao, M., Ebert, B.L., Ratcliffe, P.J. and Pugh, C.W. (1996) Drosophila melanogaster SL2 cells contain a hypoxically inducible DNA binding complex which recognises mammalian HIF-binding sites. *FEBS Lett*, **387**, 161-6.

Nobes, C.D. and Hall, A. (1999) Rho GTPases control polarity, protrusion, and adhesion during cell movement. *J Cell Biol*, **144**, 1235-44.

Ohshiro, T., Emori, Y. and Saigo, K. (2002) Ligand-dependent activation of breathless FGF receptor gene in Drosophila developing trachea. *Mech Dev*, **114**, 3-11.

Ohshiro, T. and Saigo, K. (1997) Transcriptional regulation of *breathless* FGF receptor gene by binding of TRACHEALESS/dARNT heterodimers to three central midline elements in *Drosophila* developing trachea. *Development*, **124**, 3975-3986.

Pellegrini, L. (2001) Role of heparan sulfate in fibroblast growth factor signalling: a structural view. *Curr Opin Struct Biol*, **11**, 629-34.

Perrimon, N., Noll, E., McCall, K. and Brand, A. (1991) Generating lineage-specific markers to study *Drosophila* development. *Dev. Genet.*, **12**, 238-252.

Petitjean, A., Hilger, F. and Tatchell, K. (1990) Comparison of thermosensitive alleles of the CDC25 gene involved in the cAMP metabolism of Saccharomyces cerevisiae. *Genetics*, **124**, 797-806.

Poulson, D.F. (1950) Histogenesis, organogenesis, and differentiation in the embryo of D. melanogaster. In Demerec, M. (ed.) *Biology of Drosophila.* John Wiley, New York, pp. 168-274.

Rajagopalan, S., Vivancos, V., Nicolas, E. and Dickson, B.J. (2000) Selecting a longitudinal pathway: Robo receptors specify the lateral position of axons in the Drosophila CNS. *Cell*, **103**, 1033-45.

Reich, A., Sapir, A. and Shilo, B. (1999) Sprouty is a general inhibitor of receptor tyrosine kinase signaling. *Development*, **126**, 4139-47.

Reichman-Fried, M. and Shilo, B.Z. (1995) Breathless, a Drosophila FGF receptor homolog, is required for the onset of tracheal cell migration and tracheole formation. *Mech Dev*, **52**, 265-73.

Reim, I., Lee, H.H. and Frasch, M. (2003) The T-box-encoding Dorsocross genes function in amnioserosa development and the patterning of the dorsolateral germ band downstream of Dpp. *Development*, **130**, 3187-204.

Reponen, P., Sahlberg, C., Huhtala, P., Hurskainen, T., Thesleff, I. and Tryggvason, K. (1992) Molecular cloning of murine 72-kDa type IV collagenase and its expression during mouse development. *J Biol Chem*, **267**, 7856-62.

Rhyu, M.S., Jan, L.Y. and Jan, Y.N. (1994) Asymmetric distribution of numb protein during division of the sensory organ precursor cell confers distinct fates to daughter cells. *Cell*, **76**, 477-91.

Ribeiro, C., Ebner, A. and Affolter, M. (2002) In vivo imaging reveals different cellular functions for FGF and Dpp signaling in tracheal branching morphogenesis. *Dev Cell*, **2**, 677-83.

Rothberg, J.M., Hartley, D.A., Walther, Z. and Artavanis-Tsakonas, S. (1988) slit: an EGF-homologous locus of D. melanogaster involved in the development of the embryonic central nervous system. *Cell*, **55**, 1047-59.

Ruberte, E., Marty, T., Nellen, D., Affolter, M. and Basler, K. (1995) An absolute requirement for both the type II and type I receptors, *punt* and *thick veins*, for *dpp* signaling *in vivo*. *Cell*, **80**, 889-897.

Rubin, G.M. and Spradling, A.C. (1982) Genetic transformation of Drosophila with transposable element vectors. *Science (CODEN: SCIEAS)*, **218**, 348--353.

Ruiz Gomez, M. and Bate, M. (1997) Segregation of myogenic lineages in Drosophila requires numb. *Development*, **124**, 4857-66.

Samakovlis, C., Hacohen, N., Manning, G., Sutherland, D.C., Guillemin, K. and Krasnow, M.A. (1996a) Development of the *Drosophila* tracheal system occurs by a series of morphologically distinct but genetically coupled branching events. *Development*, **122**, 1395-1407.

Samakovlis, C., Manning, G., Steneberg, P., Hacohen, N., Cantera, R. and Krasnow, M.A. (1996b) Genetic control of epithelial tube fusion during Drosophila tracheal development. *Development*, **122**, 3531-6.

Sambrook, J., Fritsch, E.F. and Maniatis, T. (1989) *Molecular cloning: A laboratory manual 2nd edition*. Cold Spring Harbour Laboratory Press, New York.

Sanger, F., Nicklen, S. and Coulson, A.R. (1977) DNA sequencing with chain-terminating inhibitors. *Proc Natl Acad Sci U S A*, **74**, 5463-7.

Scholz, H., Deatrick, J., Klaes, A. and Klambt, C. (1993) Genetic dissection of pointed, a Drosophila gene encoding two ETS-related proteins. *Genetics*, **135**, 455-68.

Sedaghat, Y. and Sonnenfeld, M. (2002) The jing gene is required for embryonic brain development in Drosophila [corrected]. *Dev Genes Evol*, **212**, 277-87.

Semenza, G.L. (2001) HIF-1, O(2), and the 3 PHDs: how animal cells signal hypoxia to the nucleus. *Cell*, **107**, 1-3.

Sheng, M. and Sala, C. (2001) PDZ domains and the organization of supramolecular complexes. *Annu Rev Neurosci*, **24**, 1-29.

Shiga, Y., Tanaka-Matakatsu, M. and Hayashi, S. (1996) A nuclear GFP/ß-galactosidase fusion protein as a marker for morphogenesis in living *Drosophila*. *Dev. Growth Differ.*, **38**, 99-106.

Shim, K., Blake, K.J., Jack, J. and Krasnow, M.A. (2001) The Drosophila ribbon gene encodes a nuclear BTB domain protein that promotes epithelial migration and morphogenesis. *Development*, **128**, 4923-33.

Shishido, E., Takeichi, M. and Nose, A. (1998) Drosophila synapse formation: regulation by transmembrane protein with Leu-rich repeats, CAPRICIOUS. *Science*, **280**, 2118-21.

Simpson, J.H., Bland, K.S., Fetter, R.D. and Goodman, C.S. (2000) Short-range and long-range guidance by Slit and its Robo receptors: a combinatorial code of Robo receptors controls lateral position. *Cell*, **103**, 1019-32.

Sonnenfeld, M., Ward, M., Nystrom, G., Mosher, J., Stahl, S. and Crews, S. (1997) The *Drosophila tango* gene encodes a bHLH-PAS protein that is orthologous to mammalian Arnt and controls CNS midline and tracheale development. *Development*, **124**, 4571-4582.

Spana, E.P., Kopczynski, C., Goodman, C.S. and Doe, C.Q. (1995) Asymmetric localization of numb autonomously determines sibling neuron identity in the Drosophila CNS. *Development*, **121**, 3489-94.

Steneberg, P., Hemphala, J. and Samakovlis, C. (1999) Dpp and Notch specify the fusion cell fate in the dorsal branches of the Drosophila trachea. *Mech Dev*, **87**, 153-63.

Sutherland, D., Samakovlis, C. and Krasnow, M.A. (1996) *branchless* encodes a *Drosophila* FGF homolog that controls tracheal cell migration and the pattern of branching. *Cell*, **87**, 1091-1101.

Tanaka-Matakatsu, M., Uemura, T., Oda, H., Takeichi, M. and Hayashi, S. (1996) Cadherin-mediated cell adhesion and cell motility in *Drosophila* trachea regulated by the transcription factor Escargot. *Development*, **122**, 3697-3705.

Taniguchi, H., Shishido, E., Takeichi, M. and Nose, A. (2000) Functional dissection of drosophila capricious: its novel roles in neuronal pathfinding and selective synapse formation. *J Neurobiol*, **42**, 104-16.

Tautz, D. (1988) Regulation of the Drosophila segmentation gene hunchback by two maternal morphogenetic centres. *Nature*, **332**, 281-4.

Treisman, R. (1994) Ternary complex factors: growth factor regulated transcriptional activators. *Curr Opin Genet Dev*, **4**, 96-101.

Turner, F.R. and Mahowald, A.P. (1977) Scanning electron microscopy of *Drosophila melanogaster* embryogenesis. II. Gastrulation and segmentation. *Dev. Biol.*, **57**, 403-416.

Uv, A.E., Roth, P., Xylourgidis, N., Wickberg, A., Cantera, R. and Samakovlis, C. (2000) members only encodes a Drosophila nucleoporin required for rel protein import and immune response activation. *Genes Dev*, **14**, 1945-57.

Vincent, S., Ruberte, E., Grieder, N.C., Chen, C.K., Haerry, T., Schuh, R. and Affolter, M. (1997) DPP controls tracheal cell migration along the dorsoventral body axis of the Drosophila embryo. *Development*, **124**, 2741-50.

Vincent, S., Wilson, R., Coelho, C., Affolter, M. and Leptin, M. (1998) The Drosophila protein Dof is specifically required for FGF signaling. *Mol Cell*, **2**, 515-25.

Whitten, J.M. (1972) Comparative analysis of the tracheal system. *Ann. Rev. of Entomology*, **17**, 373-402.

Wigglesworth, V.B. (1954) Growth and regeneration in the tracheal system of an insect. *Rhodnius prolixus. J. Exp. Biol*, **36**, 632-40.

Wilk, R., Weizman, I. and Shilo, B.-Z. (1996) *trachealess* encodes a bHLH-PAS protein which is an inducer of tracheal cell fates in *Drosophila*. *Genes Dev.*, **10**, 93-102.

Wilmzig, M. (1985) LiCl-boiling method for plasmid mini-preps. *TIGS*, **1**, 158.

Wimmer, E.A., Carleton, A., Harjes, P., Turner, T. and Desplan, C. (2000) Bicoid-independent formation of thoracic segments in Drosophila. *Science*, **287**, 2476-9.

Wolf, C., Gerlach, N. and Schuh, R. (2002) Drosophila tracheal system formation involves FGF-dependent cell extensions contacting bridge-cells. *EMBO Rep*, **3**, 563-8.

Wolf, C. and Schuh, R. (2000) Single mesodermal cells guide outgrowth of ectodermal tubular structures in Drosophila. *Genes Dev*, **14**, 2140-5.

Woods, D.F. and Bryant, P.J. (1991) The discs-large tumor suppressor gene of Drosophila encodes a guanylate kinase homolog localized at septate junctions. *Cell*, **66**, 451-64.

Zelzer, E. and Shilo, B.Z. (2000) Interaction between the bHLH-PAS protein Trachealess and the POU-domain protein Drifter, specifies tracheal cell fates. *Mech Dev*, **91**, 163-73.

Zelzer, E., Wappner, P. and Shilo, B.-Z. (1997) The PAS domain confers target gene specificity of *Drosophila* bHLH/PAS proteins. *Genes Dev.*, **11**, 2079-2089.

Hiermit versichere ich, dass ich die vorliegende Dissertation selbständig und ohne unerlaubte Hilfe angefertigt und andere als die in der Dissertation angegebenen Hilfsmittel nicht benutzt habe. Alle Stellen, die wörtlich oder sinngemäß aus veröffentlichten oder unveröffentlichten Schriften entnommen sind, habe ich als solche kenntlich gemacht. Kein Teil dieser Arbeit ist in einem anderen Promotions- oder Habilitationsverfahren verwendet worden.

Göttingen, 30. Oktober 2003

_____

Cindy Krause

Acknowledgements

This PhD thesis was done in the laboratory of Dr. Reinhard Schuh in the department of Prof. Dr. Herbert Jäckle at the Max Planck Institut für biophysikalische Chemie in Göttingen.

First of all, I give thanks to my Heavenly Father for being always there for me and helping me through every single day.

Most of all, I thank Dr. Reinhard Schuh for giving me the opportunity to do this PhD thesis and providing all the support, advice, and guidance a student can ever ask for. I learned from him how to formulate the problems in the research and approach them systematically to obtain solutions. I am ever grateful for his patience and understanding.

I appreciate Prof. Dr. Herbert Jäckle for making the resources in his department freely available during my PhD thesis. I am also thankful for his critical comments regarding the thesis.

I am grateful to Prof. Dr. Mireille A. Schäfer and her colleagues at Universität in Kassel for generously accepting me as a PhD student in Kassel at a short notice. I thank them for taking their time to supervise this PhD thesis.

I thank all the members of my lab: Christian Wolf, Matthias Behr, Nina Gerlach, Markus Stahl, Boris Adryan and Stephen Blanke for their help with various experimental protocols and critical discussions. Most of all, I am thankful for the jokes, tea, and snacks that brightened up my days in the lab.

I acknowledge Ursula Jahns-Meyer for injecting plasmid constructs into embryos for the germline transformation and Gordon Dowe and Nicole Beinert for all the sequencing.

Finally, I give thanks to my family, who always supported me with their love, understanding, and enthusiasm. I am especially grateful to my husband Andreas. Without his steadfast love and encouragement, I would not have been able to complete this PhD thesis.

Lebenslauf

Cindy Krause

25.09.1973	geboren in Seoul, Südkorea Eltern: Hui Jae Kim und Hae Ra Kim Nationalität: USA
1979-1985	Besuch der Shinwol Grundschule in Seoul, Südkorea
1986-1987	Besuch der Unbook Jr. Highschool in Seoul, Südkorea
1988-1989	Besuch der Emerson Jr. Highschool in L.A., USA
1990-1992	Besuch der University Highschool in L.A., USA
1992-1996	Hauptstudium der Molecular Cell Biology an der University of California at Berkeley, in Berkeley, USA
19.12.1996	Bachelor of Arts in Molecular and Cell Biology
1997	Grundstudium der Biologie an der Georg-August Universität in Göttingen
17.10.1997	Diplomvorprüfung im Studiengang Biologie an der Georg-August Universität in Göttingen
1997-1998	Hauptstudium der Biologie an der Georg-August Universität in Göttingen
1999	Anfertigung der Diplomarbeit am Institut für Mikrobiologie und Genetik der Georg-August Universität in Göttingen, in der Abteilung von Prof. Dr. G. Braus. „Analyse der Ras-abhängigen Regulation des „Anaphase Promoting Complexes" von *Saccharomyces cerevisiae*"
04.11.1999	Diplom in Biologie
seit 1999	Anfertigung der Dissertation im Labor von PD. Dr. Reinhard Schuh, am Max-Planck-Institut für biophysikalische Chemie, in der Abteilung von Prof. Dr. Herbert Jäckle, in Göttingen.